Sedimentology and Sequence Stratigraphy of the Corinth Canal, Central Greece

By

Sturla Vatne Meling

Master Thesis

in Petroleum Geoscience

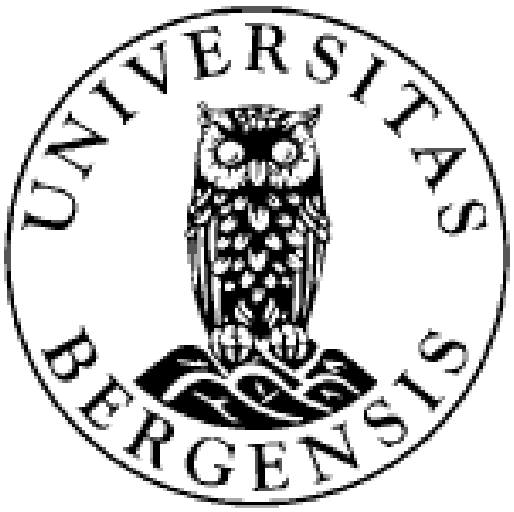

Department of Earth Science

University of Bergen

August 2016

Abstract

The following study investigate the sedimentology and sequence stratigraphy of the deposits exposed in the Corinth Canal in central Greece. Earlier studies of the Canal have been focused around the uppermost part of the Canal with minor detail paid to the deposits termed the "Corinth Marls". The aim of this study is to create a Tectono-Stratigraphic evolution of the deposits in the Corinth Canal.

The Corinth Canal features intra-rift deposits with lacustrine to marine depositional environments, changing from foreshore to offshore environments. The Corinth Canal deposits are divided into six Tectono-Stratigraphic Units, separated by major unconformities with basinward or landward shifts in facies. Tectono-Stratigraphic Units 1 to 3 are deposited within a fluvial-lacustrine basin which is capped by a major flooding surface. Tectono-Stratigraphic Units 4 to 6 are deposited within a marine environment, featuring several transgressive events cut off by falls in relative sea level.

The Corinth Canals sedimentary rocks are deposited during five Glacio-Eustatic highstands and one Glacio-Eustatic lowstand. Tectono-Stratigraphic Units 4 to 6 are deposited during five low-frequency eustatic highstand cycles (100 000 years), with deposition of the lacustrine derived Tectono-Stratigraphic Units 1 to 3 during a Glacio-Eustatic lowstand. The Tectono-Stratigraphic evolution of the Corinth Canal deposits are interpreted as lacustrine lowstand deposits overlain by five low-frequency cycles of marine deposition during the last 620 000 years.

The stratigraphic packages and bounding surfaces identified within the Corinth Canal outcrops are linked with the offshore deposits of several close by basins such as the Lechaion Gulf, the Alkyonides Gulf and the Gulf of Corinth. These correlations indicate that the Tectono-Stratigraphic evolution of the Corinth Canal deposits are closely linked with the Tectono-Stratigraphic evolution of other basins within the Corinth Rift.

Acknowledgments

This thesis is part of a Master`s Degree in petroleum geoscience at the Department of Earth Science at the University of Bergen.

Firstly, I would like to thank my supervisor Rob Gawthorpe and my co-supervisor Martin Muravchik for their helpful guidance, data processing and discussions during both the field work and during the writing process of the thesis. I would also like to thank Gijs Henstra, in addition to Haris Kranis and Manolis Skourtsos from the University of Athens, for in-field discussions.

Special thanks have to go to my fellow student Stine Hemnes Sletten, whom performed the field work for her Master`s Thesis in the Corinth Canal simultaneously as myself and acted as a field partner for much of the stratigraphic field work. Thanks have to be given to her for fruitful discussions and work performed together both during and after the field work. Thanks also have to be given to my fellow student Marthe Førland and her field-assistant, Olav Aleksander Naurstad, for their companionship during the six weeks spent in the field.

Last, but not least, I would like to thank all of my fellow students that have made my five years at the University of Bergen some of the most memorable of my life. Special thanks have to be given to the students in the "Seismic Lab" and all the wonderful people at "Midtrommet" for keeping a cheerful mood during a stressful year. None mentioned, none forgotten.

Sturla Vatne Meling Bergen, 15th of August 2016

Table of Contents

1. Introduction

1.1 Introduction and Rationale

This thesis consists of a sedimentary and sequence stratigraphic study of the exposures along the Corinth Canal in central Greece.

The study area for the thesis is the Corinth Canal, which is located on the Corinth Isthmus in central Greece, approximately 80 km west of Athens (fig. 1.1). The field work for the thesis was split into two trips of approximately 3 weeks each, from the 18th of March to the 4th of April 2015, and from the 24th of September to the 15th of October 2015. They were carried out together with my fellow students Stine Hemnes Sletten and Marthe Førland, and in co-operation with my supervisor Rob Gawthorpe, co-supervisor Martin Muravchik, and researcher Gijs Henstra.

The Corinth Canal is an excavated canal in the Corinth Basin, which shows excellent outcrops of the Corinth Basin deposits. The canal is 79 metres high in its central part, 5.8 km long and has a base width at sea level of approximately 25 metres.

The purpose of the study is to integrate traditional field work with digital outcrop interpretation techniques (LiDAR) in order to generate a detailed sedimentary sequence stratigraphic analysis of the sections exposed along the walls of the Corinth Canal. The canals deposits, which are deposited in an active offshore rift, makes it an excellent analogue for syn-rift intra-rift high deposits. No one has previously focused on the stratigraphic sequences in the lower packages of the canal. With improved data, such as LiDAR, it is now possible to get a much closer look, and in much greater detail, at the inaccessible and lower parts of the canal, and therefore get a much more precise determination of the stratigraphy. The results of the sedimentology and stratigraphy will be combined to determine the different sedimentary environments developed along the canal throughout its tectonic evolution and generate a tectono-stratigraphic evolution of the Corinth Canal deposits.

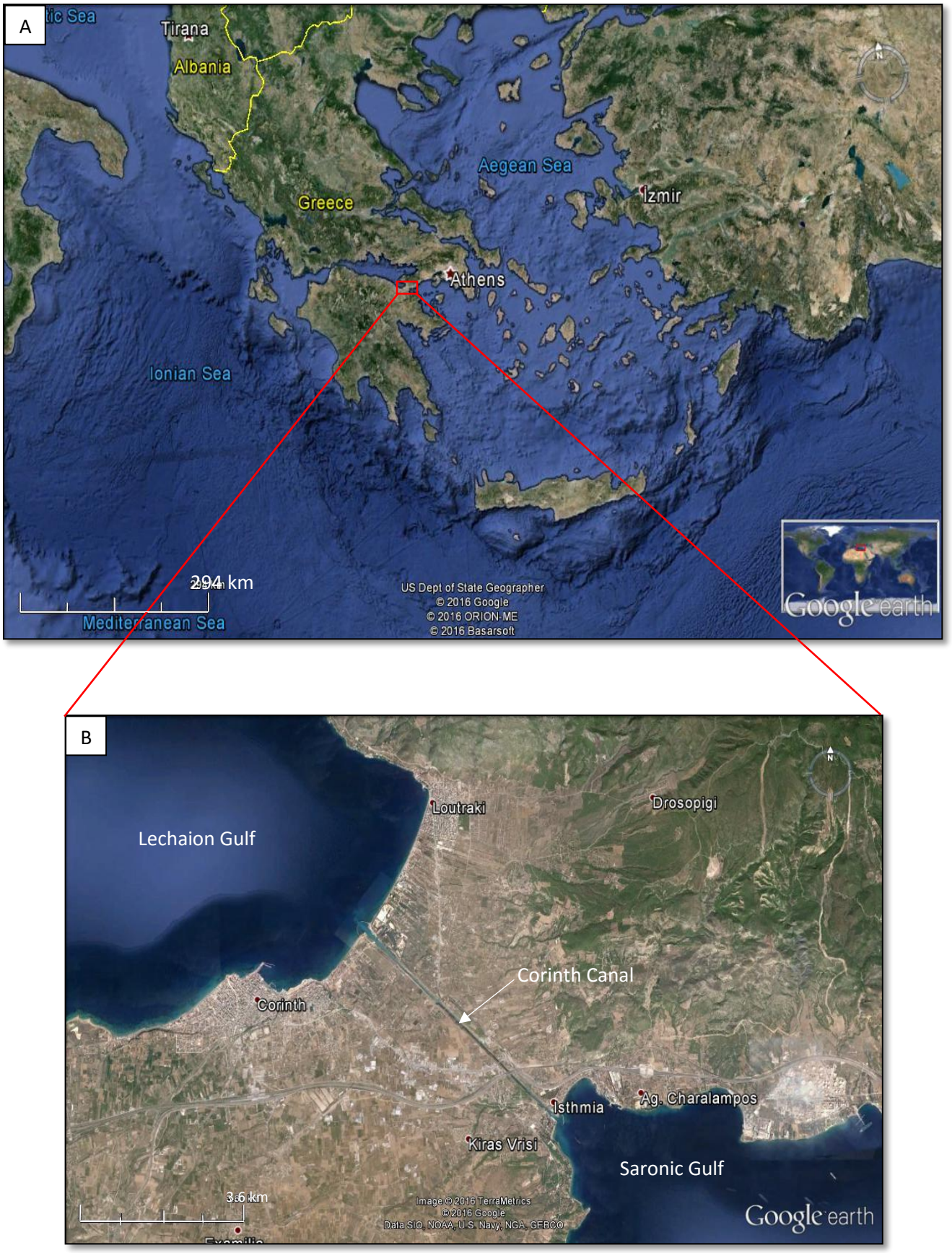

Fig. 1.1: Location maps. (A) Map of Greece and the Mediterranean region. The Corinth Isthmus is indicated with a red square. (B) Map of the Corinth Isthmus. The Corinth Canal links the Lechaion Gulf with the Saronic Gulf. Satellite images obtained from Google Earth.

1.2 Aim and Objectives

The aim of the thesis is to study the sedimentology and sequence stratigraphy of the Corinth Canal in order to develop a Tectono-Sedimentary evolution of the Corinth Canal deposits.

The specific objectives of the thesis are as follows:

I. Field-based facies analysis of the Corinth Canal
II. Characterize key stratal surfaces through field-based sequence-stratigraphic analysis of the Corinth Canal exposures
III. Fully 3D analysis of rock body geometries and syn-rift stratal architecture through digital outcrop modelling techniques (LiDAR)
IV. Paleoenvironmental analysis of the sedimentary units at the Corinth Canal and development of Tectono-Sedimentary evolution model

1.3 Previous Work

The structure and stratigraphy of the exposures found along the Corinth Canal were originally delineated in a regional geology study of the Corinth Isthmus by von Freyberg (1973). Freyberg (1973) separated the Corinth Canal outcrops into the Kalamaki Strata of Pleistocene age, which consists of two marine to freshwater cycles. This strata were overlain by the lower and upper Hauptkonglomerat with a relative sea level fall separating the Kalamaki strata from the Hauptkonglomerat. The lower and upper Hauptkonglomerat were also separated by a relative sea level fall. The uppermost sequence in the Corinth Canal were named the Gelbsandhorizont. He postulated sediment transport from east and deposition of sediments as a result of eustatic variations in sea level.

However, the sedimentology and stratigraphy received renewed attention after Collier (1988, 1990) studied the outcrops. He changed the stratigraphic boundary, environmental, and paleogeographical interpretations. Collier (1988, 1990) separated the outcrops on the Canal walls into the Corinth Marl (Freyberg's Kalamaki Strata), the 1st sub-sequence (Freyberg`s Lower Hauptkonglomerat), 2nd sub-sequence (Freyberg's Upper Hauptkonglomerat), and 3rd sub-sequence (Freyberg's Gelbsandhorizont), including a 4th and 5th sub-sequences above the existing strata interpreted by Freyberg. The earlier Kalamaki Strata were interpreted again as

the Corinth Marls, featuring a freshwater-to-marine transition. The Corinth Marls were then capped unconformably by the aforementioned sub-sequences, with subaerial exposure of the Corinth Marls before deposition of the 1st sub-sequence. Each sub-sequence was interpreted as a transgressive unit consisting of beach-to-shoreface facies, with each sub-sequence separated by an erosive or alluvial surface.

The sedimentology and structure of the Corinth Basin has been presented in Richard Collier`s Ph.D. from 1988. He then used his Ph.D. as a base to create further publications about the geology in the northern, central and southern parts of the basin (Collier, 1990; Collier and Dart, 1991; Collier and Thompson, 1991; Collier et al., 1992).

The tectonic and geological setting of the regional tectonic plates and the Gulf of Corinth Rift, are thoroughly explored in several studies (McKenzie, 1970; McKenzie, 1978; Jackson et al., 1982; Rohais et al., 2007; Bell, 2008; Ford et al., 2013).

1.4 Outline

After a brief introduction in chapter 1, chapter 2 presents the geological and tectonic setting of central Greece and the Gulf of Corinth Rift, along with the tectonic and stratigraphic history of the Corinth Basin. The 3rd chapter finishes the introductory part with the methods used to complete this thesis. The 4th chapter presents an introduction to the sedimentological field work and then presents descriptions and interpretations of the different facies and Facies Associations found in the Corinth Canal, with two simple depositional models. Chapter 5 starts with an introduction of the stratigraphic work done during the field work, before it continues with descriptions of the surfaces characteristic, the surfaces geometry and variability, and the Tectono-Stratigraphic Units interpreted in the Canal. In Chapter 6 the results from the 4th and 5th chapter are discussed in regards to Tectono-Stratigraphic evolution of the Canal outcrops, correlation with Glacio-Eustatic Sea Level Curves, local tectonism and relative sea level, and correlation of the deposits into close by offshore basins. The thesis is concluded by the summary and conclusion presented in Chapter 7.

2. Geological Framework

2. 1 Introduction

The study area is located on the Corinth Canal, at the Corinth Isthmus approximately 80 km west of Athens. The canal is located in the Corinth Basin, which is a sub-basin of the Gulf of Corinth Basin system (Collier, 1990; Collier and Dart, 1991) The Corinth Basin follows the same ESE-WNW trend as the Gulf of Corinth Basin (Collier, 1990; Collier and Dart, 1991). The Corinth Basin lies in a seismically active region, with faulted margin boundaries towards both north and south, defining a large-scale half-graben configuration for the Gulf of Corinth (Jackson et al., 1982; Collier, 1990; Collier and Dart, 1991).

2.2 Regional Geology and Tectonic Setting

The Gulf of Corinth Basin lies on the Aegean plate, which is controlled by the movement of three plate boundaries: The African, the Eurasian and the Arabian plates, with collision between the Eurasian plate and the African and Arabian plates (McKenzie, 1970; Jackson et al., 1982). Plate movement recordings for the last 3 million years show that the Arabian plate moves with a speed between 18-25 mm/year at N21-25^{o}, while the African plate moves at 5-6 mm/year toward north. (DeMets et al., 1990; McClusky et al., 2000).

The interaction between the African plate and the southward motion of the Aegean plate results in the NE to N-directed Hellenic subduction zone, where the African plate is subducted underneath the Aegean plate (fig. 2.1) (McKenzie, 1972; Le Pichon and Angelier, 1979; Le Pichon et al., 1981). Associated crustal thickening and thinning processes are due to the Hellenide Orogeny and the back-arc extension originated in the Oligocene (Le Pichon and Angelier, 1979; Le Pichon et al., 1981; Ford et al., 2013).

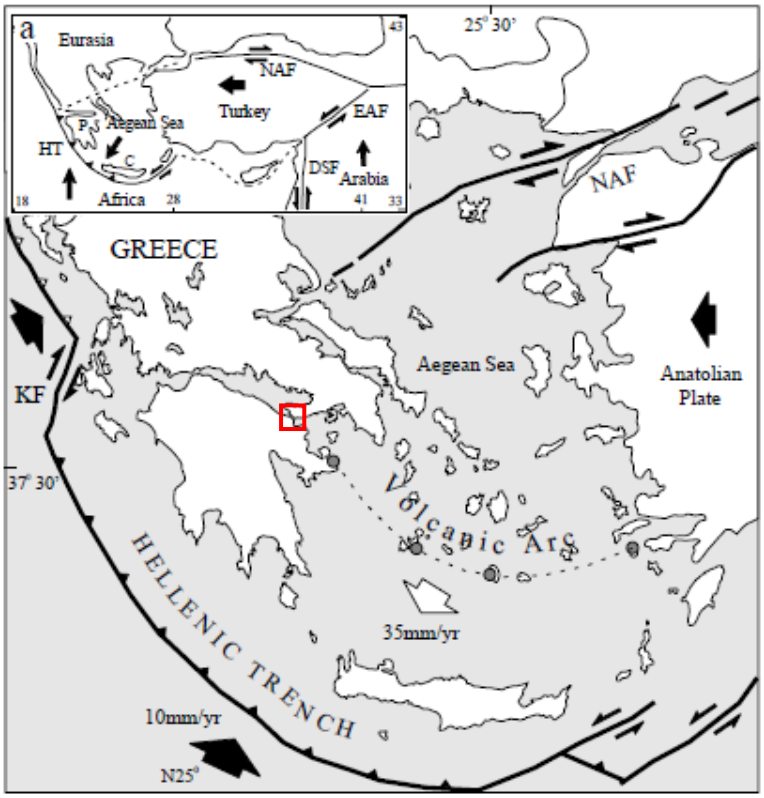

Fig. 2.1: Map showing the main structural features of the Hellenic Trench and the Aegean plate. The study area of the Corinth Canal is indicated with a red square. KF = Kefallonia Fault, NAF = North Anatolian Fault, EAF = East Anatolian Fault, DSF = Dead Sea Fault, HT = Hellenic Trench, P = Peloponnese. From Doutsos & Kokkalas (2001). Motion vectors of the African and Aegean plates from Kahle *et al*. (1998).

Extension in the Aegean basin started in middle or late Miocene (2.12 – 15 Ma), with a peak in the lower Pliocene, and has created numerous extensional systems with a NW-trend in central Greece (Jackson et al., 1982; Armijo et al., 1996; Rohais et al., 2007). The origin of the extension in central Greece is interpreted as a combination, or by one of the following processes:

1. The back-arc extension caused by the African Plate being subducted at the Hellenic Trench (fig. 2.1) (McKenzie, 1972; McKenzie, 1978; Doutsos et al., 1988; Bell et al., 2009).
2. The influence of westward propagating faults with motion transfer from the North Anatolian Plate to Central Greece (fig. 2.1) (Dewey and Sengor, 1979; Armijo et al., 1996; Armijo et al., 1999; Bell et al., 2009).
3. Gravitational collapse of the thickened crust resulting from the Hellenide Orogeny (Jolivet, 2001; Le Pourhiet et al., 2003; Bell et al., 2009).

2.3 The Corinth Rift

The Gulf of Corinth Basin lies within the Corinth Rift, which is one of the most active rifts in the back-arc extension of the Aegean plate (fig. 2.2) (Ford et al., 2013). The Corinth Rift started its rifting process in late Miocene to early Pliocene, about 5 Ma, and is presently the most seismically active zone in Europe, with an extension rate of up to 1.5 cm/year (Collier, 1990; Armijo et al., 1999; Briole et al., 2000; Rohais et al., 2007). The Corinth Rift is a NW-trending rift system undergoing N-S extension, with an associated fault dip of 45^{o}NNE on the southern margin (McKenzie, 1972; Jackson et al., 1982; Doutsos and Piper, 1990). The Rift system is approximately 100 km long, consisting of several faults with segments that reach up to 20 km in length (Roberts and Jackson, 1991). The large-scale geometry of the Corinth Rift is that of an half-graben bounded by large normal faults and a series of en-echelon N-dipping faults on the southern margin (Brooks and Ferentinos, 1984; Armijo et al., 1996).

The onshore syn-rift deposits of the Corinth rift consist of 3 groups: Lower, Middle and Upper groups (Ford et al., 2013). The Lower Group (5-1.8 Ma) consists of fluvial-lacustrine deposits, the Middle Group (1.8/1.5-0.7 Ma) consists of coarse-grained conglomeratic Gilbert-type fan deltas in alternating marine and lacustrine conditions, and the Upper Group (0.7/0.5-Present) consists of sandy to conglomeratic Gilbert-type deltas, with marine terraces and limestone notches deposited in alternating marine and lacustrine conditions (Rohais et al., 2007; Ford et al., 2013). The offshore sediments found in the Gulf of Corinth are divided into 2 units: Unit A and Unit B (Ford et al., 2013). These are laterally equivalents to the onshore syn-rift deposits of the Middle and Upper groups (Ford et al., 2013). Unit A is equivalent to the Gilbert-type deltas of the Upper Group, which are building offshore into the Gulf of Corinth, and Unit B consists of fine-grained facies which would correspond to the Gilbert-type deltas of the Middle Group (Ford et al., 2013). The lower Seismic Unit, dated at 2.1-1.5 Ma to 620 000 years old consists of lacustrine deposits, while the upper Seismic Unit, dated at 620 000 years old to present, consists of interbedded marine and lacustrine deposits (Nixon et al., 2016). The bounding surface in between, termed Horizon “U”, is a major basin-wide unconformity where the deposits change from purely lacustrine to interbedded marine and lacustrine deposits (Nixon et al., 2016).

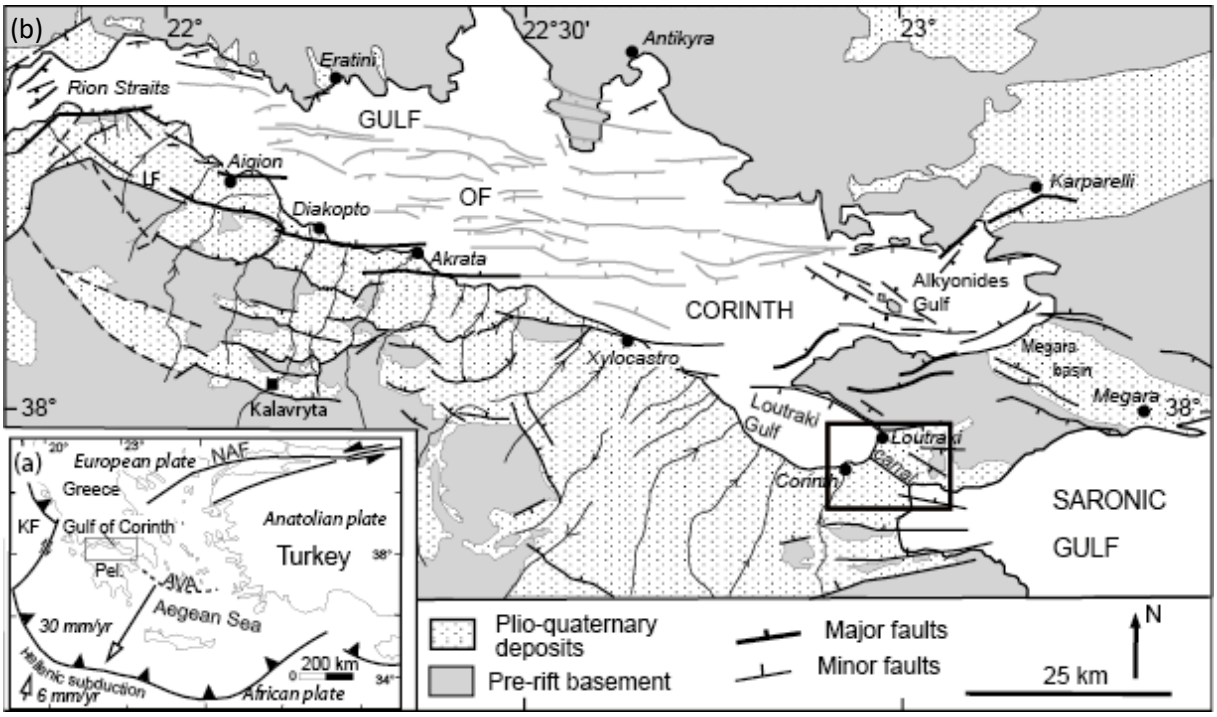

Fig. 2.2: (a) Tectonic map of the Aegean region. NAF = North Anatolian Fault, KF = Kefalonia Fault, Pel. = Peloponnese, AVA = Aegean Volcanic Arc. (b) Tectonic map of the Corinth Rift with faults and onshore stratigraphy. The Corinth Basin and the Corinth Canal study area is indicated with a rectangle (From Ford *et al*. 2013).

2.4 Chronology and Stratigraphy of the Corinth Basin

The sedimentary fill in the Corinth Basin is interpreted to overlie the basement rocks of the Pindus Nappe Mesozoic limestones and the Mesozoic carbonates and Tertiary flysch of the Gavrovo-Tripolitsa series, as it does in other parts of the Gulf of Corinth. (Collier and Dart, 1991; Flotté et al., 2005). The Basin fill stratigraphy is divided into two areas: The Northern Basin and the Southern Basin (Collier, 1988; Collier, 1990; Collier and Dart, 1991; Collier and Thompson, 1991).

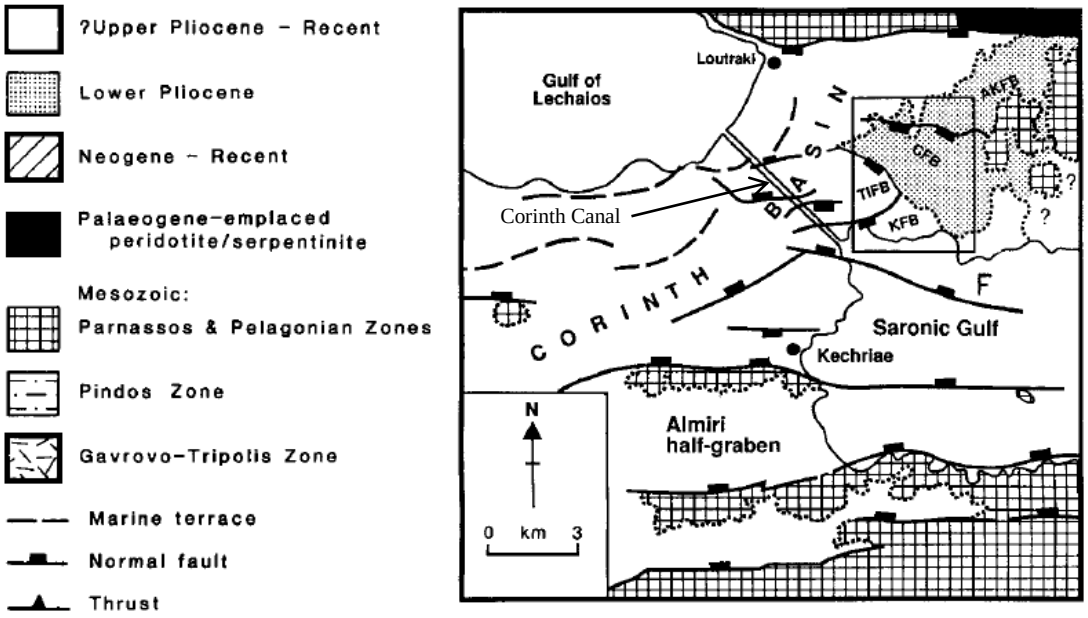

Fig. 2.3: Map indicating the major structural and stratigraphic features of the Corinth Basin. The Northern Basin includes the Corinth Canal and the region to the north while the Southern Basin comprises the area south of the Corinth Canal. AKFB = Asprakhomata-Kalamona Fault Block, CFB = Charalampos Fault Block, TIFB = Trapeza-Isthmos Fault Block, KFB = Kalamaki Fault Block. The rectangle in the square indicates the study area used by Collier & Dart to interpret the sedimentology and stratigraphy in the Northern Basin (From Collier & Dart, 1991).

2.4.1 The Northern Basin

The Northern Basin consists of The Lower Pliocene Group which crops out in the Asprakhomata-Kalamona- and Charalampos fault blocks, the Upper Pleistocene deposits of the Trapeza-Isthmus Group, and a Holocene fan-delta which is exposed in the Kalamaki fault block (Collier, 1988; Collier and Dart, 1991). The Lower Pliocene deposits found in the Asprakhomata-Kalamona fault block are interpreted to be the oldest sediments exposed in the Corinth Basin (Collier, 1988).

The Lower Pliocene Group are syn-rift deposits, characterised by syn-depositional faulting (Collier, 1988; Collier and Dart, 1991). The more than 800 m thick Lower Pliocene Group consists of the Charalampos Marl Formation, the Charalampos Conglomerate Formation, White Marl Formation, Kitrinovuni Sand Formation , Koudounistra Conglomerate Formation, Drosia Conglomerate Formation, and is capped by andesites with an age of 3.5 – 4.5 million years (Collier, 1988; Collier and Dart, 1991).

The central part of the basin consists of the Trapeza-Isthmos Group, exposed in the Trapeza-Isthmos Fault Block (Collier and Dart, 1991). They are seen westward in the Upper Pleistocene deposits of the Corinth Canal (Collier and Dart, 1991). The Corinth Canal is interpreted to have a structure which consists of a central horst and subsequent fault blocks toward both NW and SE, including development of a Graben in SE (fig. 2.4).

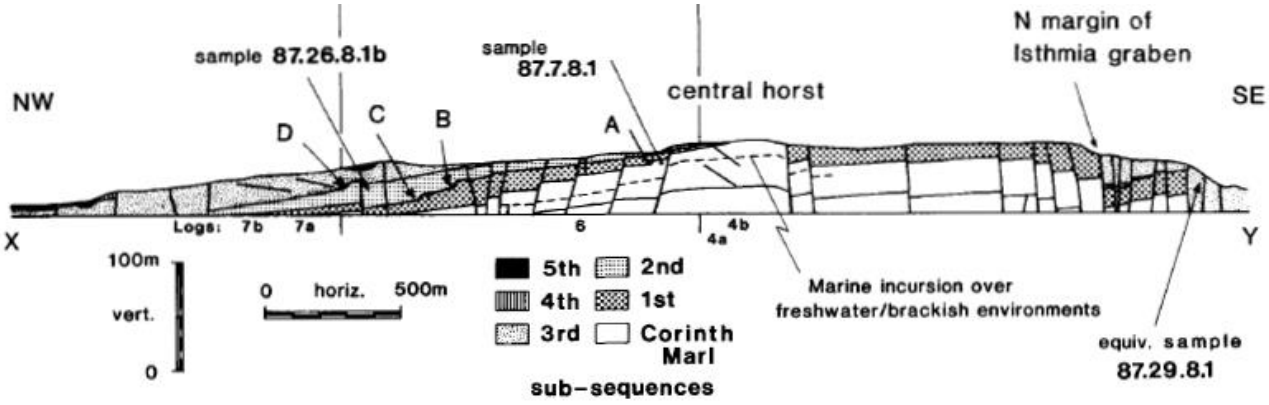

Fig. 2.4: Cross-section of the Corinth Canal. A-D marks the location of paleo cliffs (From Collier, 1990).

The outcrops exposed in the Canal have been have been interpreted by Collier (1990) to consist of the Corinth Marls capped unconformably by 5 sub-sequences (fig. 2.4). The Corinth Marls consist of marl deposited in a lacustrine to marine environment, marked by a marine incursion in the upper part of the central horst (fig.2.4) (Collier, 1990). The sub-sequences consist of a series of marine transgressive cycles, each of which is made of beach/foreshore conglomerates which fine upwards into shoreface sandstones (Collier, 1990). The 4th and 5th sub-sequences also features soil profiles, alluvium soils and fluvial bearing sands indicating fluctuations in sea level within the two sub-sequences (Collier, 1990). The 4th and 5th sub-sequences are only located in a few small areas of the canal, with the Corinth Marls and the 1st, 2nd, and 3rd sub-sequence dominating the canal outcrops (fig. 2.4). The Canal features 4 paleo cliffs created between some of the sub-sequences due to a relative fall in sea level. The sea level fall have allowed waves to re-work the sediments below creating paleo cliffs A-D (Collier, 1990).

Age determinations on the Isthmus have been performed by Vita-Finzi and King (1985), Collier (1990), and Dia et al. (1997). Vita-Finzi and King (1985) determined by ^{14}C technique the age of *Pinna fragilis* and *Crassostrea* sp. bivalves found the NW and SE margins of the canal from 35 to 38 000 years old. The two bivalves from the Vita-Finzi & King study are taken from the same stratigraphic package (Collier`s 3rd sub-sequence) as the corals dated at c. 205 000 years old by Collier (1990) and 193 000 and 212 000 years old by Dia et al. (1997).

Collier (1990) on the other hand, dated corals found in three locations by $^{230T}Th/^{234}U$. The corals were sampled from the marine marls and the upper parts of the 2nd and 3rd sub-sequences (samples 87.7.8.1, 87.26.8.1b, and 87.29.8.1, respectively in Collier (1990)) (fig 2.4). The dates obtained were older than 350 000 years for the Corinth Marl, ca. 312 000 years old for the 2nd subsequence, and ca. 205 000 years old for the 3rd subsequence. Dia et al. (1997) also used the $^{230}Th/^{234}U$-dating method on corals found near the canal. Their results are similar to Collier (1990) ages: two samples older than 350 000 years in the Corinth Marl, a sample determined at 306 000 years in the 2nd subsequence and two samples in the 3rd subsequence near the Isthmia Graben, at 193 000 and 212 000 years.

The Kalamaki fault block features a Holocene fan-delta that stretches from the S-dipping fault separating the Trapeza-Isthmus- and Kalamaki fault blocks to the coastline of the Saronic Gulf (Collier and Dart, 1991).

2.4.2 The Southern Basin

The Southern Basin contains marine deposits spanning from beach to shelf environment (Collier, 1988). Time equivalent deposits to the ones found in the Corinth Canal (Upper Pleistocene) include carbonate shelf and shoal environment facies (Collier and Thompson, 1991). The sediments were transported from the Aegean sea in the north, through a seaway created by a narrow structural trough at the now developed Isthmia Graben (Collier, 1988; Collier and Thompson, 1991). The area is dominated by tidally reworked oolitic calcareous sandstones in large transverse and linear dunes, with only minor coarser clastic sediments as observed in the northern/central basin (Collier, 1988; Collier and Thompson, 1991). After a sea level fall, the Southern Basin became dominated by alluvial deposition (Collier, 1988).

2.5 Tectonic setting of the Corinth Basin

2.5.1 The Northern Basin

The Northern Basin consists of 4 fault blocks: the Asprakhomata-Kalamona- (AKFB), the Charalampos- (CFB), the Trapeza-Isthmos- (TIFB) and the Kalamaki Fault Blocks (KFB) (fig.2.5) (Collier and Dart, 1991). Each of the fault blocks are bounded by southerly dipping faults with a throw of more than 300 m (Collier and Dart, 1991). The extensional faults which cuts through the Northern Basin features characteristics such as listric, planar and curved normal faults with both N- and S-dip (Collier and Dart, 1991). The faults generally have a dip up to 65^{o} and the structures may be up to 500 meter (Collier and Dart, 1991). Most of the structures seen in the Lower Pliocene sediments are post-depositional, but there are signs of normal faulting which are deemed syn-depositional such as a rollover anticline (fig. 2.5), angular unconformities between different members, and sedimentary dykes within the Drosia Conglomerate Formation (Collier and Dart, 1991).

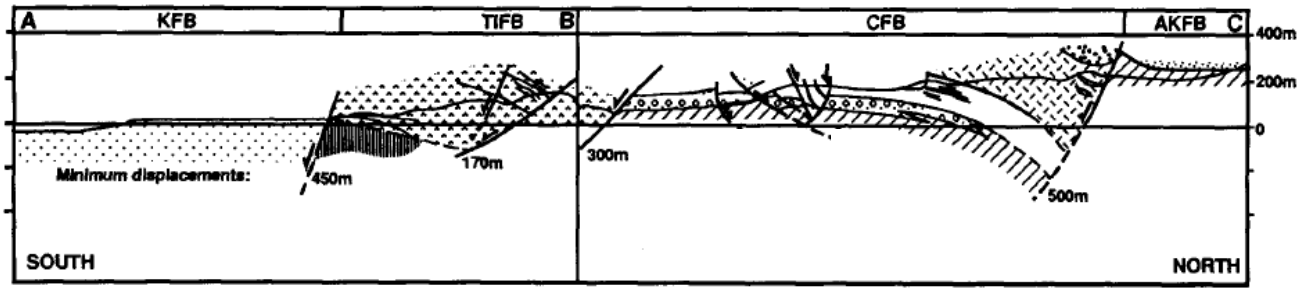

Fig. 2.5: A cross-section of the northern Corinth Basin. KFB = Kalamaki Fault Block, TIFB = Trapeza-Isthmos Fault Block, CFB = Charalampos Fault Block, AKFB = Asprakhomata-Kalamona Fault Block (From Collier & Dart, 1991)

There are evidences of fault block rotation during the deposition of the Corinth Marls and during the formation of the unconformity between the Corinth Marls and the 1st sub-sequence (Collier, 1990). The Corinth Canal is divided up into a central horst, with a series of fault blocks towards NW and SE (fig.2.4) (Collier, 1990). Block faulting during Upper Pliocene-Pleistocene controlled the deposition of the Trapeza-Isthmos Group (Collier and Dart, 1991). Syn-sedimentary faulting also created the Isthmia Graben, which is found in the SE-part of the canal (fig. 2.4) (Collier, 1990). Normal fault growth is the main control over the deposition of the 3rd subsequence in the Isthmia Graben (Collier, 1988).

The Lower Pliocene Group of the Kalamaki Fault Block has been submerged with only a Holocene fan-delta extending through the fault block (Collier and Dart, 1991). The fan-delta

was deposited due to fault-controlled subsidence of the fault block during Late Pleistocene (Collier and Dart, 1991).

2.5.2 The Southern Basin

The accumulation of the southern basin deposits from the Aegean Sea were possible through a fault-bounded seaway in the now known Isthmia Graben (Collier, 1988; Collier and Thompson, 1991). At this time the western part of the Saronic Gulf was subaerial, which made the creation of a trough through Isthmia possible (Collier, 1988). The sediments where then routed by a syn-sedimentary topography created by a normal fault scarp in the southern part of the basin (Collier, 1988). This topography lead the sediments towards NW after passing southwards trough the Isthmia seaway (Collier, 1988; Collier and Thompson, 1991). Other facies in the basin also show deposition with respect to topographic normal faults, which indicates that these are pre-existing faults (Collier, 1988). The alluvial deposits in the upper part were controlled by syn-sedimentary tilt block faulting (Collier, 1988).

2.5.3 Uplift rates on the Corinth Basin

There are several events indicating uplift of the Corinth Basin. Uplift of the northern basin area is most likely the reason for absence of Early and Upper Pleistocene sediments in the two northernmost fault blocks (Collier and Dart, 1991). Uplifted marine terraces in the Charalampos Valley show sign of uplift rates of 0.4 – 0.8 m/1000 yr in the northernmost fault blocks (Collier and Dart, 1991).

Uplift is also evident in the Upper Pleistocene marine sediments of the Corinth Isthmus, reaching almost 100 metres above the maximum sea level experienced in the Quaternary (Collier, 1990; Collier et al., 1992). Dating of canal deposits show that the Isthmus have a minimal uplift of 0.3 m/1000 year over the last 205 000 years (Collier, 1990; Collier et al., 1992). The main driving cause for this uplift is yet unknown, since the basin does not appear to be in a footwall position, and the nearest active fault with footwall uplift is too distant (Collier, 1990). However, White et al. (1987) interpreted the uplift to result from the isostatic response to accretion of igneous material. Another theory is that it is due to “underplating of the North Peloponnesian area by subducted sediment” (McKenzie, D.P., pers. comm. to Collier (1990)).

3. Methods

3.1 Field Work

The field work was conducted during two different seasons, from the 18th of March to the 4th of April 2015, and from the 24th of September to the 15th of October 2015.

Traditional field techniques were utilized to obtain sedimentological data from the Corinth Canal. These included detailed logging at centimetre scale, with particular emphasis in describing lithology, bedding, sedimentary structures, textures, bioturbation, fossils and boundaries. Samples of bivalves, gastropods and sediments were taken and brought to UiB for further investigation. Due to the steep nature of the Corinth Canal walls, detailed field observations and logging was restricted to the central horst and the fault blocks to the NW, as these were the only locations where direct access to the exposures was possible.

Sequence stratigraphic analysis in the field was performed by visual analysis of the facies stacking patterns and stratal terminations aided by the use of photo panels and a laser range finder that was later complemented with the analysis of LiDAR scans in the lab. Due to oblique-angled faults and fault blocks all the distances described in the further chapters are, unless otherwise mentioned, performed on the western margin of the horst.

3.2 Lab work

3.2.1 LiDAR

LiDAR (**Li**ght **D**etection **A**nd **R**anging) is a surveying method used to examine different aspects of the Earth's surface and atmosphere (NOAA, 2015). The LiDAR scanner normally consists of a laser scanner, high resolution digital photographic camera and a DGPS receiver (fig. 3.1) (NOAA, 2015). The use of LiDAR terrestrial scanning in this study is based on the geological interpretation of fully 3D digital outcrop models of the Corinth Canal in Virtual Reality Geological Studio software (VRGS; workflow developed in Hodgetts (2009) and Rarity et al. (2014)). The acquisition and processing of the LiDAR data was undertaken by Martin Muravchik and collaborators. The digital outcrop models thus obtained consist of high-resolution 3D meshes that were subsequently interpreted in VRGS. The interpretations consisted in digitizing the sedimentary surfaces (bedding, rock body boundaries, and unconformities) and deformational structures (fault planes) mapped in the field on the 3D meshes that integrate the digital outcrop model of the Corinth Canal. Analysis and interpretation

of the LiDAR datasets allowed for complementing the observations made in the field and obtain data from areas that were inaccessible in the Corinth Canal.

Fig. 3.1: Terrestrial LiDAR scanner (Riegl VZ-1000) used in the Corinth Canal. Photo taken by Martin Muravchik.

3.2.2 Digitalizing sedimentary logs and stratigraphic surfaces

The sedimentary logs were drafted at 1:20 scale and can be found in the appendix.

After the processing of the LiDAR-data, the main interpretations were carried out in Virtual Reality Geological Studios v1.0.0.1. VRGS allows the user to open the LiDAR data and study the outcrops in 3D view. It allows one to interpret and draw lines directly on the virtual outcrop. The software was used mainly for interpreting the stratigraphic surfaces. The stratigraphic interpretations were performed by identifying known and previously unknown markers, and then by creating polylines following the position of the stratigraphic surface on the virtual outcrop. Each polyline was a representation of a larger surface in a fault block, so each surface created in VRGS consisted of several smaller polylines.

The polylines were subsequently exported into a GIS (ArcGIS: ArcCatalog v. 10.3.1 and ArcMap v. 10.3.1) and interpolated into surfaces representing the different sedimentary unit boundaries that allowed for generation of isochoric maps for different stages of the evolution of the Corinth Canal.

4. Facies and Facies Associations

4.1 Introduction

The sedimentary strata cropping out in the Corinth Canal have been divided into 12 different facies based on; lithology/composition, sedimentary structure, texture, bioturbation, trace fossils and colour. The lithofacies descriptions and interpretations are presented in table 4.1. The lithofacies have then been further categorized into 7 different Facies Associations based on recurring associations of facies (Table 4.2).

.

Table 4.1: Lithofacies

Facies	Composition	Thickness (m)	Structures	Geometry	Texture and Other	Interpretation
F1 - Marl	Calcite, silica clay and silt.	0.6 – 2 m thick units	Weakly laminated to non-structured massive marl	Tabular bodies. Planar non-erosive lower boundary. Some beds exhibits undulating, erosive upper contacts	Some areas rich in fossils consisting of burrows and *Pecten* sp. Non-fissile.	Deposited in a low energy environment with deposition of silt and calcite, in an offshore marine setting (García-García et al., 2009). Calcite may be deposited through precipitation from water column, or calcite supplied from weathered limestones.
F2 - Siltstone	Silt	0.4 – 8 m thick units	Mostly bedded to massive with presence of wedge-shaped intercalation between grey and brown colouring. Horizontal bedding, tilted-inclined and slumped bedding.	Tabular to wedge-shaped bodies. Planar, non-erosive contacts. Areas with erosive, irregular upper surface.	*Viviparus* sp. in some silt beds. Darker coloured silt contain the largest amounts of the gastropod. Very thin beds of coarser grains with orange/dark brown colouring. Bioturbation present.	Deposited in a low energy environment allowing suspension and deposits of very fine grained material, typical for offshore facies in lacustrine (Campbell, 1971; Benson, 2016).
F3 – Sandstone	Very fine to fine sand	0.4 – 12 m thick units	Structureless massive to laminated strata	Tabular and lenticular, sheet-like bodies. Both irregular and planar upper surfaces with both erosive and non-erosive contacts.	Contain rare shells and granule clasts. Poorly lithified.	Deposited in a low energy environment below fair-weather wave-base, with deposition of fine grained sand. Shells indicate an offshore transition zone in either a lacustrine or marine setting (Campbell, 1971).

F4 - Mixed siliciclastic carbonate facies	Very fine to fine sandstone	0.2 – 5 m thick units	Massive sandstone.	Tabular small-scale to sheet-like shaped large-scale bodies. Sharp planar non-erosive lower boundary with no upper boundary experienced in the logged sections.	High abundance of bivalves, gastropods and corals. Some sections are highly cemented. Corals are also present in some areas	Deposited in a moderate to high energy environment where abundance of marine fauna indicate marine shoreface environment. High abundance of large bivalves indicate an upper shoreface environment with wave and current activity.
F5 - Poorly lithified sandstone	Very fine to fine sandstone	Up to 10 m thick units	Massive	Tabular bodies. No upper or lower boundary seen in logged section	Very poorly lithified sandstone with a large amount of small marine shells within. Abundance of glauconite. Presence of vertical orange lines	Low to moderate energy environment with scattered marine fauna indicating lower shoreface marine environment.
F6 – Cemented shells	Very fine sand	0.35 m thick unit	Massive	Lenticular body. Sharp, irregular, lower boundary and a more gradual change with lesser shells toward the top. Sharp, irregular, upper contact	Strongly lithified shells, with very small whole and fragmented shells.	Deposited in a high energy environment responsible for imbrication of shells. The marine fauna indicate a marine upper shoreface environment affected by strong currents.
F7 - Sandstone with cemented carbonate bands	Fine sandstone	0.2 – 5 m thick units	Sandstone intercalation with irregular carbonate bands. Areas of slumped facies. The sand has areas with trough cross-bedded	Lenticular bodies. Planar to irregular upper and lower boundaries	Semi-lithified sandstone. Different minerals present, with glauconite dominating. Pebble sized clasts are present in some areas.	Deposited in a moderate energy environment. Glauconite indicate marine environment, most likely shoreface deposition, with influence of calcite responsible for deposition of

			sediments			carbonate bands.
F8 - Planar parallel-stratified sandstone	Fine sandstone	0.05 – 0.2 m thick units with mm to 0.01 m bedding	Planar parallel-stratified sandstone.	Tabular and lenticular bodies. Planar to irregular sharp non-erosive lower and upper boundary.	Fine sand consisting of different minerals with glauconite quartz dominating	Deposited in upper or lower flow regime with a unidirectional current, with glauconite presence indicating marine shoreface environment (Clifton, 1971).
F9 - Planar cross-stratified sandstone	Fine to coarse sandstone.	0.05 – 0.25 thick units with bed thickness from mm to 0.02 m	Planar cross-stratified sandstone. Normal graded to ungraded. Coarse grained sand seen represents foreset laminae. Planar-crested 2D dunes. Low-to high-angled and curved cross-stratification with tangential/asymptotic and angular contacts.	Tabular and lenticular bodies. Both erosive and non-erosive irregular upper and lower boundaries.	Fine sand consisting of different minerals with glauconite and quartz dominating. Presence of granules.	Created by deposition and migration of 2D dunes by a unidirectional current in lower flow regime. Typical for unidirectional currents in a marine shoreface environment (Clifton, 1971).
F10 - Trough cross-stratified sandstone	Very fine to very coarse sandstone.	Each bed between 0.03 and 0.10 with each unit from 0.1 to 0.5 m	Non-parallel, amalgamated, curved, bundled up built sets of sandstone. Ungraded and normal graded sets with larger clasts in the lower part of the set. Sinuous-crested 3D dunes.	Lenticular bodies with concave up beds. Irregular upper and lower boundary.	Different minerals with glauconite and quartz dominating. Some granule sized clasts are present. Subrounded grains.	Created by deposition and migration of 3D dunes in the upper flow regime by a unidirectional current (Clifton, 1971). Glauconite indicate marine deposition in upper shoreface environment highly affected by currents.

F11 – Massive conglomerate	Granule to pebble conglomerate	0.03 – 0.10 m thick beds	Mainly massive, ungraded conglomerate. Inverse-normal grading is present.	Tabular and lenticular bodies. Often show sharp erosional lower boundary with irregular upper boundary	Polymict conglomerate with sub-rounded to rounded clasts. Fine sand matrix. Both matrix- or clast-supported conglomerate.	High energy environment with strong currents capable of transporting pebbles. Deposition in upper shoreface marine environment (Nemec and Steel, 1984)
F12 – Cross-stratified conglomerate	Granule to pebble conglomerate.	Ca. 0.2 m beds with units up to 16 m.	Planar to convex cross-stratified with normal to ungraded conglomerate. Mostly low-angled. Abundant amount of pebbles. Most clasts align according to cross-bedding, but also regularly appearance of vertically clasts. Both tangential and angular contacts toward lower boundary.	Tabular and wedge-shaped bodies. Often show a sharp erosional lower boundary.	Clast-supported, polymict orthoconglomerate with sub-rounded to rounded grains. Fine to medium sand matrix. Immature matrix due to high variation in minerals.	A high energy environment with a unidirectional current. Low-angle stratification indicate a beach/foreshore environment (Nemec and Steel, 1984).

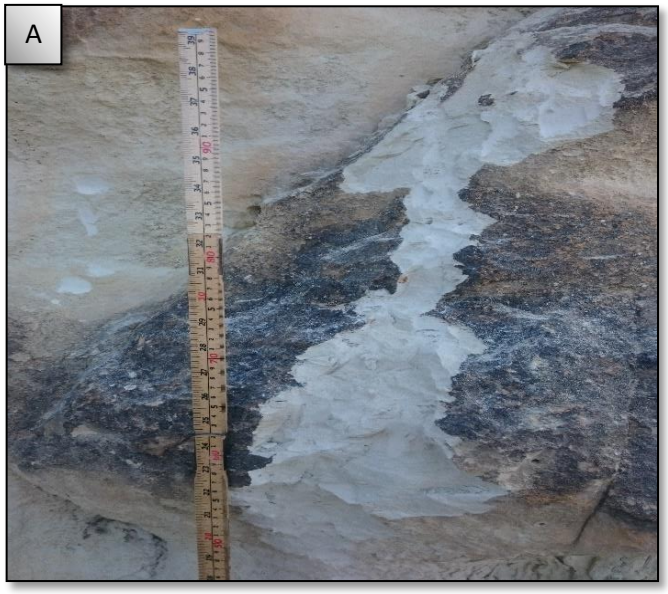
A

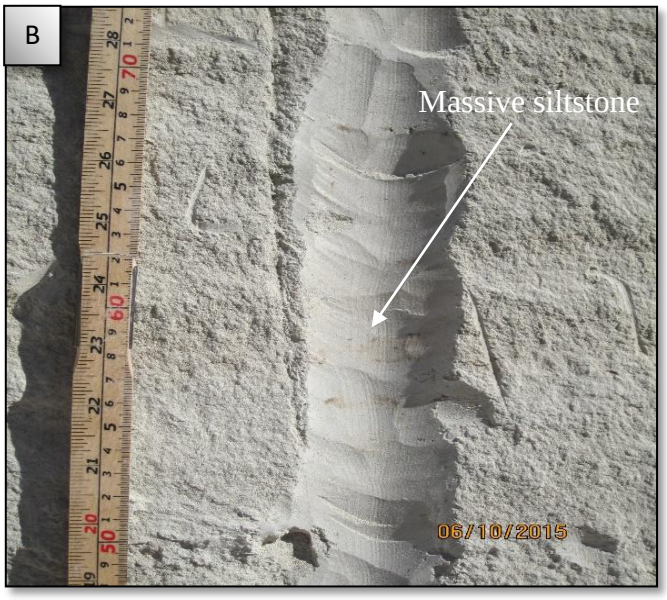
B
Massive siltstone
06/10/2015


C


D
28/03/2015

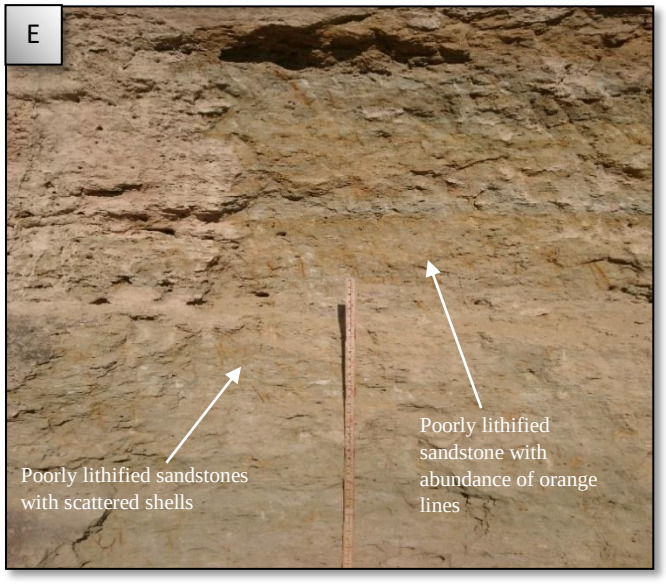
E
Poorly lithified sandstones with scattered shells
Poorly lithified sandstone with abundance of orange lines

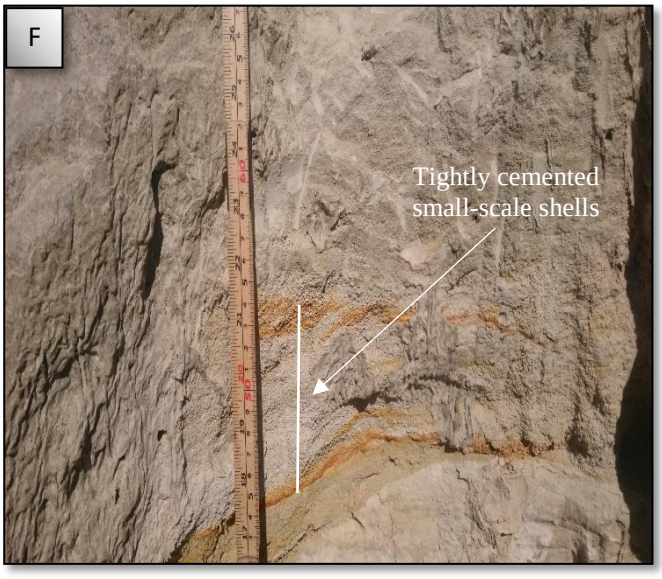
F
Tightly cemented small-scale shells

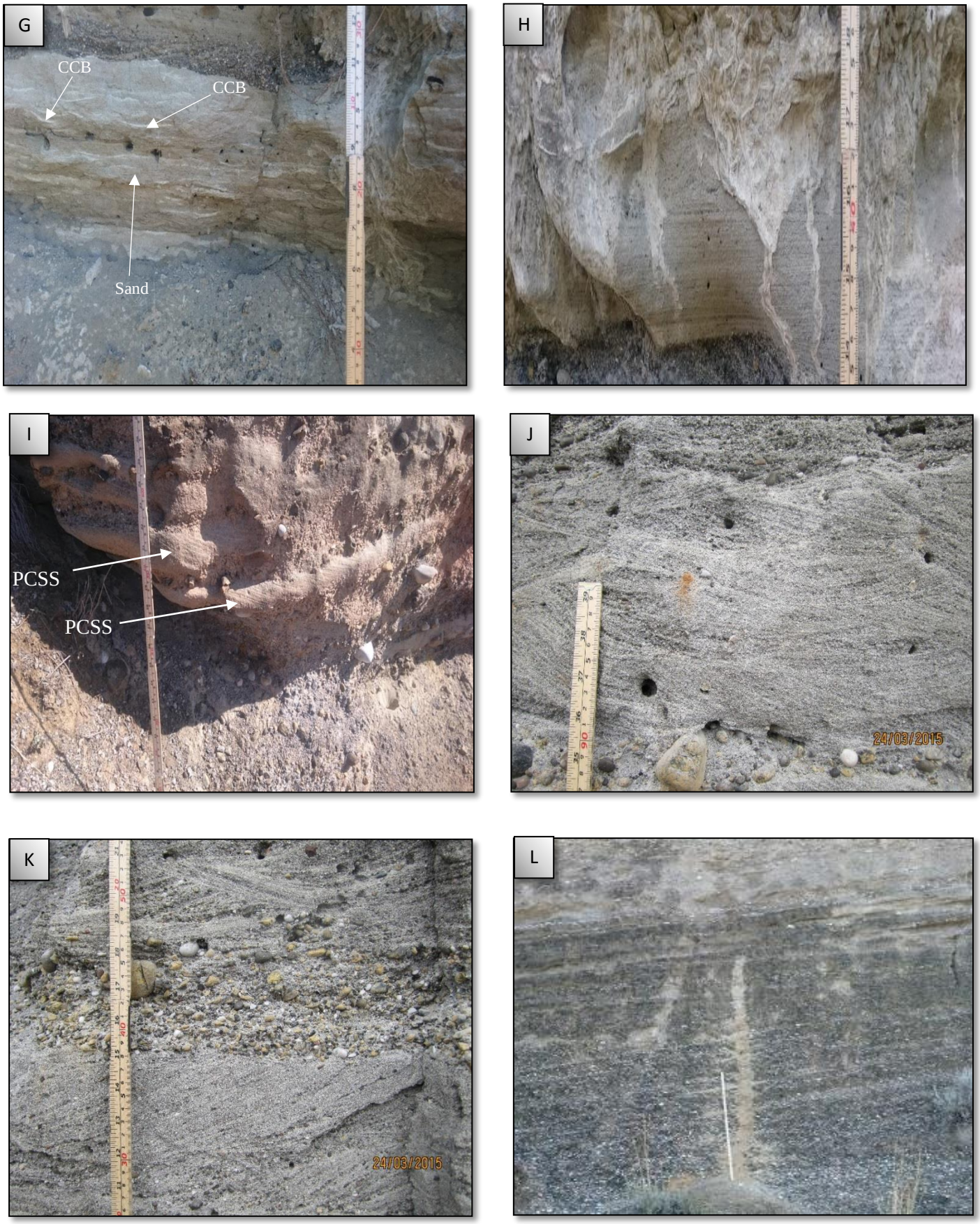

Fig. 4.1: (A) F1 - Marl (B) F2 - Siltstone (C) F3 - Sandstone (D) F4 - Mixed siliciclastic carbonate facies (E) F5 - Poorly lithified sandstone (F) F6 – Lithified shells (G) F7 - Sandstone with cemented carbonate bands (CCB) (H) F8 - Planar parallel-stratified sandstone (I) F9 - Planar cross-stratified sandstone (PCSS) (J) F10 - Trough cross-stratified sandstone (K) F11 - Conglomerate (L) F12 - Planar cross-stratified conglomerate

4.2 Facies Associations

Table 4.2: Facies Associations and their lithofacies

Facies Association	Environment	Depositional Environment	Lithofacies
FA1	Terrestrial	Lower Littoral to Upper Sublittoral lacustrine sandstones	F3
FA2		Lower Sublittoral to Upper Profundal lacustrine siltstones	F2, F3
FA3	Sub-aqueous	Foreshore/Beach conglomerates	F9, F12
FA4		Foreshore conglomerate spit deposits	F12
FA5		Shoreface sandstones	F3, F4, F5, F6, F7, F8, F9, F10, F11
FA6		Offshore-transition to offshore sandstone and siltstone	F2, F3
FA7		Offshore calcareous mudstone	F1, F4

4.2.1 Facies Association 1: Lower Littoral to Upper Sublittoral lacustrine sandstone

Description

Facies Association 1 is composed of light brown, very fine to fine sandstone, which consists of lithofacies F3 (Sandstone). The facies association stretches laterally further than 1300 m in NW-SE direction and at least 50-60 m in E-W direction. The thickness of packages may be up to 12 m thick and stretches laterally as a large tabular package.

The sediments in the Facies Association are mainly horizontally bedded with some areas showing massive very fine to fine sandstone. The sediments also show small fragmented shells determined as the gastropod *Viviparus* sp. (Collier, 1990). There are no signs of evaporation, or other major amounts of organic material within the Facies Association, indicating a clear dominance of siliciclastic material.

Interpretation

The presence of the gastropod *Viviparus* sp. indicate a freshwater environment (e.g. Benson, 2016) with deposits of *Viviparus* sp. located in several lacustrine deposits (Burch, 1989; Cavinato et al., 2000; Nury, 2000; Mandic et al., 2015). The fauna, in combination with no apparent structures on the deposited very fine to fine grained sandstone, indicate freshwater lacustrine deposits in a lower littoral to possibly upper sublittoral zone (Bohacs et al., 2000). The presence of freshwater biota and no organic content, in combination with a clear dominance of siliciclastic material, indicate deposition in a *Fluvial-Lacustrine* Facies Association, as suggested by Carroll and Bohacs (1999). This lacustrine basin type would get a regular input of freshwater and siliciclastic material, creating the dominance of siliciclastic deposits seen here, with no deep-water settlement with anoxic waters, no high grade of organic content, or any evaporite formation (Bohacs et al., 2000).

4.2.2 Facies Association 2: Lower Sublittoral to Upper Profundal lacustrine siltstone

Description:

Facies Association 2 is composed of light brown and light grey siltstone with beds of dark grey, very fine to fine sandstone and consists of F2 (Siltstone) and F3 (Sandstone). The Facies Association is approximately 15 m thick, with a lateral extension of at least 900 m in NW-SE direction and 50-60 m in E-W direction.

The siltstone, which dominates FA1, show both planar-laminated to wedge-shaped intercalation of light brown and light grey lamination, or it is more massive lacking lamination and with no apparent colour changes over several metres. The wedge-shaped intercalation is only present in a 2 m interval which feature beds of 2 cm to 10 cm thickness with sharp, planar boundaries. The massive siltstone could be up to 2 m thick without any discernible colour or textural changes. The boundaries between the massive packages of different colour show sharp and planar features. An entire siltstone package can be up to ca. 30 m thick without lithological changes. The horizontal lamination and massive sediments show no visible lateral constraints and extend extensively laterally and possibly along the entire length of the Facies Association. The siltstone feature sharp, planar boundaries towards two packages, one 20 cm and one 2 m thick, which consists of dark grey, very fine to fine sandstone interbedded with small packages of grey siltstone (fig. 4.2). Both the 20 cm and 2 m thick interbedded siltstone and sandstone package features a tabular, sheet-like body which stretch laterally at least 450 metres in NW-SE direction, and with an E-W extension of at least 50-60 metres without any visible constraints.

The siltstone and sandstones contain the small fragmented gastropod *Viviparus* sp. (fig 4.2) (Collier, 1990), with a considerable increase in the 20 cm and 2 m packages of interbedded, dark grey silt- and sandstone. The Facies Association does not exhibit any other pronounced fauna in its deposits and other fauna is hard to distinguish due to the fragmented feature of the gastropods. Bioturbation is also noticed amongst the fragmented *Viviparus* sp. and in areas of massive siltstone.

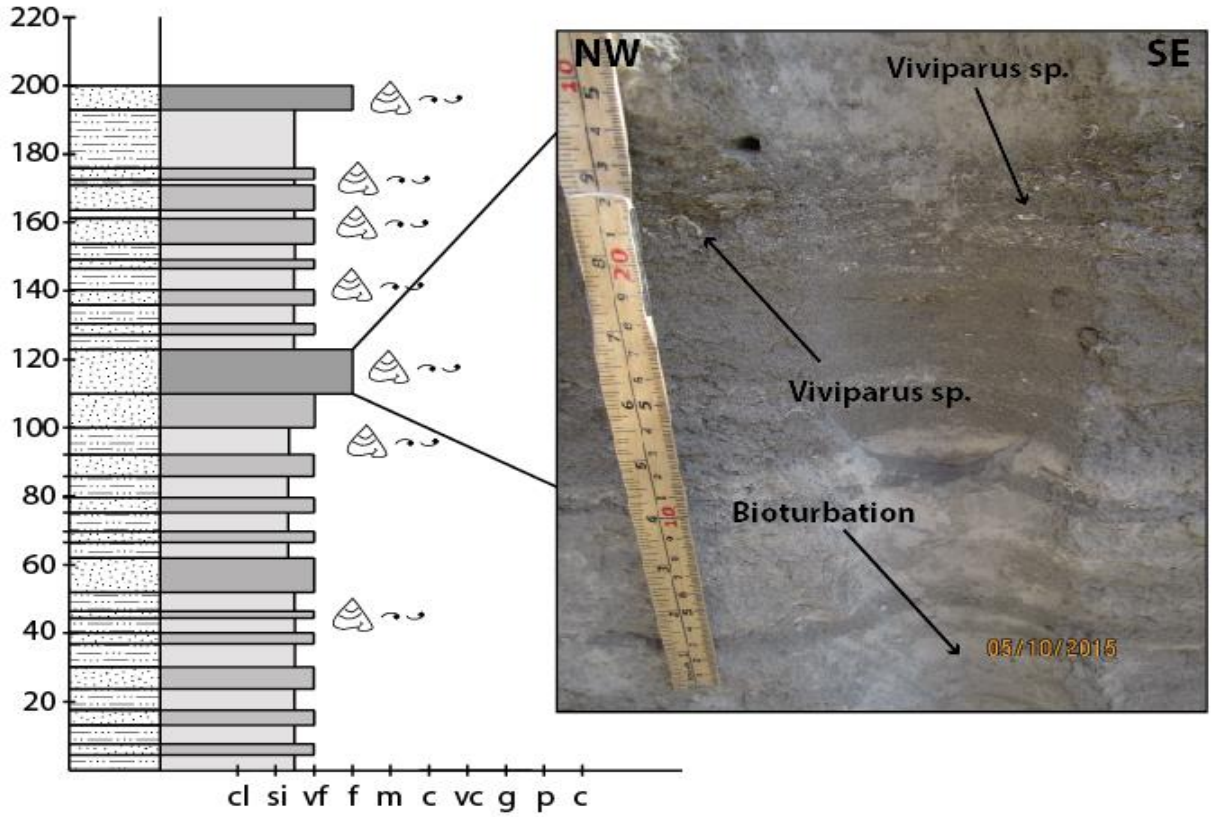

Fig. 4.2: Log section from the central horst, featuring lacustrine deposits with the influence of a subaqueous flow depositing a lot of fragmented Viviparus sp. The log is taken approximately 28 metres up on the horst. The log scale is in centimetres.

Interpretation:

The presence of *Viviparus sp.*, a fresh water mollusc inhabiting other lacustrine basins e.g. (Burch, 1989; Cavinato et al., 2000; Nury, 2000; Mandic et al., 2015), indicates a freshwater environment (Benson, 2016). The laminated to massive siltstone indicate deposition below the fair-weather and storm-weather wave-base, which together with the fauna suggest a deep-water, possibly lower sublittoral to upper profundal, in a freshwater lacustrine basinal setting, with accumulation of the finest grained sediments through suspension during highstand sea level (Olsen, 1990; Bohacs et al., 2000; Changsong et al., 2001). The interbedded 0.2 to 2 m packages of very fine to fine sandstone, could be deposited as a result of subaqueous flows in a lake basin, resulting in deposition of very fine to fine sandstone containing a lot of fragmented *Viviparus* sp. (fig. 4.2). The lack of evaporites and general low degree of organic matter, except for the small dark grey sandstone packages (fig.4.2), indicate deposition in a *Fluvial-Lacustrine* Facies Association e.g. Carroll and Bohacs (1999). The deposits indicate an hydrologically open lake with abundance of siliciclastic material and freshwater biota, such as *Viviparus* sp., with no evaporites and minimal organic content present (Carroll and Bohacs, 1999; Bohacs et al., 2000).

4.2.3 Facies Association 3: Foreshore/Beach conglomerate

Description:

Facies Association 3 is composed of inclined bedded conglomerates with small beds of planar-cross stratified sandstone, and consists of facies F9 (Planar cross-stratified sandstone) and F12 (Cross-stratified conglomerate). The thickness of the packages range from 1 to 12 m, and the Facies Association can extend laterally at least 1000 m in NW-SE direction, where there is a considerable thickness increase towards NW, and at least 50-60 metres in E-W direction, as it is found on both margins of the Canal.

The Facies Association features pebble to granule sized orthoconglomerate, where the clasts longest axis rarely exceeds 64 mm, with mature, subrounded to rounded, and discoidal to spherical clasts. The clasts are polymict with a large variance of lithologies, with red chert and serpentinite identified as some of the lithologies. The conglomeratic packages feature a low-angled inclined bedding with a 12-15^{o} dip (F12) towards N to NW (fig. 4.3). The individual sets of dipping conglomerate are ca 0.2 m thick, and clast-supported with imbricated conglomerate clasts. The individual conglomerate sets laterally extends up to 30 m in NW-SE direction. They are constrained either by the thickness of the Facies Association itself, or by the climbing form of conglomerate beds depositing above. The conglomerate feature both angular and tangential contacts towards the lower boundary of the Facies Association. Some clasts have their longest axis orientated vertically, although most clasts longest axes are aligned according to the overall low-angled inclination. The matrix in the conglomerate is immature fine to medium sand. The conglomerates are both ungraded and fining upwards. The uppermost part of the conglomerate often does not feature the same imbrication as the lowermost units, as the area seems to get more sand, and fewer clasts in some areas. The fining upwards units of conglomerates, transition into FA5 (shoreface sandstones).

Although most of the Facies Association is composed of N to NW inclined cross-stratified conglomerates, there are also areas with conglomeratic cross-stratification directed SE. These packages are ca. 2 m thick. These cross-bedded foresets show a higher angled cross-stratification, up to 50 degrees, than the NW-dipping conglomerate sets. The sharp, planar, upper and lower boundaries of the SE-directed cross-beds often show an NW-dipping inclination aligned with the NW-dipping conglomerates. In other exposures the NW-inclined conglomerate beds are interbedded with SE-directed planar cross-stratified sandstones (F9) (fig. 4.4). The sandstones are generally 10-20 cm thick and laterally extends for at least 3-4 m in NW-SE direction. The sandstones show sharp, irregular contacts with the NW-inclined

conglomerates and feature lenticular shaped bodies. The set laminae is high-angled, up to 45-60 degrees, and in some cases consists of small granules. The same sandstone packages interbedded with NW-dipping conglomerate are found directly across, on both margins of the canal, which indicates that the area depositing them has an E-W extension of at least 50-60 m.

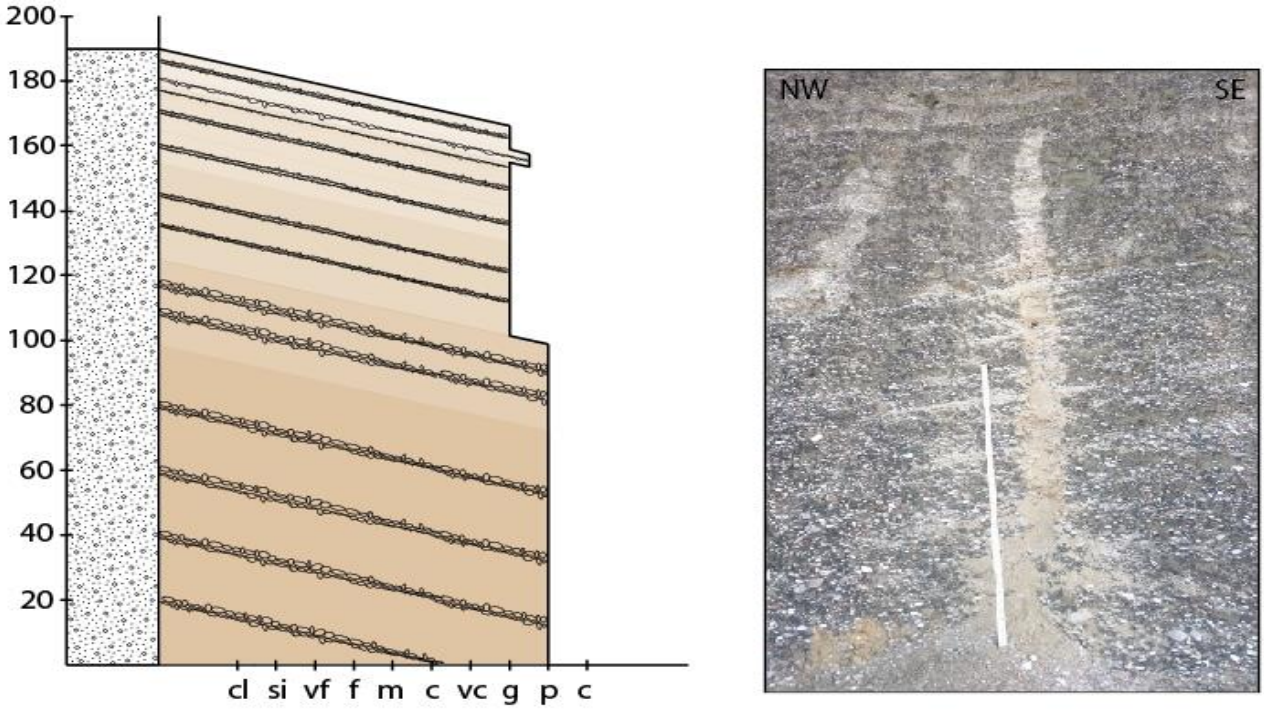

Fig. 4.3: Low-angled NW-dipping conglomerate packages featuring fining upwards strata of FA3. Measuring stick is 1 metre and the vertical scale on the log is in cm.

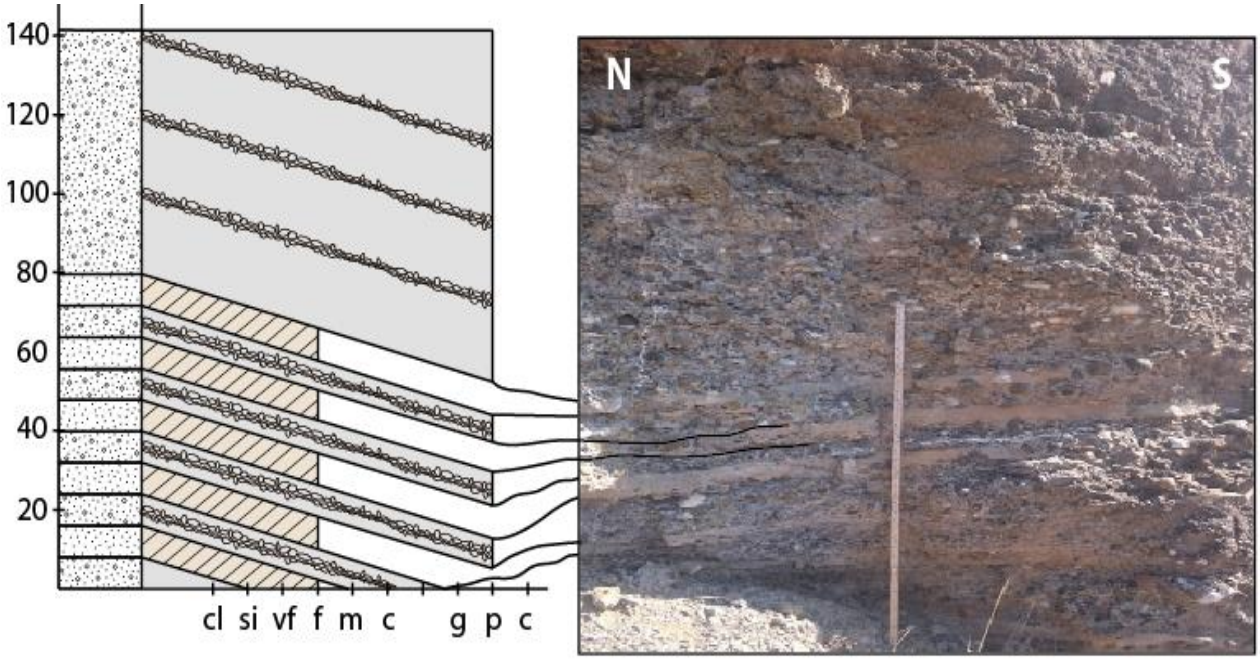

Fig. 4.4: FA 12 with low-angled NW-dipping conglomerate (F12) featuring SE-directed planar cross-bedded sandstone (F9), with a NW-dipping inclination in its lower part. Measuring stick is 1 metre and the vertical scale of the log is in centimetre.

Interpretation:

The low matrix content, the roundness and maturity of the clasts, and the low-angled inclined imbrication of the clasts indicates a high energy environment (Clifton et al., 1971; Clifton, 2006; Reading, 2009). These observations, especially the low-angled stratified conglomerate beds, in combination with a fining upwards character into shoreface sandstone, indicate a beachface/foreshore depositional environment (Campbell, 1971; Clifton et al., 1971; Nemec and Steel, 1984; Murakoshi and Masuda, 1992; Clifton, 2006). An increasing thickness of the Facies Association along with the NW-dipping strata, indicate progradational and aggradational packages of beach/foreshore conglomerate (Catuneanu, 2002).

The SE-migrating horizontal or inclined packages of clasts may indicate periods of current reversal, caused either by strong tidal currents or storm waves, or by minor fluctuations in base level creating a high energy landward directed current responsible for landward directed sediment deposition (Clifton, 2006; Reading, 2009). The same interpretation can be made about the high-angled landwards cross-bedded sandstone seen in-between the NW-dipping conglomerate in some areas (fig. 4.4), only these current reversals have deposited cross-bedded sand instead of cross-bedded conglomerate.

4.2.4 Facies Association 4: Foreshore conglomerate spit deposits

Description:

Facies Association 4 is composed of a package of cross-stratified conglomerates (F12). The Facies Association varies from 1 to 8 m in thickness and laterally extends for at least 155 m in NW-SE direction and at least for 50-60 m in E-W direction.

The Facies Association is comprised within a single unit consisting of inclined SE-dipping, convex to planar climbing sets of lateral accretion surfaces with an angular lower contact. The SE-directed foresets of this package is the only package in the area which features SE-dipping foresets, with the surrounding packages showing a NW-directed dip of their foresets (fig. 4.5). Each lateral accretion surface show a lateral extension which is up to 17 m, depending on its location in the package, as the package features a changing thickness. The entire Facies Association is comprised within a lenticular body, with sharp, irregular upper and erosive lower contacts with the surrounding sediments of FA3 (foreshore conglomerates) below and FA5 (shoreface sandstones) above (fig. 4.5).

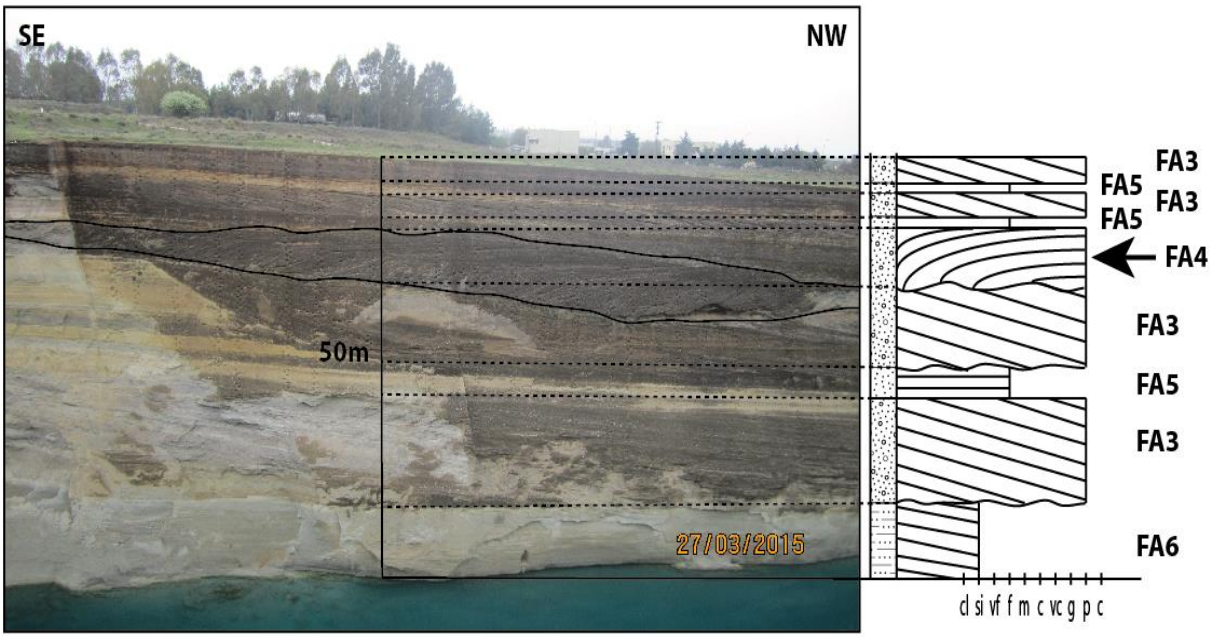

Fig. 4.5: The section featuring the SE-dipping lateral accretion surfaces comprised within the continuous black lines, with a sketch log of the area showing the vertical changes in deposits, with the arrow representing the described Facies Association, FA4.

Interpretation:

The deposition of SE-inclined lateral accretion surfaces, which are opposite of the general paleo-basinward stratification in the canal, indicate that these deposits where created by currents depositing strata in a paleo-landward direction. With the bounding strata consisting of FA3 (foreshore) and FA6 (shoreface) the deposits will most likely derive from a close by environment, and gravel foresets indicate a near-shore environment due to the amount of energy needed to transport the conglomerates (Nemec and Steel, 1984; Clifton, 2006). Deposition of sets dipping the opposite way of prograding foreshore conglomerates could have happened as a result of influence by oblique-angled waves, which creates a longshore current along the shoreline (Komar and Inman, 1970; Nicholls and Webber, 1987). These longshore currents could then result in the deposition of landward-directed foresets, and form a spit (Hiroki and Masuda, 2000). An environment such as this, with a spit and prograding foreshore conglomerates affecting each other, could be responsible for the vertical changes in landward and basinward foresets. Similar deposits of paleo-landward directed gravelly foresets are found in the Pleistocene Higashikanbe Gravel, central Japan, where the foresets are interpreted as a spit platform during a Transgressive Systems Tract (Hiroki and Masuda, 2000).

4.2.5 Facies Association 5: Shoreface sandstones

Description:

Facies Association 5 comprises different sections generally consisting of either very fine to fine sandstone packages with occasional reworked trough-cross bedded strata, or gastropod, bivalve, and coral packages in a mix of broken shells and sand (fig. 4.6), or packages with interbedded coarse to very coarse sandstone and conglomerates with planar- and trough cross-beds (fig 4.7). The Facies Association consists of lithofacies F4, F5, F6, F7, F8, F9, F10, and F11. The thickness of the individual packages could vary from 1 to 15 m. Individual packages could feature a lateral extension of up to 1000 metres in NW-SE direction, often with a marked increase in thickness towards NW, and a lateral extension of at least 50-60 m in an E-W direction.

The largest sections of the Facies Association are made up by F4, F5, and F7. Lithofacies F4 (mixed siliciclastic carbonate facies) feature with up to at least 5 m thick packages containing abundant, reworked bivalves and gastropods with laterally extensive bodies up to at least 50-60 m in E-W direction. Lateral extension along the canal, NW to SE, is difficult to determine precisely, but at least 100-200 m sections of the bivalves and gastropods are seen. Large bodies of F5 (Poorly lithified sandstone), featuring scattered gastropods and bivalves stretches laterally in NW-SE and E-W for at least 100 m in an up to ca. 10-15 m thick sediment body. Sections of F7 (sandstone with cemented carbonate bands) could stretch up to at least 5-6 m thickness with a variance in bed thickness between each carbonate band, from 5 to 60-70 cm. F7 also included slumped or deformed bodies of the sand to carbonate sediments and an occasional occurrence of pebbles. Sections of S7 were found in an area laterally extending 50-60 m in E-W direction and at least 20 m in NW-SE direction.

Other areas included a small, up to 0.35 m thick package of F6 (cemented shells), with sharp irregular contacts and a lenticular body, which is found located between sections of F7 and F10. It shows tightly cemented small-scale shells. 5-20 cm units of fine-grained sandstones of F8 (planar parallel-stratified sandstone) with bedding in mm scale, were found in between sections of F7, F9, F10 and F11. They feature both tabular and lenticular bodies with sharp irregular contacts to the surrounding sediments and show lateral extension in NW-SE direction of at least 10-20 metres. Areas of F10 (Trough cross-stratified sandstone) could feature in packages from 10 to 50 cm. The larger trough cross-bed packages normally consist of very fine to fine sand while the trough cross-beds featuring coarse to very coarse sand, often with small granules

making up the lower part of the bundled foresets, are generally thinner and are found in combination with F8, F9 and F11 (fig. 4.7).

The interbedded packages of coarse to very coarse sand and conglomerate packages of F8, F9, F10, and F11 (fig. 4.7), which are found directly below FA3 (foreshore conglomerates), show a lateral extent at least 50-60 m in E-W direction. The lateral extent in NW-SE direction is difficult to determine due to limited exposures of these sections.

Generally, the sand grains found in the different facies mentioned above are made up by several lithologies, with glauconite in high abundance. The grains are immature and range from angular to rounded. The sandstones generally show very poor to poor lithification with sediments often being easy to carve into. A general exception were the areas with high abundance of bivalves, gastropods, or corals.

The sediments vary from areas with no bioturbation to areas with a high degree of bioturbation (fig. 4.6), with the highly bioturbated areas dominated by vertical and horizontal burrows, bivalves, gastropods, and corals such as: *Acropora* corals, *Cardium* sp., *Archimediella* sp. *Solen* sp., *A. noae, C. glaucum, L. lacteus, Lutraria* sp., *Natica, Tellina, Glycymeris glycymeris, Ostrea edulis, Chama, Pecten* sp., *Pectunculus* and *Pinna* sp. (von Freyberg, 1973; Vita-Finzi and King, 1985; Collier, 1990). The bivalves and gastropods vary from very small to large, between whole and fragmented, and are found in the massive very fine to fine sandstones with a mixture of broken shell fragments. The shells are often reworked. They also vary in abundance with some areas only featuring scarce examples of fossils, while they in other areas are almost imbricated and impossible to carve through. In areas with low abundance, the bivalves are almost exclusively smaller.

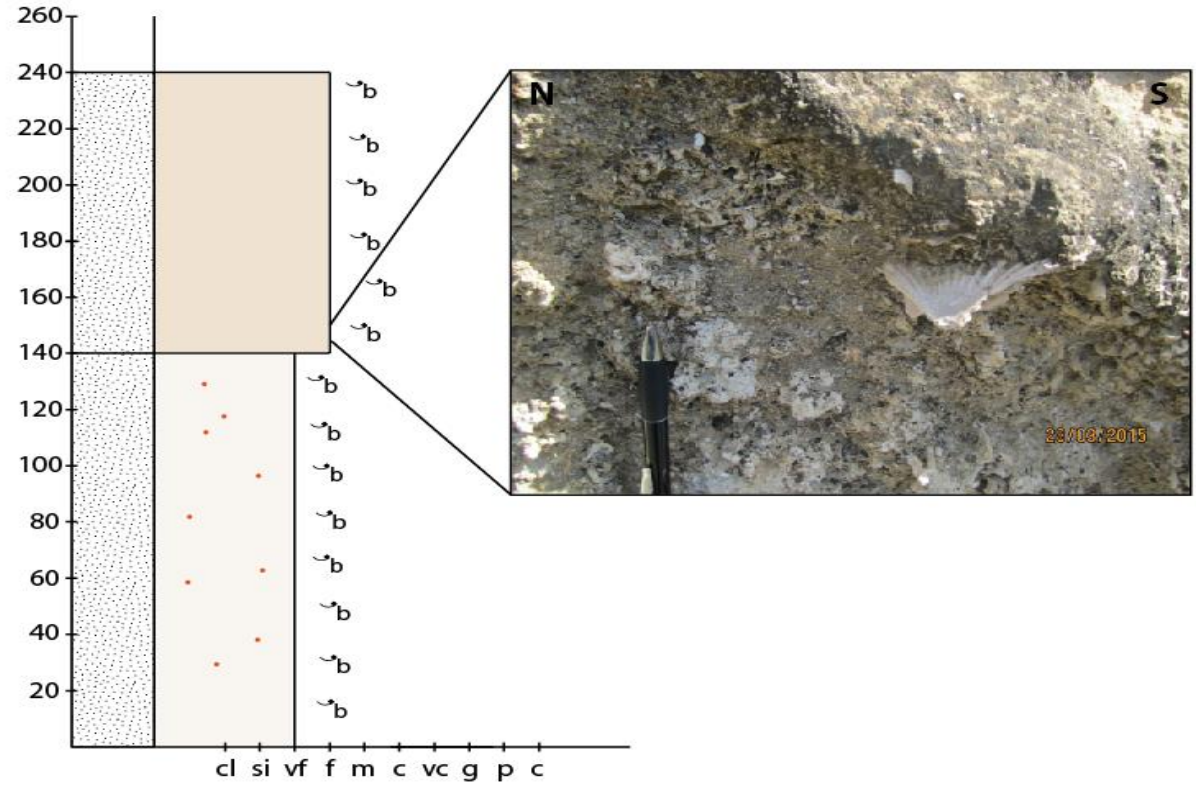

Fig. 4.6: A logged section of the shoreface sandstone featuring a high abundance of bivalves with lithofacies F4 (Mixed carbonate siliciclastic facies) within Facies Association FA5 (shoreface sandstones). The pen is 12 cm. Vertical scale on the log is in centimetre.

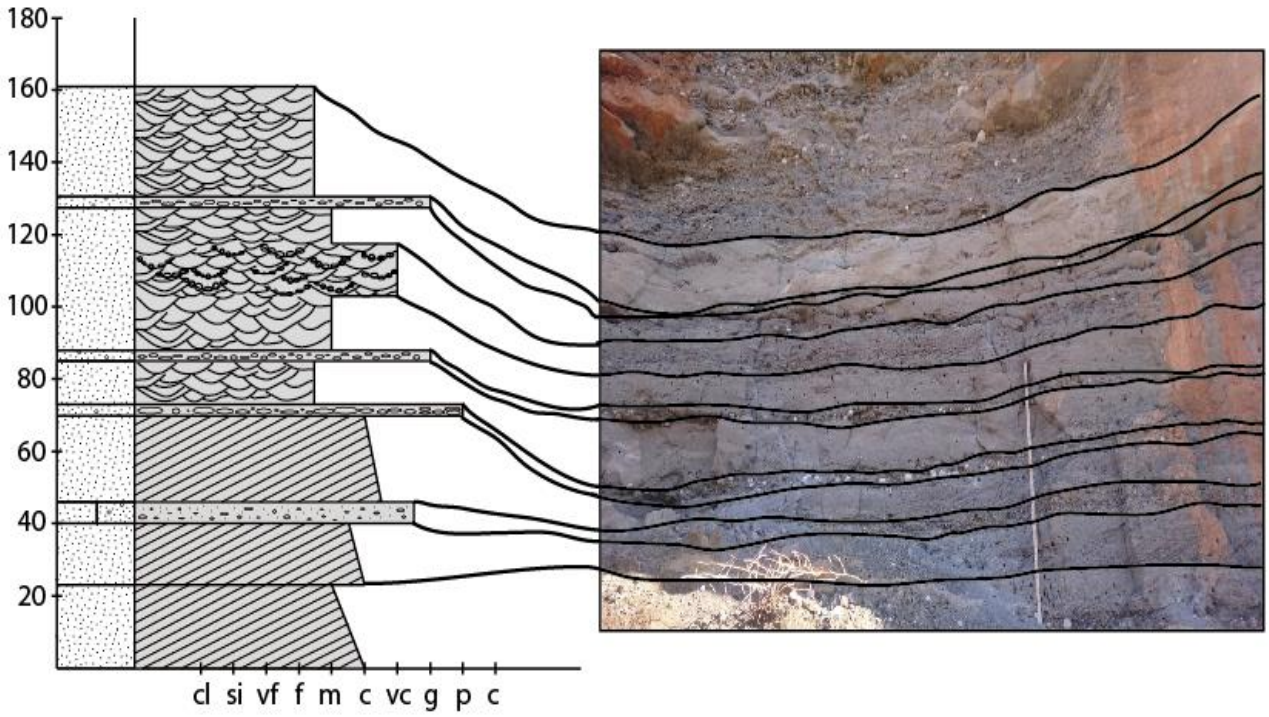

Fig. 4.7: A logged section of the upper shoreface sandstones featuring planar- and trough cross-bedded sandstone packages, featuring lithofacies F8, F9, F10, and F11 within Facies Association FA5. Measuring stick is 1 metre, and the vertical scale of the log is in centimetre.

Interpretation:

The planar- and trough cross-bedding found in the sandstone are good indicators of a near-shore marine environment. Fine to medium planar cross-stratified sandstone and fine to coarse trough cross-stratified sandstones are good indicators of migration of longshore bars as a result of unidirectional currents in a shoreface environment (Campbell, 1971; Clifton et al., 1971; Clifton, 2006; Collinson et al., 2006; Reading, 2009).

The dominance of glauconite found in the sediments is another strong indication of a marine environment (Odin and Matter, 1981). The larger clasts may have been transported into such an area during periods of high energy, i.e. during storms, or by strong tidal currents.

The bivalves and gastropods present in the sediments are all marine molluscs (Vita-Finzi and King, 1985; Collier, 1990; Dia et al., 1997). The reworking of gastropods indicate a wave influence on the deposits, suggesting deposition above fair-weather wave base (Murray-Wallace et al., 1996). The changes in abundance of the marine molluscs also indicate changes between higher and lower energy environment, with high mollusc abundance and mollusc-reworking indicating a high energy, most likely in a near-shore environment (Murray-Wallace et al., 1996).

The sediments, structures and molluscs discovered in this Facies Association combined, indicate sandstone bodies formed in a shoreface environment (Clifton et al., 1971; Clifton, 2006; Collinson et al., 2006; Reading, 2009). The differences in bioturbation, grain size and structures indicate changes between a low and high energy shoreface environment. The area featuring the deposits presented in fig. 4.7 indicate high-energy environment with wave influence most likely in an upper shoreface transitioning to a foreshore environment (Clifton et al., 1971). The same is likely for the deposits consisting of corals and high abundance of reworked bivalves and gastropods, while the very poorly lithified sandstone with a few scattered small shells, probably are deposited in a middle to lower shoreface environment (Murray-Wallace et al., 1996). The increase in the thickness of different units of the Facies Association towards NW, indicate an aggradational pattern to the deposition.

4.2.6 Facies Association 6: Offshore transition to offshore sandstone and siltstone

Description:

Facies Association 6 is composed of silt and very fine to fine sand and lithofacies F2 (Siltstone) and F3 (Sandstone). The individual thickness of the Facies Association varies in its different locations from 40 cm to 13 m.

The very fine to fine sand is massive and contain different immature grains with abundant *glauconite*. The sandstone packages are up to 3 m thick and show a lateral extension of at least 50 m in NW-SE and 50-60 m in E-W direction. The packages feature sharp, planar to irregular boundaries with tabular to lenticular bodies and a sheet-like larger scale body. The siltstone features horizontal bedded strata with a small section featuring scattered small granule-sized clasts. The siltstone units are up to 13 m thick and has a lateral extension of at least 700 m in NW-SE and 50-60 m in E-W direction. There are small, almost invisible colour changes between light grey and light brown sediments in the siltstone.

There are no signs of bioturbation or structures in the sand or in the NW-dipping silt.

Interpretation:

The immature glauconite grains in the sandstone indicate a marine environment (Odin and Matter, 1981). The sandstone is also massive and feature no structures, which indicates a depositional environment not affected by waves and currents, most likely below fair-weather or storm-weather wave base, in an offshore-transition to offshore zone. The siltstone also indicates deposition in a low energy environment, allowing deposition through suspension, in this case deemed as marine offshore zone deposits, due to its vertical transition from shallower shoreface marine deposits, and its composition consisting of fine grained silt (Campbell, 1971). The sediments are therefore interpreted as offshore transition to offshore deposits.

4.2.7 Facies Association 7: Offshore calcareous mudstone

Description:

Facies Association 7 consists of non-fissile, light grey to white calcareous silt, with interbedded sandstone bodies featuring burrows and bivalves, consisting of lithofacies F1 (Marl) and F4 (Mixed siliciclastic carbonate facies). The Facies Association laterally extends for at least 1000 m in NW-SE direction and with an extension of at least 50-60 m in E-W direction. It stretches as a large tabular to wedge-shaped package, which gets eroded by overlying sediments of FA3 (foreshore conglomerates). The individual marl packages show a thickness from 15 cm to 12 m, while the smaller sandstone bodies range from 20 to 80 cm.

An area of bivalves with horizontal and vertical burrows in high abundance, within calcareous silt, is located in the lowermost part of the Facies Association. The bivalves include *Cardium* sp. and *Pecten* sp. The area featuring burrows and bivalves in the lowermost part extend laterally for at least 450 metres in NW-SE direction and at least 50-60 metres in E-W direction and is only constrained by faults. The Facies Association is followed upwards by horizontal laminated and massive calcareous silt of F1, with a dominance of massive silt. In most parts the bedded silt seem to extend laterally without any constrains, along an at least 450 m NW-SE extent. The Facies Association also features interbedded sandstone bodies within the calcareous siltstone. These sandstone bodies have a measured thickness between 20 and 80 cm, and consist of very fine to fine sand with a presence of vertical and horizontal burrows along with other bivalves. Some of the sandstone packages also features granule clasts within. The sandstone bodies show both tabular bodies with sharp, planar boundaries and lenticular bodies with sharp, irregular boundaries to the surrounding calcareous siltstone. The largest sandstone package can be seen extending for at least 200 m in NW-SE direction, while some of the smaller ones are only seen over a distance of a few metres.

Interpretation:

The bivalves of *Pecten* sp., *Cardium* sp. are marine molluscs indicating that the marlstones have been deposited in a marine environment. The deposition of calcareous mudstone indicate a depositional environment below storm-weather wave base, sheltered from exterior forces and near-shore currents, in an area with mainly pelagic sedimentation (Sanders and Pons, 1999; García-García et al., 2009; Lubeseder et al., 2009). This would allow deposition of silt and calcium carbonate in an offshore zone on a siliciclastic shelf (Sanders and Pons, 1999; García-García et al., 2009; Lubeseder et al., 2009). The small areas of bivalves and burrows in

sandstone deposits are possibly deposited as a result of episodic supply of siliciclastic material during periods of higher energy, possibly due to small fluctuations in sea level, storm ebb surges, or turbidity flows (García-García et al., 2009). Marlstone deposition with interbedded sandstone layers make these deposits very similar to the Marlstone deposits found in the Guadix Basin, Spain (García-García et al., 2009).

Marlstone deposition indicate a mixture of calcite and silt in an offshore environment. The silt is normally transported to offshore zones either via suspension during mass transport, or by pelagic sedimentation (Aurell et al., 1998). The calcite would have a similar transport process, but with deposition seaward of what seems to be a siliciclastic-dominated shelf, derivation from mass transport from upper shelf seems unlikely for the calcite. The calcite may have been deposited offshore either due to chemical precipitation and carbonate production directly from the area, or through chemical weathering of carbonate bedrock located onshore or offshore (Aurell et al., 1998; Lubeseder et al., 2009). The chemical weathering would create chemical ions, which then in turn could have been transported to an offshore setting either via groundwater or rivers, if the bedrock was onshore. When reaching the marine environment the chemical ions could have been transported via suspension in the water column and been deposited along with the silt below storm-weather wave base, to create a mixture of silt and calcite (Aurell et al., 1998; Lubeseder et al., 2009).

4.3 Depositional models

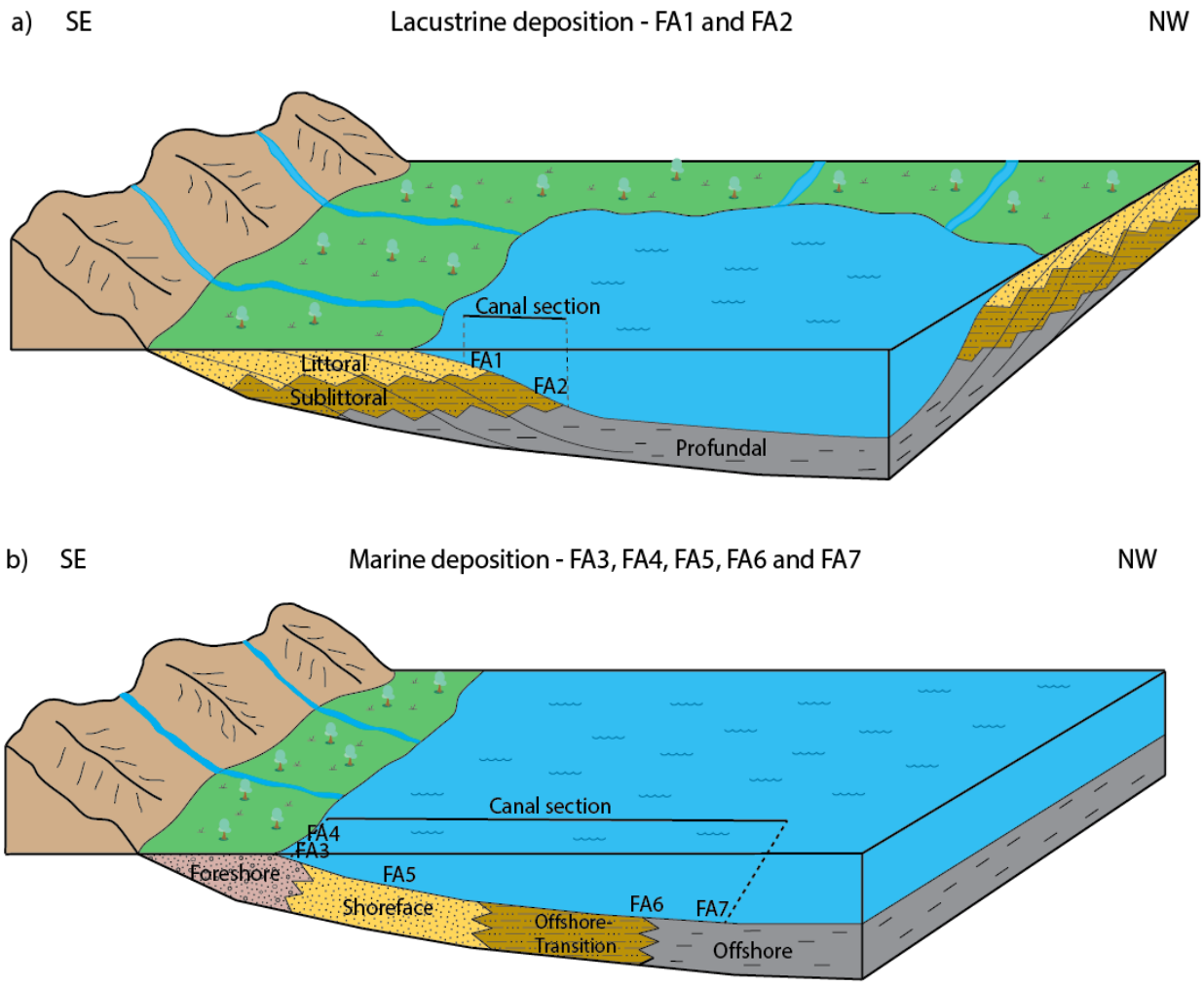

Fig. 4.8: Two simple depositional models for the *(A)* lacustrine and *(B)* marine deposits exposed in the Canal.

To summarize the Facies Associations, two simple sketches, fig. 4.8, has been created. The purpose is to show an approximate deposition of how the Facies Associations are distributed within the respective lacustrine and marine depositional environments. FA1 and FA2 are deposited in a fluvial-lacustrine basin with deposition from lower littoral to upper profundal zone. FA3 and FA4 are deposited in a foreshore area within a marine environment. FA5 consists of sandstones deposited in a marine shoreface environment. FA6 consist of sandstones and siltstones in a marine offshore-transition to offshore environment, and FA7 consists of calcareous mudstones (marlstones) which are deposited in an offshore marine setting. The Canal section represent approximately how the Facies Associations are distributed, from SE to NW, in the Canal outcrops. No structures or faults are added to these sketches, as the Tectono-Stratigraphic evolution of the outcrops is discussed and presented in Chapter 6.

5. Sequence Stratigraphy

5.1 Introduction

The stratigraphic analysis was performed by visual analysis of the stratal geometry and facies above and below the surfaces, in combination with sedimentary logging. This allowed sub-division of the succession exposed in the Corinth Canal based on: I) bedding geometry, II) facies characteristics, III) abrupt shifts in facies, and IV) colour changes.

This has led to observation of 5 key sequence stratigraphic surfaces and a divide into six Tectono-Stratigraphic Units (fig. 5.1a) which are found in the various fault blocks in the canal. The key sequence stratigraphic surfaces generally include major shifts in angularity, erosion, and major landward/basinward shift in facies. There are also several other minor sequence stratigraphic boundaries, such as landward and basinward shift in facies in addition to lithology-boundaries with no indications of landward and basinward shifts. The Tectono-Stratigraphic units are separated by using the characteristics of the individual surfaces and the facies within the Tectono-Stratigraphic Units, which lead to indications of major Tectono-Stratigraphic Units separated by period of non-deposition. The Tectono-Stratigraphic Units are also divided into smaller Stratal Units, which are bounded by smaller sequence stratigraphic surfaces (fig. 5.1b).

5.2 General overview of interpreted surfaces

There are a number of observed surfaces in the canal with different importance, therefore the term *key stratal surfaces* is used throughout this chapter to describe the key sequence stratigraphic surfaces which are used to separate the Canal into six Tectono-Stratigraphic Units. A simple overview, with characteristics of the key stratal surfaces, minor sequence stratigraphic surfaces and lithology-boundaries, are found in table 5.1.

Table 5.1: Overview of different surfaces and their characteristics

	Surfaces	**Characteristics identified on different surfaces**
Key stratal surfaces	2, 3, 4, 5, 8	Angular unconformity, truncation, onlap, downlap, facies shift, subaerial exposure, wave-eroded cliff
Landward shift in facies	5.2, 6.2, 9, 11, 13	Facies shift, flooding surface
Basinward shift in facies	5.1, 7, 8, 8,1, 8,2 10, 12	Facies shift, conglomerate lag, downlap, wave-eroded cliffs
Lithology-boundaries	1.1, 1.2, 4.2, 4.3, 4.4	Facies shift

The surfaces show a wide variety of characteristics with the observations uncovering unconformities, marker beds, planar/non-planar surfaces, erosive surfaces, lithology-boundaries, wave-eroded surfaces, and surfaces were the lithology transition across the surface may differ from fault block to fault block.

5.2.1 Types of surfaces

Table 5.2: Surface type table

	Surface Type
ST1	Angular unconformity
ST2	Disconformity
ST3	Wave-eroded cliff
ST4	Subaerial exposure

ST1 – Angular unconformity

Description:

Several of the surfaces in the Canal show angular differences between strata, with truncation of the underlying angled beds, indicating several angular unconformities within the canal outcrops. The surfaces are both horizontal and tilted. They have different characteristics with them featuring a combination of clutches of crushed shell and siltstone in the area right above the unconformity and clear erosion of the underlying strata packages. The surfaces separates lithologies of siltstones from siltstones, siltstones from conglomerates, marlstones from conglomerates, and sandstones from conglomerate.

Interpretation:

The angular unconformities seen in the Canal are due to rotation of fault blocks, which have created an inclined strata which is later truncated by an overlying Unit depositing, in addition to erosion from overlying Units which have created angular differences between Units.

ST2 – Disconformity

Description:

There are several surfaces that divide parallel bedded strata with no clear sign of an unconformity. When traced further into surrounding fault blocks however, the surface often changes towards angular unconformities with truncations, indicating an unconformity along the entire surface. The surfaces separated sandstones from sandstones.

Interpretation:

The surfaces are interpreted as disconformities, or paraconformities, with parallel-bedded strata where there are no clear signs of an unconformity, but correlates with identified unconformities.

ST3 – Wave-eroded paleo cliffs

Description:

Some surfaces experience cliffs with a sudden step in elevation, which incises and erodes the unit below. It creates an increase in accommodation space for the unit above. There are in total four cliffs (A, B, C, and D) found along the surfaces and they vary in height from 3 to 10.5 m. Surfaces onlap onto the eroded cliffs in the Unit above. They separate marlstones below from foreshore conglomerates above, and most commonly shoreface sandstones below from foreshore conglomerates above.

Interpretation:

The cliffs are created due to a stillstand in relative sea level, where wave motion have been able to erode the sea floor for a prolonged time period (Collier, 1990; Papanikolaou et al., 2015). These stillstand in sea level are part of smaller sea level fluctuations during a larger sea level fall, or due to smaller sea level fluctuations due to tectonic forces.

ST4 – Subaerial exposure

Description:

The upper boundary of the marlstones depositing on the central horst show small depressions and strongly cemented calcite along the boundary between marlstones below and foreshore conglomerate above.

Interpretation:

The depressions in the marlstones indicate a dissolution of calcium carbonate with karstic features along the surface. The strongly cemented and hardened marlstones indicate calcrete formation. Both karst and calcrete formation are indicators of subaerial exposure of calcareous rocks, which leads to the interpretation of subaerial exposure of the marlstones on the horst (Lauritzen, 2011).

5.3 Variability & Geometry

Description

The geometry of the surfaces is mostly dependant on the general geometry of the individual fault blocks. The dip-directions of the key stratal surfaces are generally towards NW, from FN1 until FN5 (fig.5.1). At this point the dip-direction changes towards W to NW. This gradual shift from NW-dipping towards W-dipping surfaces is evident NW of FN6, where all the key stratal surfaces have a W-dip. The paleo cliffs all have a W-dip, even if the surrounding surfaces show N to NW dip.

The dip of the surfaces varies throughout the fault blocks. They generally vary between 1 and 4 degrees in their extent NW of FN1. A general observation, which is present throughout, is the low angle of surface 4, the base of Tectono-Stratigraphic Unit 4. While the surfaces below show a higher dip between 3 & 4 degrees towards NW, surface 4 generally show a 0.5-1.5 degree dip. The different key stratal surfaces, Surfaces 3, 4 and 8 are all angular unconformities where the Tectono-Stratigraphic Unit above truncates the dipping strata in underlying Unit. The truncation and angular unconformities are noticed between FN1 and FN4 for Surface 3, between FN1 and FN4 for Surface 4, and between FN1 and FN1.1 and NW of FN6 for Surface 8 (fig. 5.1).

The geometry of the key stratal surfaces SE of FS1 follows the general geometry of the fault blocks, with some small exceptions. The individual fault blocks vary between N & NW-dipping surfaces. The key stratal surfaces between FS1 and FS4 have an N-dipping geometry, the key stratal surfaces between FS4 and FS5 have a NW-dip, between FS5 and FS7 they have a mix between N and NW-dip, with dominance towards N-dip, and between FS7 and FS8 they show a NW-dip.

As with the dip-direction, the dip of the individual key stratal surfaces also mostly depends on the fault block. Although the dip of an individual key stratal surface may have a very small decrease from one fault block to another, the general dip of the surfaces show a dip increase towards SE. This is exemplified by the average dip of the key stratal surfaces being c. 1 degree between FS1 and FS3, before it increases to 3 degrees between FS3 and FS4, 4 degrees between FS4 and FS6, 5 degrees between FS6 and FS7 and eventually increased to around 7-8 degrees between FS7 and FS8 (fig. 5.1).

All dip and strike measurements of interpreted surfaces are attached within a table in the appendix

Interpretation

With both the dip-direction and dip-angles showing the same data vertically in almost every surface in the Fault Blocks SE of FS1, the dip-direction and dip-angles are interpreted to derive from post-depositional rotation of the fault blocks in the area SE of FS1.

The geometry and dip of surfaces in the fault blocks NW of FN1 are interpreted as results of various stages of fault block rotation. The angular unconformities and truncations witnessed at the key stratal surfaces 3, 4, and 8, indicate a rotation of the fault blocks which have cause the strata to tilt towards W to NW. With tilting of strata in various fault blocks and truncation and angular unconformities at each key stratal surface, this indicate rotation of the fault blocks after deposition of each Tectono-Stratigraphic Unit NW of FN1.

5.4 Tectono-Stratigraphic Units

This subchapter focuses on describing and interpreting the different Tectono-Stratigraphic Units found in the Corinth Canal. The Canal has been divided into six different Tectono-Stratigraphic Units (fig. 5.1a) separated by key stratal surfaces, with 14 minor Stratal Units (fig. 5.1b), separated by minor sequence stratigraphic boundaries within the Tectono-Stratigraphic Units. The Tectono-Stratigraphic Units are divided due to characteristics of facies within each of the Units and their stacking pattern, in addition to a divide based heavily on the interpretation of surfaces. The bounding key stratal surfaces are interpreted to feature either major landward/basinward shifts in facies and/or clear truncation and angular unconformity between the deposits, indicating a time period of non-deposition. The surfaces separating the minor Stratal Units are interpreted as minor landward or basinward shifts in deposits.

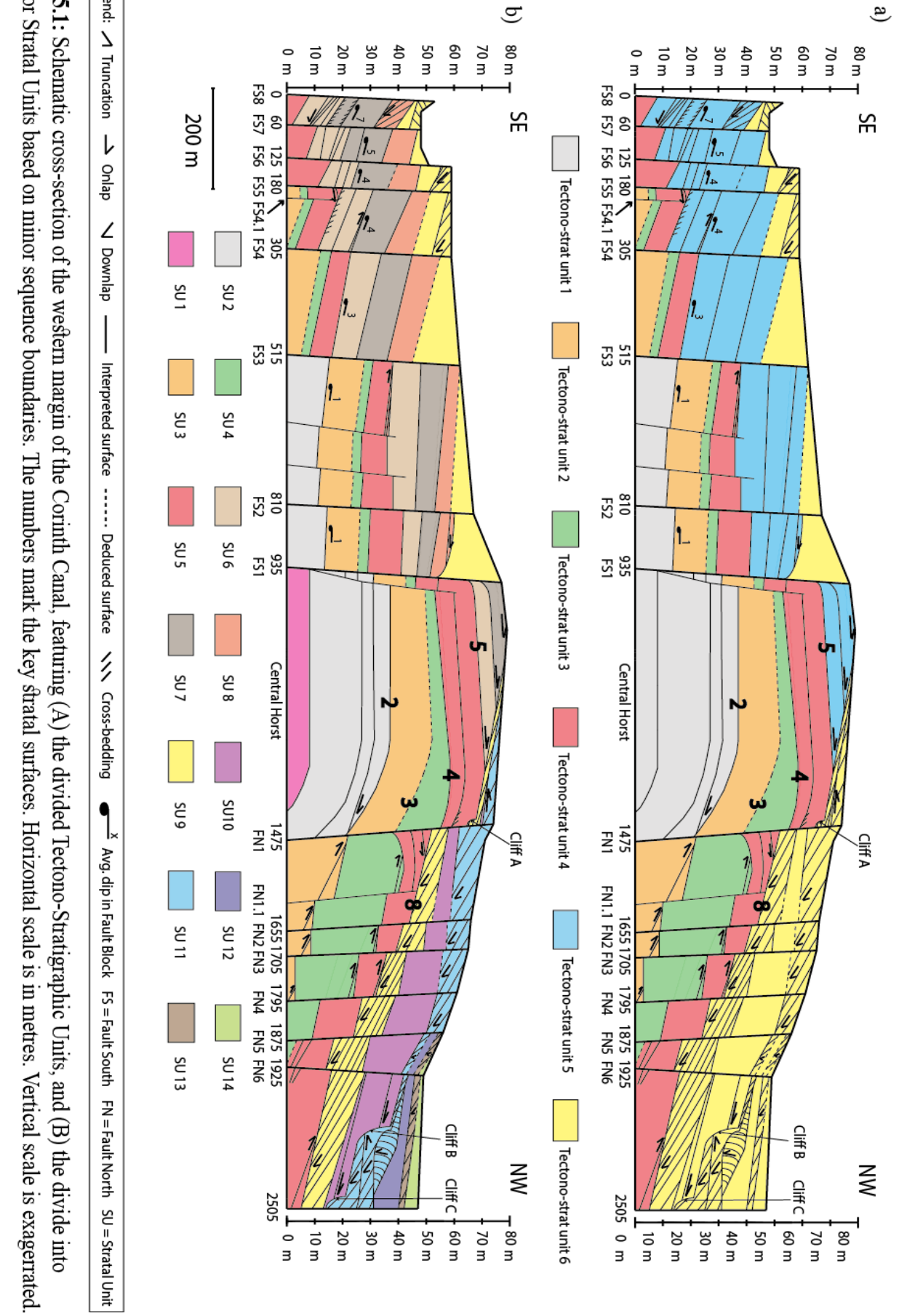

Fig 5.1: Schematic cross-section of the western margin of the Corinth Canal, featuring (A) the divided Tectono-Stratigraphic Units, and (B) the divide into minor Stratal Units based on minor sequence boundaries. The numbers mark the key stratal surfaces. Horizontal scale is in metres. Vertical scale is exaggerated.

5.4.1 Tectono-Stratigraphic Unit 1

Description

Tectono-Stratigraphic Unit 1s base is not exposed as it lies under sea-level and is bounded at the top by Surface 2. The Unit consists of lacustrine siltstone bodies with a few packages of very fine to fine sandstone (Lithofacies F2 and F3 and Facies Association FA2). The Tectono-Stratigraphic Unit is divided into two smaller Stratal Units separated by an angular unconformity. The Unit extends from FS3 to FN1, across 960 m (fig. 5.1a).

Stratal Unit 1 consists of siltstone with a high-angled dip towards NW

Stratal Unit 2 consists of horizontally laminated to massive siltstone. There are fragmented gastropod shells of *Viviparus* sp. (Collier, 1990) scattered throughout the siltstone. The upper part of the unit is characterized by two packages of dark grey very fine to fine sandstone 0.2 to 2 m thick, containing abundant small fragments of *Viviparus* sp. interbedded with the siltstone (fig. 4.2). The sedimentary beds of the Unit dip towards FN1 on the NW part of the horst. The dipping is seen up to 200 m SE of FN1 (fig. 5.2).

No exposed base surface makes thickness measurements impossible.

On the horst, the Unit is mainly horizontal with no tilt, but folding in the beds towards FN1 creates a NW to N tilt. The tilt and tilt-angles both NW and SE of the horst is further described and interpreted in subchapter 5.3 and will not be repeated for the individual Tectono-Stratigraphic Units, as the Units SE of FS1 are very similar which would make it very repetitive.

The upper boundary, surface 2, truncates the top beds of Unit 1 over the fold developed towards FN1 (fig.5.2).

Interpretation

The sediments are deposited in a lacustrine lower sublittoral to possible upper profundal environment in a fluvial-lacustrine basin (FA2) (Bohacs et al., 2000). This environment is responsible for the large subparallel bedded siltstone packages featuring the freshwater gastropod *Viviparus* sp. (Collier 1990) and an occurrence of subaqueous flows depositing thin sandstone packages near the upper boundary (Bohacs et al., 2000).

The folding of the beds and the upper surface of the Unit towards FN1, indicate the development of a monocline fold due to the vertical propagation of blind fault FN1 (fig. 5.2) (Gawthorpe and

Leeder, 2000; Willsey et al., 2002). This would have created a dip towards N to NW in the beds of the upper Stratal Unit and the upper surface experienced in the Canal (fig 5.2).

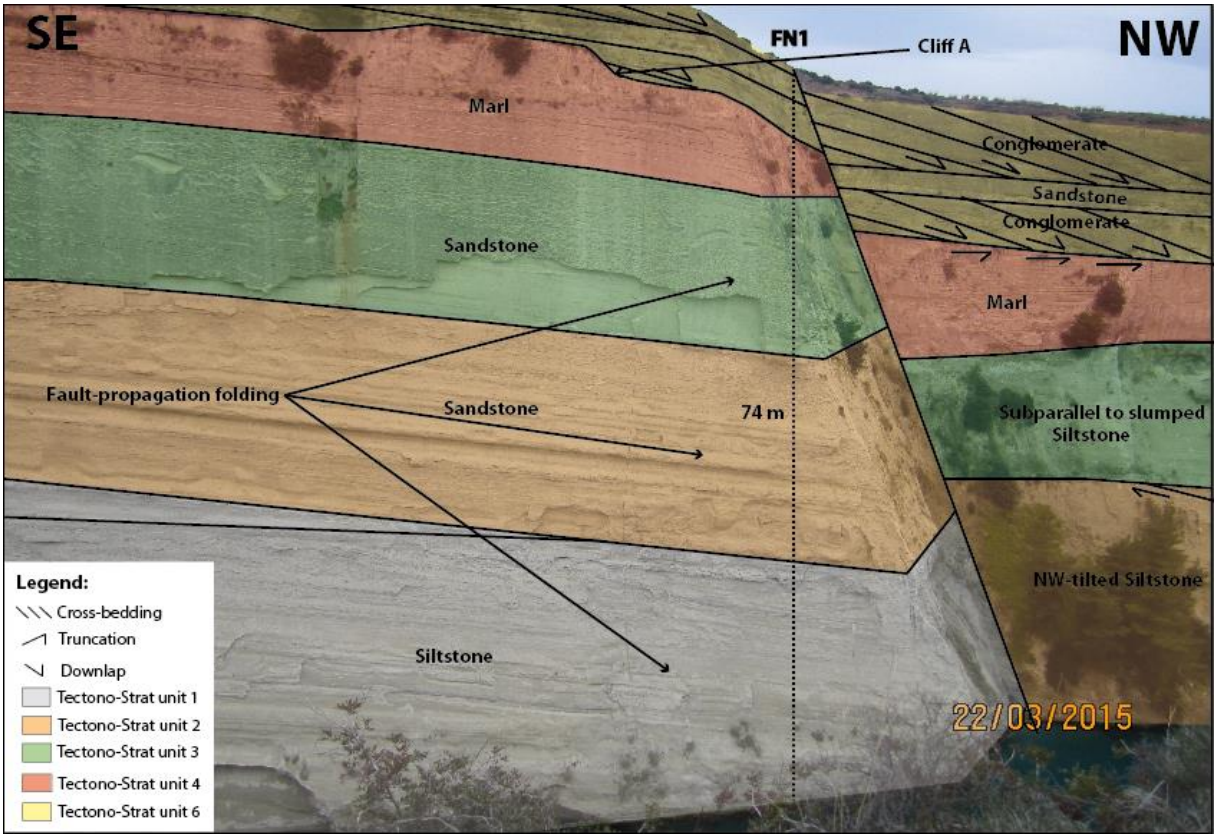

Fig. 5.2: Tectono-Stratigraphic Units 1, 2, 3, 4, and 6 in the vicinity of FN1. The Tectono-Stratigraphic Units 1 to 3 all show evidences of fault-propagation folding towards FN1, due to fault breaching of the earlier monocline structure after deposition of Tectono-Stratigraphic Unit 3.

5.4.2 Tectono-Stratigraphic Unit 2

Description

Tectono-Stratigraphic Unit 2 is bounded by Surface 2 at the base and surface 3 at the top. This Unit consists of lacustrine sandstone and siltstone with a lateral change between the two lithologies across FN1. It consists of lithofacies F2 and F3 and Facies Association FA1 and FA2. The Unit extends from FS5 to FN4, across 1615 m (fig.5.1a). It has a tabular external geometry.

Unit 2 composition varies laterally from massive or laminated sandstones southeast of FN1 to parallel-bedded siltstones northwest of FN1 (fig. 5.2). The laminated or massive sandstones on the horst contain very small fragments of *Viviparus* sp. (Collier, 1990) and folds towards FN1 (fig. 5.2). The parallel-bedded siltstone NW of FN1 is tilted towards NW and is truncated by the upper surface, which is an angular, erosional unconformity featuring crushed clutches of shell and siltstone in the area above the surface.

The base, surface 2, features a change from siltstone below to sandstone above. Surface 2 truncates the top beds of Unit 1 over the monocline fold developed towards FN1. The surface is down-faulted NW of FN1. SE of FS1 Surface 2 is down-faulted beneath sea level SE of FS3.

Thickness measurements are constant throughout the Unit, with an approximate thickness of 12 m.

Unit 2 is folded in the horst, dipping to the SE towards FS1 and dipping to the NW towards FN1 (fig. 5.1 and 5.2). The dipping towards FN1 is seen up to 200 m SE of FN1.

Interpretation

The base, Surface 2, marks a change from lacustrine lower sublittoral to upper profundal (FA2) below, to lacustrine lower littoral to upper sublittoral (FA1) above (Bohacs et al., 2000). This change indicates a basinward shift of facies in the lacustrine basin, as littoral to sublittoral sandstone packages prograded towards the basin centre and deposited on top of the deeper lacustrine siltstones (Bohacs et al., 2000).

The sandstone sediments SE of FN1 are deposited in a lacustrine littoral to sublittoral zone (FA1), evident by the freshwater gastropod *Viviparus* sp. NW of FN1 the Unit consists of lacustrine siltstone of sublittoral to profundal zone (FA2) (Bohacs et al., 2000). These are deposited in a fluvial-lacustrine basin (Bohacs et al., 2000).

The reason for lateral variation across FN1 might be a blind propagating fault which have affected the beds of this, and the underlying deposits, and created a monocline. With a monocline already affecting the below lying Tectono-Stratigraphic Unit 1, before deposition of Tectono-Stratigraphic Unit 2, it could have created increased accommodation space NW of the horst. This might have created a deeper water environment NW of FN1, where it changes from lower littoral/upper sublittoral sandstones in the horst, to lower sublittoral/upper profundal siltstone NW of FN1 (fig. 5.2) (Bohacs et al., 2000; Gawthorpe and Leeder, 2000; Willsey et al., 2002). The blind propagating fault creating the monocline, also affects these deposits after deposition, as it could be the reason for the NW-dipping beds and bounding surfaces of this Unit towards FN1. The blind propagating fault created a monocline structure within this Unit as well, before eventually surface breaching after Tectono-Stratigraphic Unit 3, creating the folding presently seen in the outcrops (fig. 5.2) (Gawthorpe and Leeder, 2000; Willsey et al., 2002).

5.4.3 Tectono-Stratigraphic Unit 3

Description

Tectono-Stratigraphic Unit 3 is bounded by Surface 3 at the base and Surface 4 at the top. Unit 3 consists of lacustrine sandstone and siltstone with lateral variation of facies across FN1. This unit consists of lithofacies F2 and F3, and Facies Association FA1 and FA2. Unit 3 is exposed between faults FS5 and FN6 (fig. 5.1a). The Unit has a tabular external geometry.

SE of FN1 the Unit consists of subparallel bedded to massive sandstones, while it NW of FN1 consists of subparallel to minor tilted parallel-laminated and slumped siltstone (fig. 5.2). The subparallel to massive sandstone contains fragmented bits of the gastropod *Viviparus* sp. (Collier 1990) and is folded towards FN1 (fig. 5.2). The subparallel to slightly tilted parallel-bedded and slumped siltstone NW of FN1, show a higher inclination of beds between FN2 and FN4, than between FN1 and FN2, and F4 and FN5, where the beds are almost subparallel.

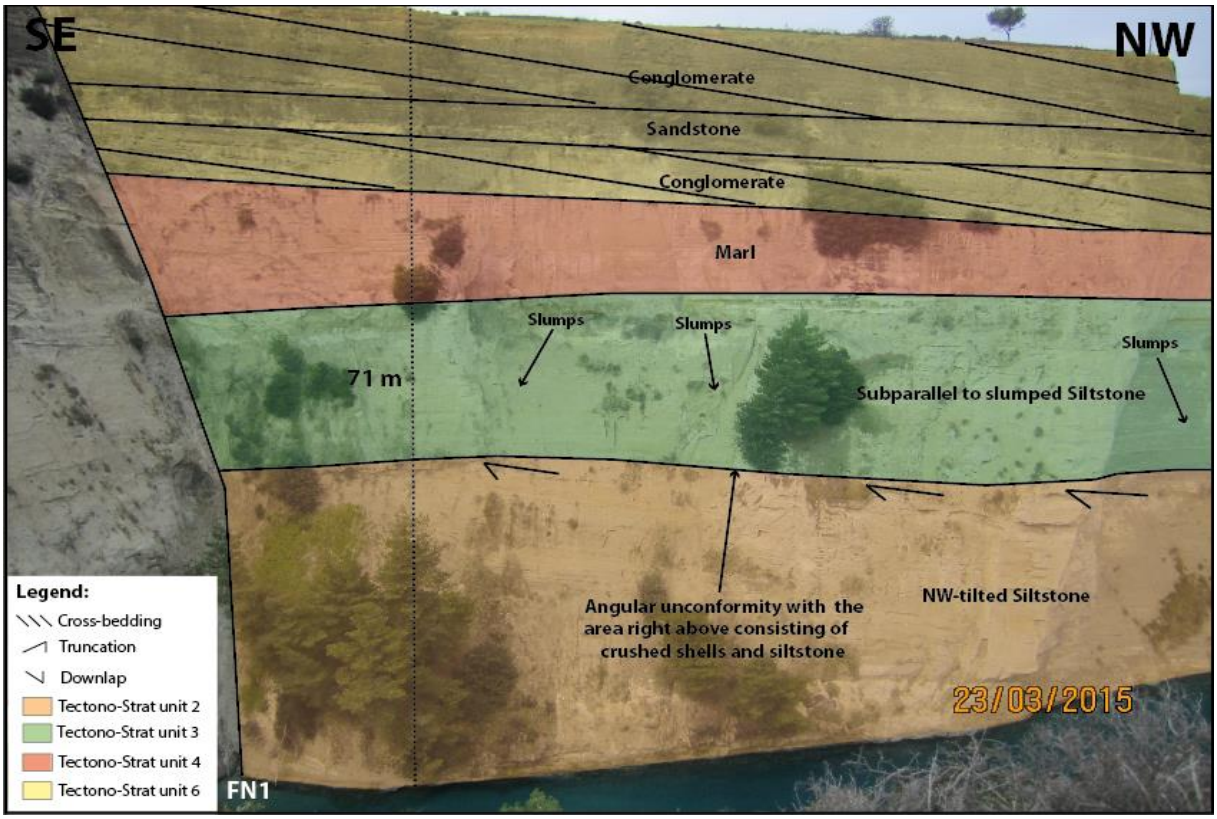

Fig. 5.3: The Tectono-Stratigraphic Units immediately NW of FN1, with the angular unconformity between Unit 2 and 3.

Tectono-Stratigraphic Unit 3 base is Surface 3 (fig. 5.1a). SE of FN1 the surface marks a change between massive and subparallel bedded sandstones across the surface. NW of FN1 the surface marks a change from parallel-bedded siltstone with a NW tilt below, to subparallel laminated

and slumped siltstone above (fig. 5.3). Between FN1 and FN4 the unconformity has crushed shells and siltstones above, in the lowermost part of this Unit (fig. 5.3).

Southeast of FS1 the Unit has an even thickness of approximately 3 m (fig 5.1). From FS1 towards FN1 the thickness increases from ca. 3 m at FS1 to ca. 14 m at FN1. NW of FN1 the thickness is ca. 16 m, but would be thicker if it were not for the wedge-shape in Tectono-Stratigraphic Unit 4 above, which erodes the beds if this Unit immediately NW of FN1 (fig 5.1). The maximum thickness is reached between FN1.1 and FN4 where the thickness is 25 m (fig. 5.1).

The unit is folded on the horst, dipping to the SE towards FS1 and dipping to the NW towards FN1 (fig. 5.2). The dip towards FN1 is seen up to 200 m SE of FN1.

Interpretation

The lower surface marks a separation of lower shoreface to offshore transition lacustrine deposits and is angular unconformity with truncation of the Unit below, as the NW-dipping siltstone below is truncated by the slumped unit above in the Fault Blocks towards NW.

The sandstones SE of FN1 are deposited in a lacustrine lower littoral to upper sublittoral zone (FA1) (Bohacs et al., 2000). NW of FN1 the Unit is deposited in a lacustrine lower sublittoral to upper profundal depositional environment (FA2) (Bohacs et al., 2000). The sediments are deposited in a fluvial-lacustrine basin (Bohacs et al., 2000).

The lithology change across FN1, from sandstone to siltstone, in addition to the beds on the NW part of the horst folding towards FN1, might come as a result of the same faulting event. FN1 acts as a blind propagation fault during deposition of the Unit and have already created a monocline in the below lying Tectono-Stratigraphic Units. The continued blind propagation of this fault could be responsible for the sediment packages in the horst to fold towards FN1, as it has created a monocline structure as it has propagated through the deposits, before eventually surface breaching after deposition of this Unit and created the folding seen in the outcrops (fig. 5.2). With a monocline created in the underlying Tectono-Stratigraphic Units, before deposition of these beds, the change from sandstone to siltstone across the fault may result from differences in water depth from the footwall to the hanging-wall of FN1. This resulted in a change from lower littoral/upper sublittoral to a lower sublittoral/upper profundal zone across FN1. The slumped siltstone in this Unit, located between FN1 and FN4, is likely caused by syn-

sedimentary slumping of the Unit as it has been deposited down-slope above the monocline feature in the deposits below (Collinson et al., 2006).

The increase in thickness observed from the horst across FN1, is interpreted to result from the development of the monocline fold discussed earlier, where an increase in accommodation space NW of FN1 could be responsible for the thickness increase of the Unit.

The lacustrine deposits of Tectono-Stratigraphic Unit 1 to 3 show an overall progradational stacking pattern, with a basinward movement of the lacustrine shoreline which deposits littoral to sublittoral facies above sublittoral to profundal facies. Progradation of a lacustrine basin indicates a sediment supply which exceeds the available accommodation space, characteristic of an overfilled lake basin (Bohacs et al., 2000).

5.4.4 Tectono-Stratigraphic Unit 4

Description

Tectono-Stratigraphic Unit 4 is bounded by Surface 4 at the base and Surfaces 5, SE of the horst, and 8, NW of the horst, at the top. The Unit show lateral variation in facies, and generally consists of marine deposits of carbonate to siliciclastic sediments, deposited in foreshore, shoreface and offshore environments. The unit consists of lithofacies F1, F2, F3, F4 and F11, and Facies Associations FA3, FA5, FA6, and FA7. The Unit has a tabular geometry. The Unit is exposed for 2505 m, across the entire interpreted Canal section (fig. 5.1).

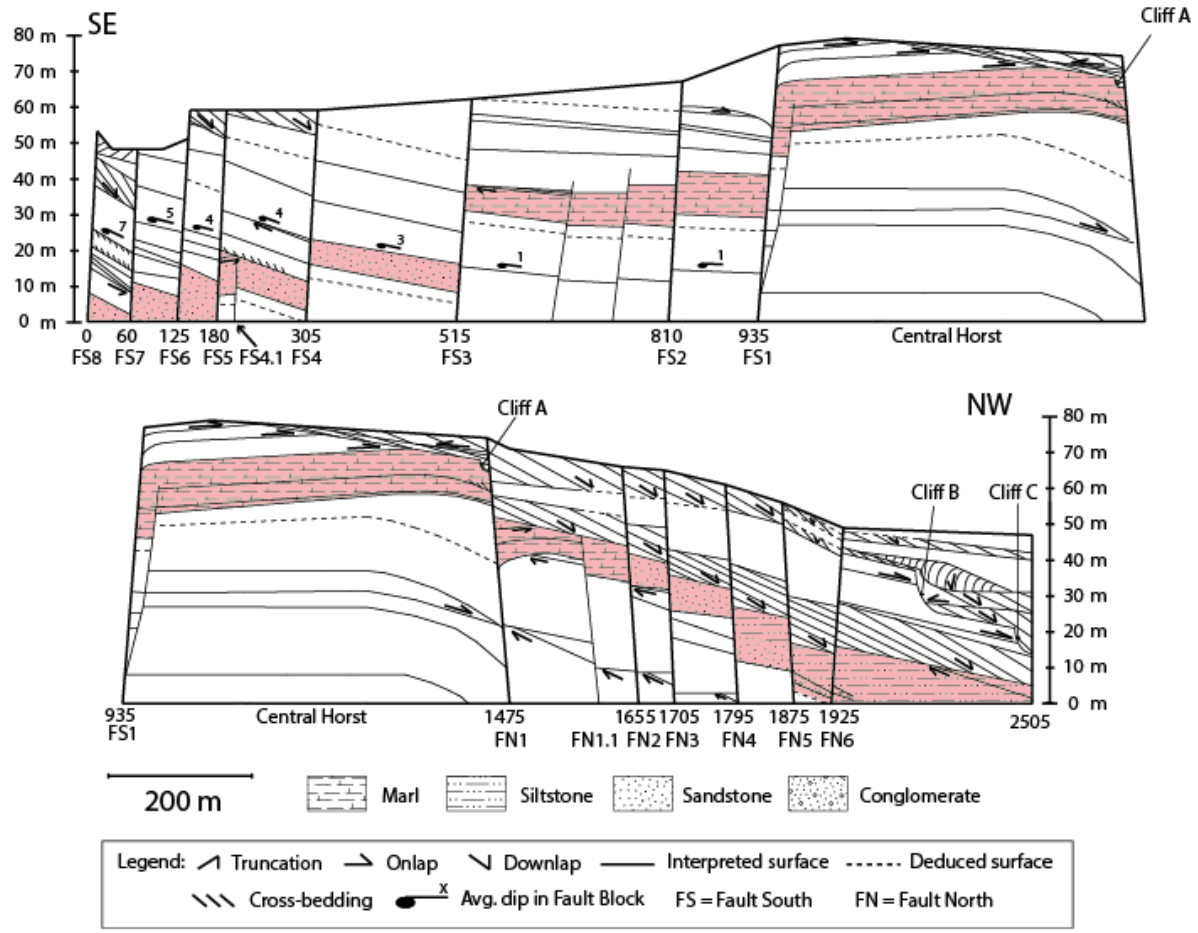

Fig. 5.4: The lateral variation in facies occurring in Tectono-Stratigraphic Unit 4. Horizontal scale in the figure is in metres.

From 0 to 515 m (fig.5.4) the Unit consists of sand with a minor presence of shells. From 515 to 1655 m (fig.5.4) the Unit consists of massive to subparallel bedded marl with burrows and shells, interbedded with small sandstone packages. The distance from 1655 to 1795 m (fig.5.4) feature a sandstone package with gastropod and bivalve-filled sandstone, before the Unit between 1795 and 1875 m (fig.5.4) feature a transition from the gastropod and bivalve-filled

sandstone in its lower parts, to siltstones in its upper part. Between 1875 and ca 1950 m (fig.5.4) the gastropod and bivalve-filled sandstone is separated from the siltstone by beds featuring highly fragmented shell and sand, clast-supported conglomerate, and highly fragmented shell and sand-filled matrix-supported conglomerate. The siltstone above these beds show a parallel-bedded tilt towards NW from 1875 to 2505 m (fig.5.4), with siltstone beds getting truncated by the overlying Unit.

The base, Surface 4, marks a change from lacustrine sandstone and siltstone below, to foreshore conglomerates, shoreface sandstones and offshore marl above. The base surface truncates inclined beds of the underlying Unit between FN1 and FN1.1, and FN2 and FN4 (fig. 5.1).

The thickness variations in the Unit change across faults, and due to erosion from the overlying Unit. SE of FS1 the thickness slightly decreases between FS2 and FS3 (fig 5.1), and feature thickness increases from footwall to hanging-wall across FS4 and FS4.1 (fig 5.1 and 5.5). On the NW part of the horst, the Unit gets thinner due to erosion by overlying conglomerates, in addition to creation of paleo cliff A, which decreases the thickness by ca. 3 m (fig. 5.1 and 5.2). NW of FN1 there is a wedge-shape onto the horst which increases the thickness across FN1 (fig. 5.2). The thickness increases across FN1.1, before a small antithetic fault in relation to FN3 decreases the thickness slightly. It reaches its maximum thickness NW of FN1, between FN4 and FN5, of 14-15 m, after a large thickness increase across FN4.

Between FS1 and FN1 the Unit is folded with tilt towards SE to E in the SE part of the Horst, with a small change towards NW-tilt towards FN1.

Interpretation

The base, Surface 4, indicates a major landward shift in deposits and a major flooding surface at this boundary. NW of FN1 the surface is interpreted to have a period of non-deposition with enough time span to rotate the 1st, 2nd and 3rd fault blocks, to allow it getting a dipping strata in Tectono-Stratigraphic Unit 3, which is later truncated by the deposition of Tectono-Stratigraphic Unit 4. The marine incursion across this surface has either occurred due to a eustatic rise in relative sea level, which have flooded the area, or a major subsidence of the area, which would result in a marine incursion above the lacustrine sediments with no variations in eustatic influence.

The unit is interpreted to be deposited in foreshore, shoreface and offshore zone marine environments (FA3, FA5, FA6, and FA7). The decrease in sediment grain-size from sandstones

in the SE towards marlstones in the horst and siltstones towards the NW is interpreted to reflect a SE source of sediments. The sandstones and conglomerates between 1655 and 1950 m (fig. 5.4), may be deposited due to a transgressive lag where shoreface sandstones and foreshore conglomerates have been deposited above the base surface as the sea starts to rise, with siltstones depositing above after the sea level have risen.

The thickness changes experienced in the unit seem to be dominated by changes across specific faults, or by truncation by the overlying Unit. The slight decrease in thickness experienced between FS2 and FS3, is due to a higher inclined base than upper surface. The upper surface show an angular unconformity as the Unit above truncates the tilted parallel-bedded strata of this Unit, and causes the slight decrease experienced in this interval. The following faults; FS4.1 (fig. 5.5), FS4 (fig. 5.5), FN1, FN1.1, FN3, and FN4, all show a thickness increase in the hanging-wall of the Unit. These faults show signs of syn-sedimentary normal fault growth, indicated by a clear increase in thickness from footwall to hanging-wall, including a wedge-shape of the Unit onto FN1 (fig. 5.2 and 5.3) (Gawthorpe and Leeder, 2000; Hongxing and Anderson, 2007). This happens due to surface breaching of the individual faults at the Units base, Surface 4, creating increased accommodation space in the hanging-wall (Cartwright et al., 1998; Hongxing and Anderson, 2007). FS5 also features fault-propagation folding as the fault have blindly propagated and folded the strata into a monocline, before at a later point breaching it, and created folding of the Units strata on each side of the FS5, as seen in the outcrops (fig. 5.5).

Since the upper surface on the NW part of the horst and NW of FN1 separates Tectono-Stratigraphic Unit 4 and 6, and not Tectono-Stratigraphic Units 4 and 5, as it does SE of FS1, the two upper surfaces of this Unit are not time-equivalent. The upper surface NW of FN1, surface 8, actually truncates the upper surface extending SE of FS1, surface 5. This makes aspects like comparing thicknesses across the horst difficult, as the Unit have experienced differences in erosion. The upper surface NW of FN1 is a major unconformity and Tectono-Stratigraphic Unit 5 is missing from the succession in this area.

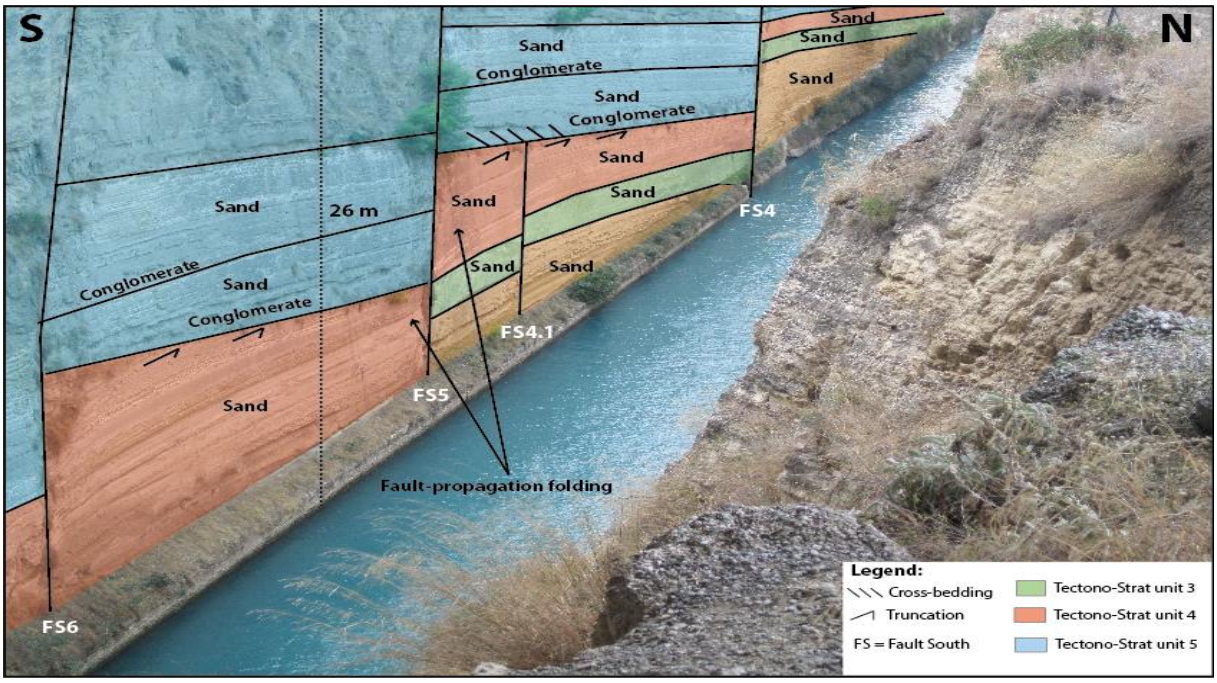

Fig. 5.5: Area between FS4 and FS6, featuring Tectono-Stratigraphic Units 3 to 5. Both FS4 and FS4.1 show normal fault growth with increase in thickness of Tectono-Stratigraphic Unit 4 in the hanging-walls. FS5 show a fault-propagation fold.

5.4.5 Tectono-Stratigraphic Unit 5

Description

Tectono-Stratigraphic Unit 5 is bounded by surface 5 at the base and surface 8 at the top. This Unit consists of deposits of carbonates to siliciclastics, deposited in foreshore to shoreface and offshore marine environments. The unit consists of lithofacies F1, F3, F4, F9, F10, F11, F12, and Facies Association FA3, FA5, and FA7. The Unit has a tabular external geometry. The Tectono-Stratigraphic Unit is divided into 3 smaller Stratal Units separated by minor sequence stratigraphic boundaries (fig. 5.1b and fig. 5.6). It is exposed laterally from FS8 to the central part of the horst (fig 5.1a).

The lowermost stratal unit, Stratal Unit 6 (fig 5.1b), consists of marlstones from the horst until FS3. Between faults FS4 and FS6 it is composed of NW-dipping cross-bedded conglomerate, SE-dipping cross-bedded sand and laminated to massive sand in the lower part of the package. From 0 to 305 m the Unit also features a conglomerate bed in the middle part of the unit, which increases in thickness towards SE, before fining upwards to laminated sand towards the top.

Stratal Unit 7 (fig 5.1b) consists of marlstones from the horst until FS3. From FS3 to FS7 the uppermost part of the unit contains gastropods and bivalves, while surface 6 features a conglomerate lag in the area above the surface, from FS3 to FS8. Other features include a varied abundance of clasts in the area above the conglomerate lag, thin layers of conglomerate, planar- and trough cross-bedded sandstone, and some scattered bivalves which have been noticed in exposed sections between FS5 and FS6. From 0 to 60 m there are also two NW-dipping conglomerate packages.

The uppermost stratal unit, Stratal Unit 8 (fig 5.1b), is composed of marlstones which is both massive and horizontally bedded until FS3. From FS3 to FS4 the Unit has small pieces of shell/clasts near the lower surface. From FS4 to FS8 the stratal unit consists of matrix supported conglomerate. The strata is mainly horizontally bedded, with NW-dipping cross-bedded strata with climbing sets between FS7 and FS8.

The base, Surface 5, marks a change from marine marl and shoreface sandstones below, to marine marl, shoreface sandstones and foreshore conglomerates above. It represents an angular unconformity and a truncational surface in the interval between FS4 and FS5, with a separation of shoreface sandstones below, and foreshore conglomerates above (fig. 5.5). Between FS1 and FS4 the surface does not feature any erosional traits and is characterised as a disconformity.

The Tectono-Stratigraphic Unit thickens from the horst and until FS8. The thickness is decreased immediately SE of FS1, by a wedge-shape of the Unit above (fig. 5.1), which erodes the sediments of this units. The thickness of the Unit is approximately 20 m after the wedge-shape before it increases towards SE. There are thickness increases noticed within the different Stratal Units of Tectono-Stratigraphic Unit 5. These increases are related to changes across faults, from footwall to hanging-wall. These increases are seen across faults FS2, FS3, and FS4. The increase in thickness across these faults is focused around an increase in the middle and upper Stratal Units.

The Unit show a SE tilt on the horst.

Interpretation

The change from marl to shoreface sand and foreshore conglomerate packages in its span SE of FS1 could indicate an antecedent shoreline SE of the sediments which have supplied the area SE of FS4 with more foreshore conglomerates, wave-current influenced sandstones with planar- and trough cross-bedded strata and reworked molluscs. The area spanning NW of FS4 would then have been further into a shelf and offshore environment, reflected in the sediments by the change from coarser grained sediments in SE to offshore marl deposits in the near vicinity of, and on the horst.

The base, Surface 5, does not show any major changes across its surface SE of SF1, until the interval between FS4 and FS5 (fig. 5.5). There, the basal surface separates shoreface sand below from cross-bedded NW-dipping conglomerate above. This change is most likely caused as a result of a relative fall in sea level, which have allowed coastal sediments to be transported from SE with the NW-dipping conglomerate above the surface being deposited in a paleo-basinward direction. There are indications of a sea level fall across the lower surface in the area furthest SE, which is not that prominent towards NW, as the base surface only separates packages of marl on the horst. This may indicate an antecedent shoreline to SE, which supplies the sediments. With an antecedent shoreline in SE, a minor sea level fall would have a larger effect on the deposits furthest SE, as they are closer to the shoreline, then i.e. the marls on the horst, which lies further into and offshore zone and might not experience the sea level variations as much. The angular unconformity and truncation of beds in the Unit below, especially between FS4 and FS5 (fig. 5.5), and FS4.1 breaching the base surface of this Unit and dying out (fig. 5.5), indicate that there have been a time-period between deposition of the Tectono-

Stratigraphic Units 4 and 5. This would allow tilting of the Unit below, and FS4.1 to be buried at the base, before the deposition of Tectono-Stratigraphic Unit 5.

The internal thickness changes seen towards SE seem to revolve around small thickness changes across the faults FS2, FS3 and FS4. Across the faults FS3 and FS4, the uppermost Stratal Unit shows a thickness increase from footwall to hanging-wall, which indicate surface breaching of the faults at the base of Stratal Unit 8 (Hongxing and Anderson, 2007).

Tectono-Stratigraphic Unit 5 features several landward and basinward shifts in facies, all of which are observed in the Fault Blocks furthest toward SE. Two significant surfaces within Tectono-Stratigraphic Unit 5 are Surfaces 6 and 7 that separate Stratal Units 6 from 7, and 7 from 8. Both surfaces separate shoreface sandstones below from foreshore/coastal conglomerates above, implying basinward shift in facies for each case. They feature conglomerate lag and NW-dipping conglomerates above surface 6 and climbing sets of conglomerates, possibly representing foreshore conglomerates, above surface 7.

There are also several minor landward and basinward shift in facies within the individual Stratal Units (fig. 5.6). Stratal Unit 6 has two internal flooding surfaces and one basinward shift in facies, represented by changes from foreshore conglomerates to shoreface sandstones, separating the Stratal Unit into two minor sets of fining upwards strata, separated by a fall in relative sea level (fig. 5.6). In Stratal Unit 7 there is generally a large fining upward from the conglomerate lag and clasts at the base of the Stratal Unit, to upper shoreface sandstones (fig. 5.6). However, in the interval from 0 to 60 m, there are two sets of cross-bedded NW-dipping conglomerate packages, one at the base of the Unit, and one in the centre of the Unit, indicating two flooding surfaces and one basinward shift in facies within the Stratal Unit. Thus this Stratal Unit may also be divided into two smaller sets of fining upwards strata between FS7 and FS8. Stratal Unit 8 consists of the same facies throughout, and does not show any internal landward or basinward shifts in facies.

The fining upwards from foreshore conglomerates to shoreface sandstones indicate several transgressive events during deposition of the sediments, which are cut by a relative sea level fall. The repeated deposits of prograding conglomerates overlain by aggrading shoreface sandstones as the sea level start to rise, indicate a repeated deposition of Lowstand- (LST) and Transgressive Systems Tract (TST), which is then cut off by a falling relative sea level, before repeating itself (Catuneanu, 2002). The first flooding surface between the conglomerates and sandstones, which show a change from LST to TST is termed a *Maximum Regressive Surface*

(Helland-Hansen and Martinsen, 1996), while the base of the LST, created after a sea level fall, is interpreted as a *Correlative conformity* sensu Hunt and Tucker (1992).

A series of transgressive events cut off by a fall in relative sea level, which is seen throughout Tectono-Stratigraphic Unit 5, is characteristic of an uplifting shoreline, which the Corinth Canal area features (Collier, 1990).

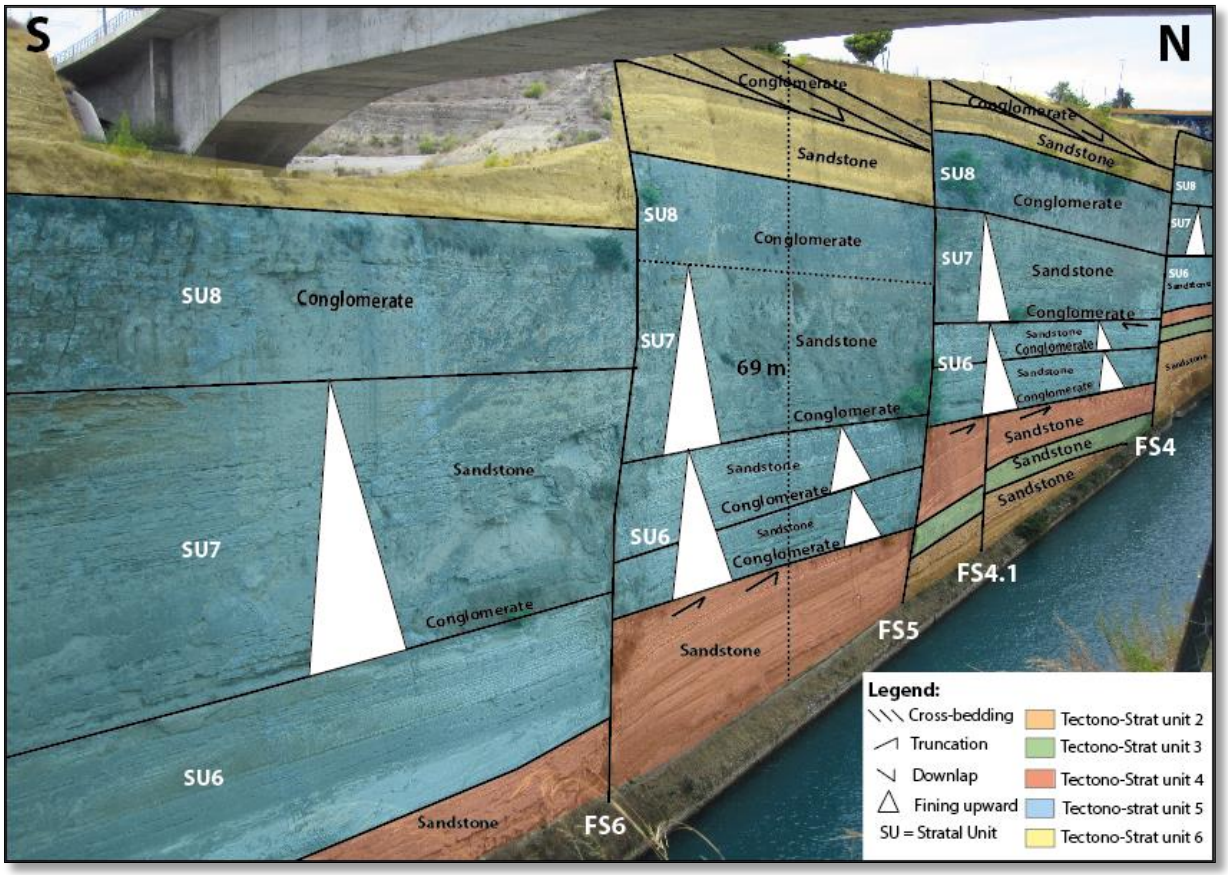

Fig. 5.6: Fault Blocks between faults FS4 and FS6, with stratal units 6 and 7 within Tectono-Stratigraphic Unit 5 showing fining upwards trends. Stratal Unit 6 shows two smaller fining upwards packages, with Stratal Unit 7 showing a fining upwards throughout its package. Stratal Unit 8 consist of the same facies throughout the stratal unit and does not feature any internal facies shifts.

The interpretation of shifts between shoreface and foreshore/coastal conglomerate deposits are supported by Papanikolaou et al. (2015) who have been able to take core samples in the south-eastern area of the canal, near the Saronic Gulf (fig. 5.7). Their core logs, taken down to 35 to 50 m depth, indicate the same kind of interbedding between foreshore/coastal conglomerates and shoreface sandstones, at depths which approximately correspond to the section found above surface 4. Their core logs show much larger sections of gravel and conglomerate interpreted as coastal conglomerates, and thinner sections of shoreface deposits. This implies sediment supply for Tectono-Stratigraphic Units 4 to 6 from the SE, with their core logs possibly taken more proximal to a possible SE antecedent shoreline (fig. 5.7). This would create a section from SE

to NW in the canal with a close by shoreline near the Saronic Gulf, with much deposits of coastal conglomerates as stated by Papanikolaou et al. (2015), before it changes towards less conglomerate and more shoreface sand in the sections present in figure 5.6, and then a change towards offshore marl deposits near and on the central horst, furthest NW of a possible SE shoreline (fig. 5.7). Other signs supporting a close-by shoreline SE of the interpreted sections, are the conglomerate packages which almost exclusively show a dip towards NW, in what would be a paleo-basinward direction, and the fining of strata towards NW in Tectono-Stratigraphic Unit 5, where the deposits of marlstones are deposited in the area around the horst, in an area distal of a possible SE antecedent shoreline (fig. 5.7).

Fig. 5.7: 3D view of the Canal based on Google Earth. Locations of the boreholes taken by Papanikolaou et al. (2015), the area present in the fig. 5.6 and the central horst are placed within the map to give the reader an approximate overview of the placement of the previous described features.

5.4.6 Tectono-Stratigraphic Unit 6

Description

Tectono-Stratigraphic Unit 6 is bounded by surface 8 at the base and its top is eroded by present day topography. The Unit consists of lithofacies F3, F4, F5, F6, F7, F8, F9, F10, F11, and F12, and Facies Associations FA3, FA4, and FA5. Tectono-Stratigraphic Unit 6 consists of six smaller Stratal Units (fig. 5.1b and 5.8), which can be summarized as three units consisting of foreshore conglomerates (FA3, FA4) and three units consisting of shoreface sandstones (FA5). The Unit extends across the entire length of the interpreted canal area.

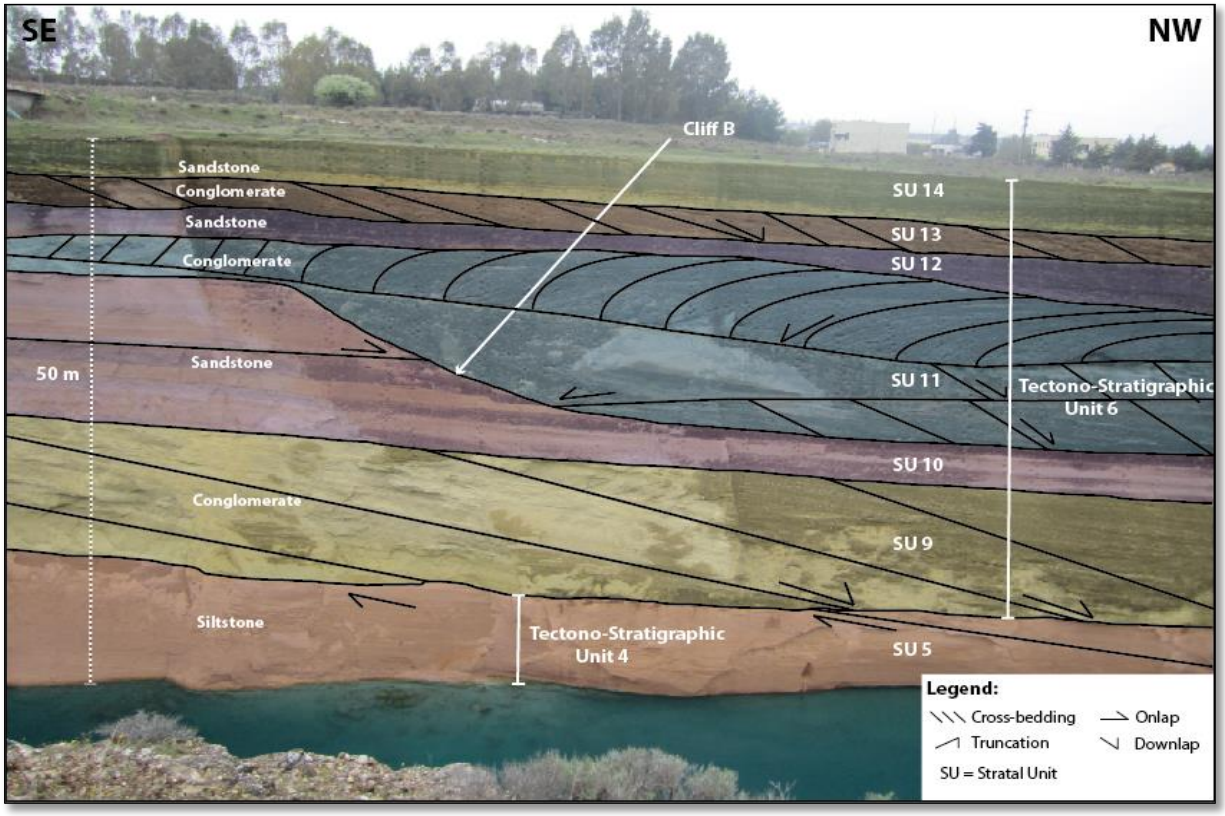

Fig. 5.8: Tectono-Stratigraphic Units 4 and 6 in the area around paleo cliff B. Tectono-Stratigraphic Unit 6 is divided into 6 smaller Stratal Units. Tectono-Stratigraphic Unit 6 shows intercalation of foreshore conglomerates and shoreface sandstones.

Stratal Units 9, 11 and 13 (fig. 5.8) consist of beach/foreshore conglomerates with low-angled cross-beds dipping towards NW, downlapping onto the basal surface (fig. 4.3). There are other structures seen within each of the stratal units. SE-dipping high-angled foresets with conglomerates, a large erosive spit deposit (FA4) are seen within Stratal Unit 11 (fig. 4.5 and fig. 5.8). Shoreface sandstones and conglomerates featuring coarse grained sand and planar- and trough cross beds are found underneath the cross-bedded conglomerate in Stratal Unit 11 (fig. 4.7). In the lower part of stratal unit 11 there are interbedded planar-cross bedded

sandstones with a SE-directed dip within the cross-bedded NW-dipping conglomerates (fig. 4.4). A package of massive sandstones is deposited beneath the cross-bedded NW-dipping conglomerate in some areas in Stratal Unit 9. SE of FS1 Stratal Unit 9 consists of shoreface sandstones with shelly sand and cross-bedded NW-dipping packages of conglomerate, sand and shells.

Stratal Units 10, 12 and 14 consist of shoreface deposits with high to low abundance of bivalves, gastropods and corals (fig. 4.6), cemented carbonate bands (fig. 4.1g), planar- and trough cross-bedded sandstones, and subparallel bedded to massive sandstones. The sandstones are often poorly lithified.

The basal surface, surface 8, stretches across the entire interpreted area. NW of FN1 the surface marks a change from marine offshore marlstones and siltstones, and shoreface sandstones below, to foreshore/beach conglomerate above. Southeast of FS1 two contrasting facies patterns occur across Surface 8: an appearance of basinwards shift immediately SE of FS1 (marl below, conglomerates above) and landwards shift of facies on the rest of the fault blocks (foreshore cross-bedded conglomerates below, shoreface sandstones above). On the horst, the surface features strongly lithified calcite, in addition to karstic features like small depressions noticed in various areas along the surface where the underlying Unit consists of marl. It features truncation and angular unconformities in several places along its extent. The surface erodes the entire length of the horst, where Tectono-Stratigraphic Unit 5 eventually is completely eroded (fig 5.1). Paleo-cliff A is created on the base surface immediately SE of FN1 (fig. 5.2).

Tectono-Stratigraphic Unit 6 shows an increase in exposed thickness towards NW and SE of the horst. No upper boundary make thickness measurements impossible, but there is generally an exposed thickness increase seen over a larger wavelength, and generally not affected by faults. The individual Stratal Units increases in thickness as they are deposited across hundreds of metres NW of FN1 (fig 5.1). The cross-bedded conglomerate of stratal unit 9, 11 and 13 show vertical up building and lateral outbuilding NW of FN1. The sandstone bodies of stratal unit 10, 12 and 14 show an increase in thickness with vertical up building NW of FN1. There are larger variations within the Stratal Units of the Tectono-Stratigraphic Unit, i.e. as paleo-cliffs A, B, C and D affect the deposits, where there is an increase of foreshore conglomerates above the cliffs, with erosion and decrease of thickness in the shoreface sandstones below. Due to the formation of paleo cliffs B (fig. 5.8) and C on its upper boundary, Stratal Unit 10 show a

decrease in thickness of approximately 18 m NW of FN6. Stratal Unit 11 however, show an increase of approximately 18 m, due to the formation of paleo cliffs B and C on its basal surface.

Interpretation

The basal surface, surface 8, is split into two parts. NW of FN1 it divides Tectono-Stratigraphic Unit 4 from 6, whereas southeast of FS1 it divides Tectono-Stratigraphic Units 5 and 6. To the northwest of FN1 the basal surface shows a change from marine marl, shoreface sandstones and offshore siltstones to foreshore conglomerate deposits (fig. 5.8). This change indicates a major basinward shift in deposits. This indicates a substantial period of time across this surface NW of FN1, as the entire package of Tectono-Stratigraphic Unit 5 is missing from the exposed outcrops NW of FN1. The surface shows signs of subaerial exposure with karstic features and strongly lithified calcium carbonate, which indicate calcrete formation, on the entire length of the horst. This indicates that at least the horst has experienced subaerial exposure before deposition of Tectono-Stratigraphic Unit 6. Creation of cliff A on the basal surface is due to a higher frequency stillstand fluctuation in sea level, during a lower frequency sea level fall, allowing waves to erode the underlying strata (Collier, 1990; Papanikolaou et al., 2015). This sea level fall has most likely occurred after deposition of Tectono-Stratigraphic Unit 5, and not after Tectono-Stratigraphic Unit 4, as the entire length of this surface on the horst feature the karst and calcrete formations, and there are no indication of a major sea level fall between the marine marls deposited in Tectono-Stratigraphic Units 4 and 5 on the horst.

Increased accommodation space have been created SE of FS1, due to surface breaching of the fault at the basal surface. Subsidence of the hanging-wall leads to isostatic uplift of the footwall, in this case the horst. This leads to subaerial exposure of the horst. The surface breaching have created a wedge-shape of Stratal Unit 9 towards FS1, with deposits of conglomerates possibly derived from the subaerial exposed horst (fig. 5.9). With an antecedent shoreline further towards SE supplying the area SE of the horst, there may be areas where the lower surface SE of FS1 changes between landward and basinward shift in deposits. The area closest to FS1 may have received conglomerates either via longshore transport from north as stated by Collier (1990), or erosion from the subaerial exposed horst. This would create an appearance of basinward shift in facies near FS1 where there previously have been deposited offshore deposits of marl below, during a highstand sea level. The fault blocks furthest towards SE however, may have been closer to an antecedent shoreline, where there have been several variations in sea level. The shoreline during deposition of Tectono-Stratigraphic Unit 5 may have been a bit further towards NW, with foreshore conglomerates depositing further NW below surface 8. Following surface

breaching of FS3 and FS5 at the base of this Unit, it would cause further subsidence of the fault blocks in SE, and lead to a retrogradation and the shoreline moving further SE. This would create a landward shift in facies in the fault blocks furthest to SE, as illustrated in fig. 5.9.

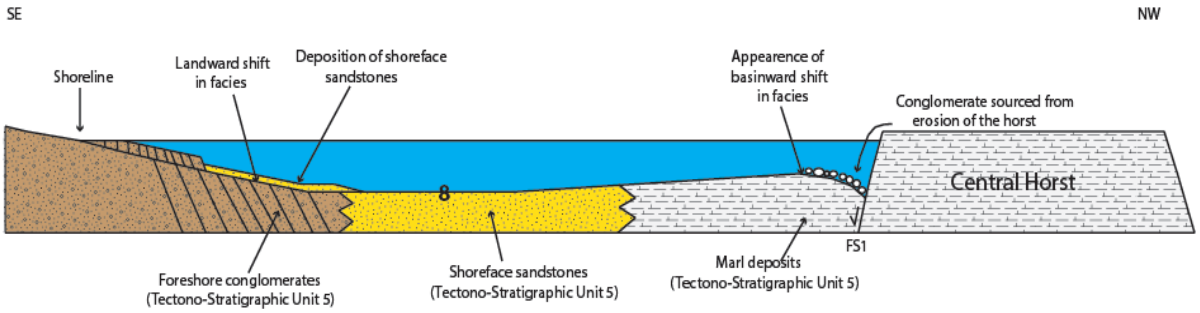

Fig. 5.9: Sketch of a possible evolution of Stratal Unit 9 SE of the horst, with surface 8 showing a landward shift in facies in SE, with an appearance of basinward shift in facies in the vicinity of FS1.

Stratal Unit 9 show two different sediment bodies on each side of the horst, with sediments SE of FS1 consisting of a mix of shoreface sandstones with some areas of cross-bedded conglomerate (fig. 5.9), whereas the sediments NW of FS1 consists of cross-bedded NW-dipping conglomerate. A possible reason for the change in sediments might be that during the lowering of sea level between Tectono-Stratigraphic Units 5 and 6, and subaerial exposure of the marls on the horst as a result of surface breaching of FS1 and FN1 creating isostatic uplift of the horst, there may have been a smaller water body between the central horst and a possible antecedent shoreline towards SE (fig.5.9), in addition to a new shoreline at the SE and NW part of the horst. This would create time-equivalent strata with two separate lithology-bodies on each side of the horst. With small inputs of foreshore sand with NW-dipping cross-beds and shoreface sand SE of FS1, the package has most likely received sediment from an antecedent shoreline SE of the horst (fig. 5.9). The conglomerate with a NW-dipping cross-beds NW of FN1, could then have been transported by longshore currents from the north, and started to prograde towards NW as suggested by Collier (1990), or through erosion of the subaerial exposed horst.

The Tectono-Stratigraphic Unit towards NW feature several facies shift within, with both landward and basinward shift in facies (fig. 5.8). There are 5 significant sequence boundaries, with 2 basinward and 3 landward shifts in facies that separates the different Stratal Units within Tectono-Stratigraphic Unit 6 (fig. 5.8). The progradational and aggradational style of the foreshore conglomerates, which happens after a period of falling sea level, overlain by a flooding surface and aggradational shoreface packages above, indicates that the Tectono-

Stratigraphic Unit is comprised of successions of Lowstand- (LST) and Transgressive Systems Tracts (TST) (Catuneanu, 2002). Progradational and aggradational packages of foreshore conglomerates, in combination with them overlying a subaerial unconformity, are indicators for a Lowstand Systems Tract (Catuneanu, 2002). The Transgressive Systems Tract deposits are then deposited when the sea level increases and aggrading shoreface sandstones replaces the progradational conglomerate bodies. These packages of foreshore conglomerates and shoreface sandstones are separated by a *Correlative conformity*, sensu Hunt and Tucker (1992), at the base of the progradational and aggradational foreshore conglomerates of LST, with a *Maximum regressive surface* (Helland-Hansen and Martinsen, 1996) separating LST and TST, between the foreshore conglomerates and shoreface sandstones. These are then cut off by a fall in sea level, before the deposition repeats itself. These repeated transgressive events with fining upwards strata, capped by a relative sea level fall are, as stated in Tectono-Stratigraphic Unit 5, common on shorelines featuring a continuing uplift (Collier 1990).

6. Discussion

6.1 Tectono-Stratigraphic evolution of the Corinth Canal deposits

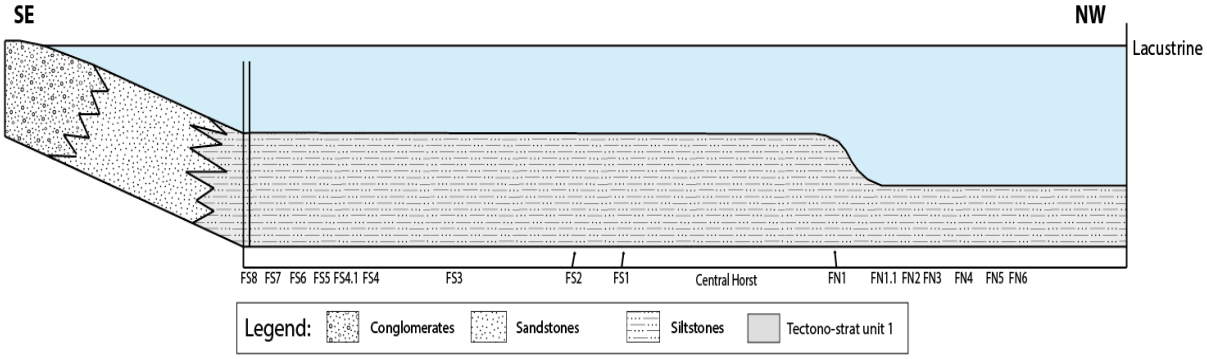

Fig. 6.1: Deposition of Tectono-Stratigraphic Unit 1. The drawing of faults below the strata indicates that they are blindly propagating, but they have not breached any of the present surfaces at the time. Not to scale.

Deposition of Tectono-Stratigraphic Unit 1 in a fluvial-lacustrine basin (fig. 6.1). The Unit consists of lacustrine siltstone in a lower sublittoral to upper profundal/deep water lacustrine setting (FA2) (Bohacs et al., 2000). FN1 is blindly propagating through the deposits creating a monocline structure. Also blind propagation of FS1 and FS2. The relative position of the faults are marked, even though they are not affecting the strata packages yet.

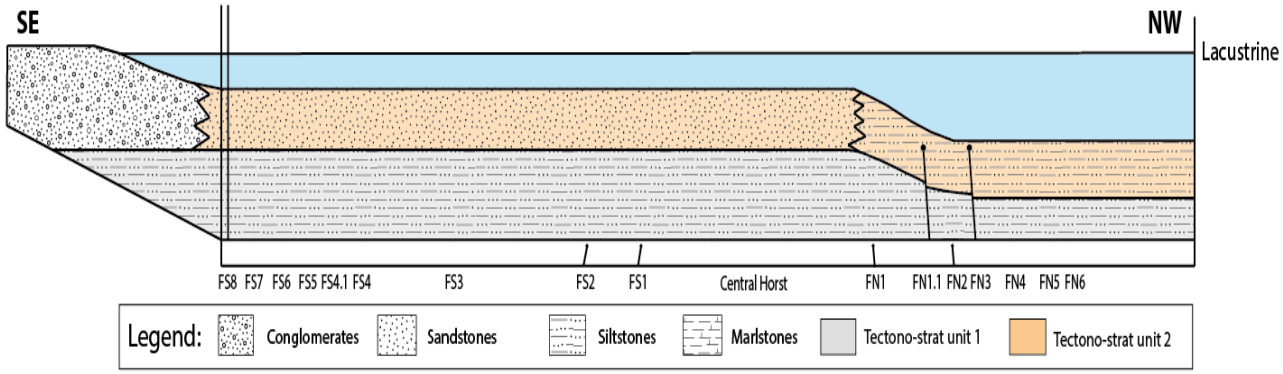

Fig. 6.2: Deposition of Tectono-Stratigraphic Unit 2. The drawing of faults below the strata indicates that they are blindly propagating, but they have not breached any of the present surfaces at the time. Not to scale.

Deposition of Tectono-Stratigraphic Unit 2 in a fluvial-lacustrine basin following a progradation and basinward shift of facies across the base key stratal surface (fig. 6.2). Southeast of FN1 the Unit consists of lower littoral to upper sublittoral sandstones (FA1), with lower sublittoral to upper profundal/deep-water siltstone (FA2) NW of FN1 (Carroll and Bohacs, 1999; Bohacs et al., 2000). The change from siltstones to sandstones across FN1, is due to an increase in water depth across FN1, due to the monocline structure created by FN1

propagating blindly. FN1 continues to propagate blindly through Tectono-Stratigraphic Unit 2, creating a monocline structure in this Unit. Blind propagation of FN1, FN1.1, FN2, FN3, FS1, and FS2 are ongoing.

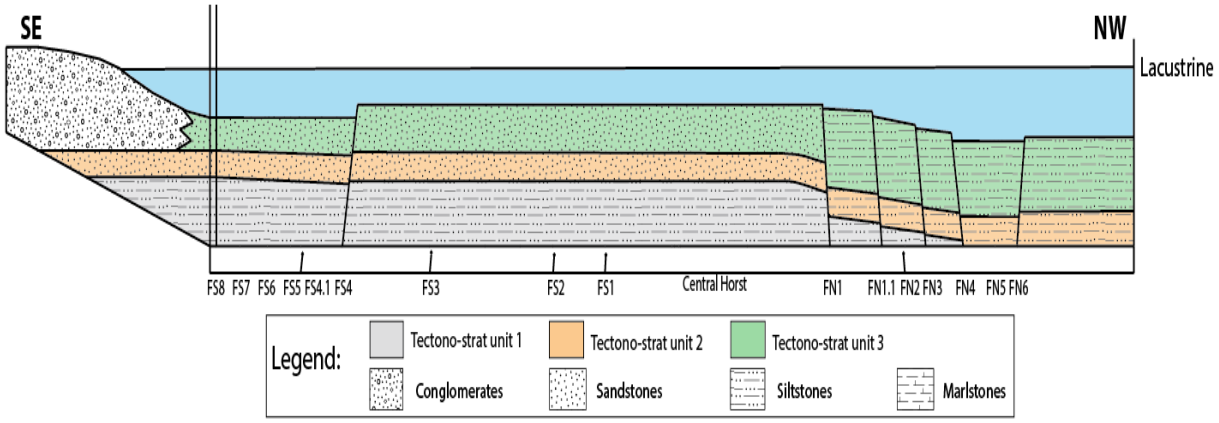

Fig. 6.3: Deposition of Tectono-Stratigraphic Unit 3. The drawing of faults below the strata indicates that they are blindly propagating, but they have not breached any of the present surfaces at the time. Not to scale.

Deposition of Tectono-Stratigraphic Unit 3 in a fluvial-lacustrine basin (fig. 6.3). The Unit consists of lower littoral to upper sublittoral zone sandstones (FA1), SE of FN1, and lower sublittoral to upper profundal siltstones (FA2), NW of FN1 (Bohacs et al., 2000). The change from sandstones to siltstones across FN1, is due to the earlier monocline structure of the sediments across FN1, which have created deeper water depths NW of FN1 (Willsey et al., 2002). FN1 breaches the upper surface of Tectono-Stratigraphic Unit 3 after deposition of this stage, which creates the fault-propagation folding seen in the exposed outcrops. Surface breaching is also experienced by the faults FN1.1, FN3, FN4, FN6 and FS4, with blind propagation of FN2, FS1, FS2, FS3, and FS4.1.

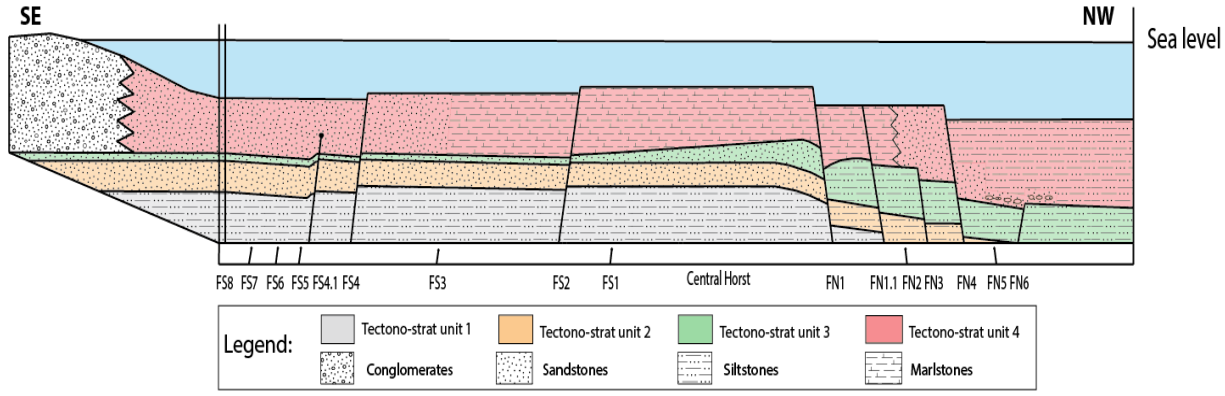

Fig. 6.4: Deposition of Tectono-Stratigraphic Unit 4. The drawing of faults below the strata indicates that they are blindly propagating, but they have not breached any of the present surfaces at the time. Not to scale.

Deposition of Tectono-Stratigraphic Unit 4 in a shoreface to offshore marine setting with FA3, FA5, FA6, and FA7, after a major landward shift in facies due to a major flooding of the Canal

area after deposition of Tectono-Stratigraphic Unit 3 (fig. 6.4). A transgressive lag is found from FN2 to immediately NW of FN6. Sediment supply from SE is inferred due to a coarsening of grains toward SE. Thickness increases are due to surface breaching faults at the base boundary of this Unit. Surface breaching of faults FN1, FN4, FS2, and FS4 at the upper boundary of Tectono-Stratigraphic Unit 4 with blind propagation of FN2, FN3, FN5, FS1, FS3, FS4.1, FS5, FS6, and FS7. FN1 and FN6 are buried at this point.

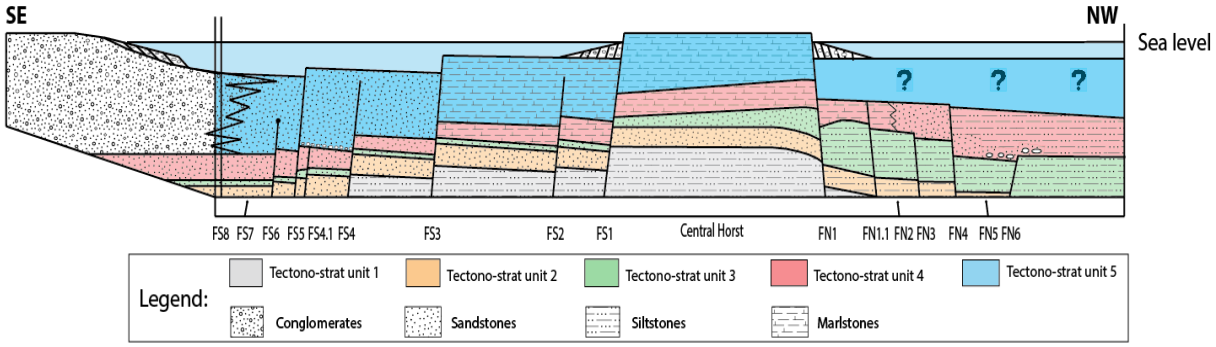

Fig. 6.5: Deposition of Tectono-Stratigraphic Unit 5. The drawing of faults below the strata indicates that they are blindly propagating, but they have not breached any of the present surfaces at the time. Not to scale.

Deposition of Tectono-Stratigraphic Unit 5 in a foreshore, shoreface and offshore marine setting with a base level fall across the lower boundary of the Unit SE of FS1 (fig. 6.5). Central horst is exposed after deposition due to surface breaching of FS1, with subsiding fault blocks towards SE, causing isostatic uplift of the horst, which may, in combination with lowering of sea level, be responsible for the subaerial exposure. Longshore currents transporting conglomerate start depositing NW-dipping foreshore conglomerates NW as stated by Collier (1990). The area SE of the horst is supplied with conglomerates either via longshore currents or due to erosion of the subaerial exposed horst, depositing immediately SE of FS1. Surface breaching of FN1, FS1, FS3, and FS5 at the upper boundary of Tectono-Stratigraphic Unit 5. Blind propagation of FS2, FS4, FS6 and FS7. FS4.1 and FN1.1 are buried at the base surface of Unit 5, with FN6 buried at the base of Unit 4. In the faults NW of FN1 it is not possible to indicate surface breaching as Tectono-Stratigraphic Unit 5 is missing from the exposed outcrops NW of the horst.

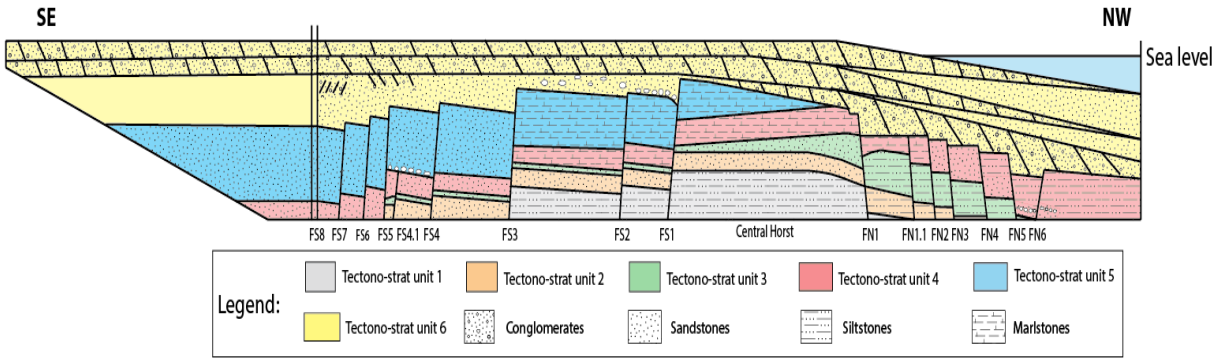

Fig. 6.6: Deposition of Tectono-Stratigraphic Unit 6. Not to scale.

Deposition of Tectono-Stratigraphic Unit 6 in a foreshore to shoreface environment with FA3, FA4, FA5, and FA6 (fig. 6.6). The Unit consist of recurring foreshore and shoreface deposits. The deposits occur due to changes in base level with regression followed by transgression. This repeats itself to create several units of foreshore-to-shoreface deposits, separated by a base level fall. Every fall in sea level is accompanied by a wave eroded cliff at the upper surface of the shoreface sandstones. They are created due to wave erosion during periods of sea level stillstand as the relative sea level sinks. No indications of fault activity within Tectono-Stratigraphic Unit 6, and the faults are drawn up to the base of surface 8, with later surface breaching of the sediments above.

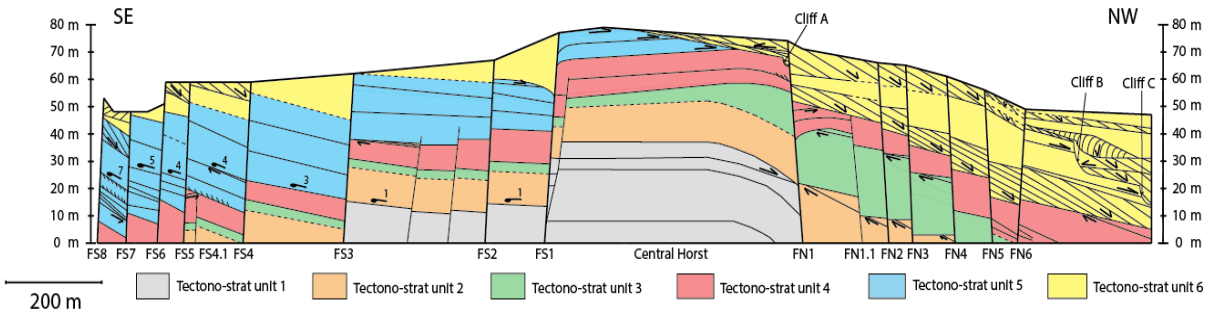

Fig. 6.7: The present exposed outcrops in the Corinth Canal.

The exposed outcrops of the Corinth Canal at present time, due to uplift and erosion. The faults are cutting through all of the strata, with exception of FN1.1 and FS4.1, which are buried at surfaces 5 and 8 (fig. 6.7). The outcrops are exposed up to 80 m above sea level due to a uplift of 0.3 mm/year affecting the Corinth Isthmus during at least the last 205 000 years (Collier, 1990; Collier et al., 1992; Dia et al., 1997).

6.2 Stratigraphic ages

Age determinations of different stratigraphic packages are particularly helpful in determining depositional control on sediments, especially in reference to well documented eustatic sea level changes. Studies by Vita-Finzi and King (1985), Collier (1990), and Dia et al. (1997) have produced age determinations for some of the stratigraphic packages in the canal, located in Table 6.1 below. Vita-Finzi and King (1985) used ^{14}C-dating method on bivalves, while both Collier (1990) and Dia et al. (1997) used U-series dating on corals.

Table 6.1: The placement of the ages determined by Vita-Finzi and King (1985) Collier (1990), and Dia et al. (1997) in reference to this study`s Tectono-Stratigraphic and Stratal Units. Two numbers within each column indicate dating on two different samples, i.e. the 193 000 age in Dia et al. (1997), is derived from a sample taken at 50 m height in Stratal Unit 14, while the 212 000 age is taken on a sample located at 40 m height in Strata Unit 14.

This studys Tectonic-Stratigraphic Unit	This studys Stratal Unit	Vita-Finzi and King (1985) ages	Collier (1990) ages	Dia et al. (1997) ages
Tectono-Stratigraphic Unit 4	Stratal Unit 5		Older than 350 000 year	Older than 350 000 year
Tectono-Stratigraphic Unit 6	Stratal Unit 12		ca. 312 000	ca. 306 000
Tectono-Stratigraphic Unit 6	Stratal Unit 14	ca. 35 000 ca. 38 000	ca 205 000	ca. 193 000 ca. 212 000

The ages from the Vita-Finzi and King (1985) study have not been taken into account in this study, with the dating method ^{14}C only working for samples younger than 50 000 years old, in addition to the similarities between Collier (1990) and Dia et al. (1997) ages.

6.3 Correlation of the Corinth Canal deposits and the Upper Quaternary eustatic variations

As described in Chapter 5, there are several changes in sea level which affect the stratigraphic packages in the Canal. These changes may derive from eustatic sea level variations, or due to tectonic activity. A possible way to determine if these are controlled by major tectonic forces, or by major changes in eustatic sea level, is to correlate the available ages (Table 6.1) with well-known eustatic sea level curves for the Upper Quaternary (Fig. 6.8) (Labeyrie et al., 1987; Shackleton, 2000; Lea et al., 2002; Waelbroeck et al., 2002; Cutler et al., 2003; Siddall et al., 2007) .

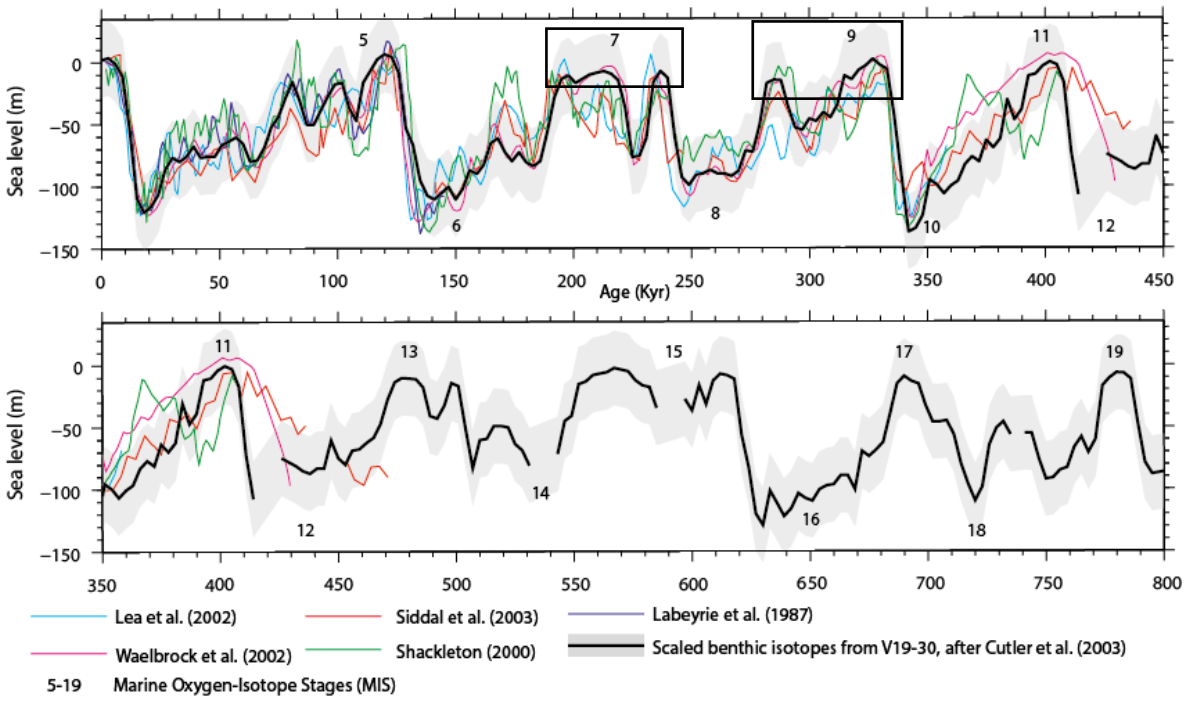

Fig. 6.8: Sea level estimates during the course of the past 800 000 years from a variety of different sources (Labeyrie et al., 1987; Shackleton, 2000; Lea et al., 2002; Waelbroeck et al., 2002; Cutler et al., 2003; Siddall et al., 2003; Siddall et al., 2007). Modified from Siddall et al. (2007).

A change in eustatic sea level could be responsible for the facies changes experienced in the Canal. The ca. 312 000 and 205 000 year ages of corals from Collier (1990) and Dia et al. (1997), are taken from Stratal Units 12 and 14 (shoreface sandstone packages) in Tectono-Stratigraphic Unit 6 (Table 6.1). These ages corresponds to two major sea level highs: Marine Isotope Stage (MIS) 9 (Stratal Unit 12) and MIS 7 (Stratal Unit 14) (fig. 6.8).

According to Collier (1990) each of his sub-sequences, consisting of foreshore to shoreface deposits, were deposited on glacio-eustatic highstands. Collier (1990)`s three sub-sequences are comprised within this studys Tectono-Stratigraphic Unit 6, with Sub-sequence 1 interpreted as Stratal Unit 9 and 10, Sub-sequence 2 as Stratal Units 11 and 12, and Sub-sequence 3 as Stratal Units 13 and 14. With stratal units of foreshore and shoreface depositing during the same highstand, it would give depositional ages for Stratal Units 11 and 12 at MIS 9, and Stratal Units 13 and 14 at MIS 7. This leads to the interpretation of depositional time for Stratal Units 9 and 10 at the highstand MIS 11.

Tectono-Stratigraphic Units 4 and 5 both feature offshore marine marls during its deposition, which indicate a highstand sea level during deposition of these sediments. In regards to the interpreted ages for Tectono-Stratigraphic Unit 6, Tectono-Stratigraphic Unit 4 and 5 are placed

at the highstands of MIS 15 and MIS 13, with ages respectively between 560 000 to 620 000 and 470 000 to 530 000 years old.

Tectono-Stratigraphic Unit 4 and Tectono-Stratigraphic Units 1,2, and 3, are separated from each other by several rises in sea level, causing the deposits to change from lacustrine (Tectono-Stratigraphic Units 1, 2, and 3) to marine offshore marls (Tectono-Stratigraphic Unit 4). The marine incursion above lacustrine deposits could have been caused by the major rise in sea level seen between MIS 15 and 16 (fig. 6.8). This would imply deposition of the lacustrine deposits of Tectono-Stratigraphic Units 1-3 during MIS 16 and give the lacustrine deposits an age of approximately 620 – 680 000 years old.

Table 6.2: These ages are interpreted due to a correlation between the deposits of the Corinth Canal and well-known eustatic sea level curves (Labeyrie et al., 1987; Shackleton, 2000; Lea et al., 2002; Waelbroeck et al., 2002; Cutler et al., 2003; Siddall et al., 2003; Siddall et al., 2007). The only certain ages are of Stratal Unit 11 and 12, and 13 and 14, with ages of 306 000 and 200 000 years respectively. In addition, Tectono-Stratigraphic Unit 4 has an age older than 350 000 years.

Tectono-Stratigraphic Units	Stratal Units	Base surface	Isotope Stage	Approximate ages
6	14 (Shoreface)	13	7	190 000 – 240 000
	13 (Foreshore)	12	7	190 000 – 240 000
	12 (Shoreface)	11	9	280 000 – 340 000
	11 (Foreshore)	10	9	280 000 – 340 000
	10 (Shoreface)	9	11	390 000 – 420 000
	9 (Foreshore)	8	11	390 000 – 420 000
5	8 (Marine)	7	13	470 000 – 530 000
	7 (Marine)	6		
	6 (Marine)	5		
4	5 (Marine)	4	15	560 000 – 620 000
3	4 (Lacustrine)	3	16	620 000 – 680 000
2	3 (Lacustrine)	2	16	620 000 – 680 000
1	2 (Lacustrine)	1	16	620 000 - 680 000
	1 (Lacustrine)			

These interpretations indicate that the deposits exposed in the Canal have a high correlation with the Upper Quaternary Glacio-Eustatic Sea Level Curve. Deposition of these highstand deposits, which show a transgressive pattern cut off by relative sea level fall, if derived from tectonism, would have to be created by major 100 000 year reversals in tectonic activity creating a repetitive change between foreshore and shoreface deposits in the upper Stratal Units. Collier (1990) states that no such major tectonic structures are found within the Canal area, indicating that the highstand deposits could not be derive from tectonic reversals. This implies that

Tectono-Stratigraphic Units 4 to 6, above the 620 000 year surface, are records of low-frequency global eustatic sea-level cycles (100 000 years), which have developed over the past 620 000 years and been deposited during five Glacio-Eustatic highstands, while Tectono-Stratigraphic Unit 1 to 3 were deposited during a Glacio-Eustatic lowstand.

6.4 Variations in relative sea level and local tectonic control

Interpretations in the previous subchapter indicate a deposition of Tectono-Stratigraphic Units 4 to 6 during Glacio-Eustatic highstands. However, there are several minor landwards and basinward shifts in deposits within Tectono-Stratigraphic 5 and 6. Foreshore conglomerates of Tectono-Stratigraphic Unit 6, featuring progradation and aggradation, found in Stratal Units 9, 11 and 13, are indicative of Lowstand periods in a sea level curve (Catuneanu, 2002). Deposition of prograding and aggrading packages during the transgression and highstand of a eustatic sea level curve, indicate that these strata packages have been deposited due to higher frequency shifts in the sea level, which have affected the Canal during deposition.

Tectono-Stratigraphic Unit 5 feature several landward and basinward shifts in facies within. The continued interpretation of fining upwards transgressive packages, capped by a fall in relative sea level, are also due to higher frequency relative sea level changes. Collier (1990) suggested that transgressive packages capped by a relative fall in sea level were characteristic of a continuing uplifting shoreline, as is seen on the Corinth Isthmus. If these changes in relative sea level are due to higher frequency variations in a sea level curve or due to tectonic changes is unknown.

Although the deposits fit with the Glacio-Eustatic Sea Level Curve, the Canal sediments are deposited within an active rift, which implies that tectonics have played a role during deposition, which is also evident by deposits in the Canal.

Local faults within the Canal have controlled changes experienced in relative sea level. In Tectono-Stratigraphic Units 1 to 3 a blind propagating fault creating a monocline, is responsible for an increase in relative sea level NW of the monocline, which have led to changes in facies from sandstone to siltstone, due to an increase in relative sea level (fig. 6.1 to 6.3). Surface breaching of faults before deposition of Tectono-Stratigraphic Unit 4, 5 and 6 has also been responsible for local increases in relative sea level.

Tectonic activity have been present during what it is interpreted as rotation of the individual Fault Blocks NW of FN1. The rotation is evident between each of the Tectono-Stratigraphic Units, as Tectono-Stratigraphic Units 3, 4 and 6 all truncates tilted strata in the underlying Tectono-Stratigraphic Units in some of the Fault Blocks NW of FN1 (fig 5.1). This implies tectonic activity present between depositions of each of the Tectono-Stratigraphic Units, causing rotation of fault blocks. Possible tectonic activity would be during MIS16 for rotation of Tectono-Stratigraphic Units 2 and 3, with tectonic activity rotating Tectono-Stratigraphic Unit 4 between MIS 11 and MIS 15. Post-depositional rotation of Fault Blocks is present SE of FS1, where tectonic activity has created N to NW tilted strata, with increasing tilt-angle further towards SE (fig. 5.1).

The subaerial exposure of the horst, after deposition of Tectono-Stratigraphic Unit 5, may come as a result of local tectonism, possibly in combination with relative sea level changes. FS1 surface breaches the upper surface of Tectono-Stratigraphic Unit 5, which creates subsidence in the hanging-wall and causes an isostatic adjustment of the footwall, in this case the horst, which might have caused enough uplift to expose the horst to subaerial conditions. This would have happened sometime between 470 000 and 420 000 years ago.

6.5 Correlating the Canal deposits and surfaces with close by offshore basins in the Corinth Rift

The Gulf of Corinth, Gulf of Lechaion and the Gulf of Alkyonides have been extensively studied through seismic imaging (Leeder et al., 2005; Bell et al., 2009; Taylor et al., 2011; Charalampakis et al., 2014; Nixon et al., 2016). Based on the main lithological characteristics of the Corinth Canal deposits and the interpreted ages obtained from the Glacio-Eustatic Sea Level Curve (Labeyrie et al., 1987; Shackleton, 2000; Lea et al., 2002; Waelbroeck et al., 2002; Cutler et al., 2003; Siddall et al., 2003; Siddall et al., 2007) (Table 6.2), a correlation with the offshore deposits of the Corinth Rift is made. The ages of several of the surfaces discovered in the Canal are similar to the ages of major flooding surfaces found within the Gulf of Corinth offshore basin, which implies a lateral extension of these surfaces into the offshore deposits (Nixon et al., 2016).

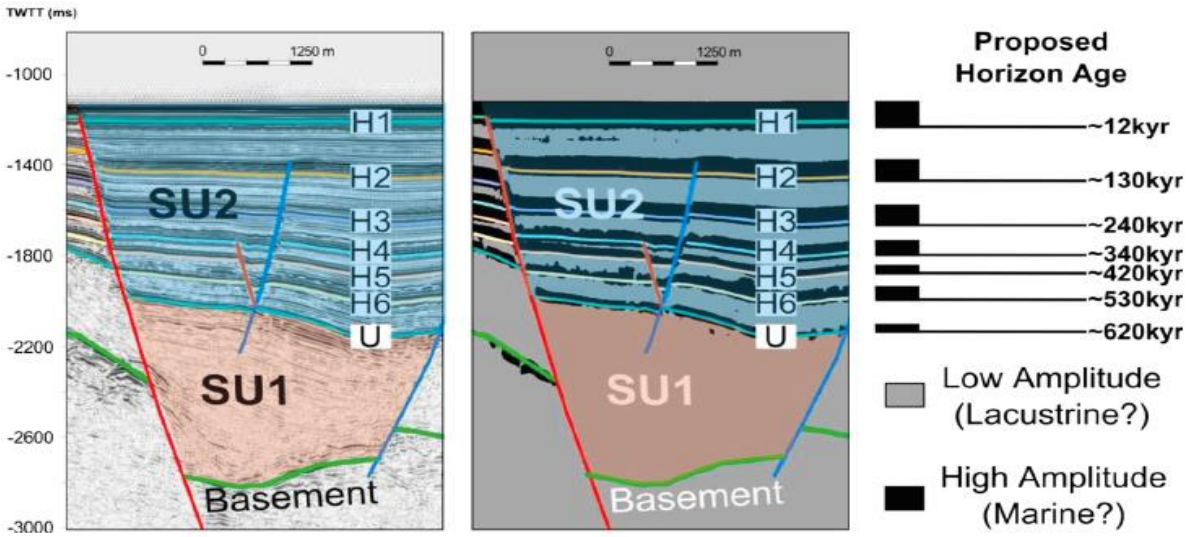

Fig. 6.9: The two Seismic Units, marked SU1 (Seismic Unit 1 – Red) and SU2 (Seismic Unit 2 – Blue), constitutes the Gulf of Corinth Offshore deposits. From Nixon et al. (2016).

The horizon between Seismic Unit 1 and 2 (fig. 6.9), horizon "U", is a major basin-wide unconformity, showing a change from a large package of lacustrine deposits below, to marine deposits above, acting as a large flooding surface and showing a major landward shift in deposits across the horizon (Nixon et al., 2016). This surface is interpreted at 620 000 years old by Nixon et al. (2016). This vertical change in facies and approximate age corresponds to surface 4 in this study, which also feature a change from a large deposition of lacustrine sediments below, to marine deposits above. Surface 4 show a major landward shift in deposits, with an age interpreted at approximately the same 620 000 years old as surface "U".

Nixon et al. (2016) interprets several flooding surface within Seismic Unit 2 (fig. 6.9). They are determined as 530, 420, 340, 240, 130, and 12 000 years old, featuring changes from lacustrine deposits below to marine deposits above, with a major landward shift in deposits across each horizon (Nixon et al., 2016). A major difference from the Gulf of Corinth deposits to the Corinth Canal deposits, is that the Corinth Canal deposit does not feature lowstand/lacustrine deposits in between the marine deposits above the 620 000 year surface. The Corinth Canal outcrops only feature the Glacio-Eustatic Sea Level highstands, while the Gulf of Corinth feature deposits of both Glacio-Eustatic highstands and lowstands.

With this knowledge it is possible to correlate several of the surfaces which appear to show basinward shift in the Canal, with major flooding surfaces in the Gulf. Key stratal surfaces 5 and 8, which in the Canal feature a change from respectively offshore marl to offshore marl, and offshore marl to foreshore conglomerate, with an interpretation of relative sea level fall in between the deposits, are interpreted with ages similar to flooding surfaces H6 and H5 in the

Gulf of Corinth (Table 6.2 and 6.3) (Nixon et al., 2016). Surfaces 5 and 8 only show a basinward change in deposits in the Canal due to the missing lowstand/lacustrine deposits of MIS 14 and 12, which are present in the Gulf of Corinth. Both surfaces in the Canal feature indications of a fall in relative sea level, i.e. subaerial exposure, where lacustrine deposits may have accumulated in the Gulf of Corinth. With a lacustrine deposition in between the marine deposits, they would both show a major flooding surface in the Canal, such as in the Gulf of Corinth and is therefore possible to correlate (Table 6.3).

A similar interpretation can be made for surfaces 10 and 12 in the Canal outcrops, which both feature a change from shoreface sandstones below, to foreshore conglomerate above, but are interpreted with similar ages to flooding surfaces H4 and H3 in the Gulf of Corinth (Table 6.2 and 6.3) (Nixon et al., 2016). Both surfaces 10 and 12 show a fall in relative sea level in the Canal, with wave-eroded cliffs characterising the surfaces. During these sea level falls, lowstand/lacustrine deposits of the Gulf could have accumulated during MIS 10 and 8, making them possible to correlate with H4 and H3. This is in line with Collier (1990) `s interpretation, where he have interpreted the formation of wave-eroded cliffs on surfaces 10 and 12 during lacustrine events.

Table 6.3: Approximate ages of surfaces featuring in the Canal outcrops, with correlation of flooding surfaces in the Corinth Offshore Rift Basin as presented in Nixon et al. (2016).

Surfaces (This study)	**Approximate ages based on Glacio-Eustatic cycles**	**Seismic Unit 2 horizons (Nixon et al. 2016)**	**Approximate ages**
Surface 12	Ca. 240 000	H3	Ca. 240 000
Surface 10	Ca. 340 000	H4	Ca. 340 000
Surface 8	Ca. 420 000	H5	Ca. 420 000
Surface 5	Ca. 530 000	H6	Ca. 530 000
Surface 4	ca. 620 000	U	ca. 620 000

Studies by Leeder et al. (2005) on the Alkyonides Gulf show six stratigraphic sequences interpreted as periodic low-frequency (100 000 year) sequences, deposited due to global sea level cycles over the course of the last ca. 600 000 years. The horizons H3 to H1 have been possible to correlate into the Alkyonides Gulf, indicating a correlation of sediments with Seismic Unit 2 (Nixon et al., 2016). This indicates a tectono-sedimentary evolution in the Alkyonides Gulf over the last 620 000 years, with changing between lacustrine and shallow marine sediments (Leeder et al., 2005; Nixon et al., 2016).

Seismic Unit 2, with the upper horizons H1, H2 and H3, can be correlated from the Gulf of Corinth Offshore Basin, into the Lechaion Gulf (Taylor et al., 2011; Charalampakis et al., 2014; Nixon et al., 2016). The lowermost interpreted horizon in the Lechaion Gulf is interpreted at an age of ca. 245 000 years old, at MIS 8 (Charalampakis et al., 2014). This implies that the lowermost interpreted horizon in the Lechaion Gulf correlate with this studys surface 12 (Table 6.2 and 6.3).

The age correlated surfaces, from the Canal deposits through the offshore Lechaion Gulf and into the Gulf of Corinth, lead to the assumption that the upper part of offshore Seismic Unit 1 correlate with the onshore lacustrine deposits of Tectono-Stratigraphic Units 1 to 3 in the Canal (Table 6.4). Offshore Seismic Unit 2 correspond to onshore Tectono-Stratigraphic Units 4 to 6, with missing Glacio-Eustatic lowstand and lacustrine deposits in the Canal outcrops (Table 6.4).

Table 6.4: Correlating the onshore stratigraphy interpreted in the Canal with the offshore Gulf of Corinth deposits interpreted in several publications (Bell et al., 2009; Taylor et al., 2011; Charalampakis et al., 2014; Nixon et al., 2016).

Onshore Stratigraphy	Offshore Stratigraphy	Age Estimates
Tectono-Stratigraphic Units 1 to 3	Seismic Unit 1	2-1.5 Ma to 620 000 years old
Tectono-Stratigraphic Units 4-6	Seismic Unit 2	620 000 years old to present

The tectono-stratigraphic evolution of the Corinth Canal deposits is interpreted to consist of middle Pleistocene lacustrine deposits overlain by marine foreshore, shoreface and offshore deposits of upper Quaternary age. With the exception of the missing lacustrine deposits above the 620 000 year surface in the Canal, the same tectono-sedimentary evolution have been interpreted for the close by Lechaion Gulf, Gulf of Corinth and the Alkyonides Gulf, indicating a large area affected largely by Glacio-Eustatic Sea Level Cycles within the Corinth Rift (Leeder et al., 2005; Taylor et al., 2011; Charalampakis et al., 2014; Nixon et al., 2016). This implies that the deposition of the Corinth Canal deposits are closely linked to other depositional basins within the Corinth Rift.

7. Summary and Conclusion

The main objective of this study is to establish depositional environments for the Corinth Canal and key stratigraphic boundaries, to be able to create a Tectono-Stratigraphic evolution of the Corinth Canal deposits. 7 Facies Associations and 6 Tectono-Stratigraphic Units have been described and interpreted.

- The Corinth Canal deposits consists of 7 different Facies Associations, divided based on the composition, structures, and fauna found in the outcrops. The Facies Associations are derived from Lacustrine and Marine environments.

- Facies Associations 1 and 2 are derived from a terrestrial environment with deposition in a lower littoral to upper sublittoral (FA1), to lower sublittoral to upper profundal (FA2) lacustrine setting. They are deposited in a fluvial-lacustrine basin with siliciclastic deposits dominating and with no indications large contents of organic matter or evaporites.

- Facies Associations 3 to 7 are derived from a marine environments, with foreshore/beach conglomerates (FA3), foreshore conglomerate spit deposit (FA4), Shoreface sandstones (FA5), offshore-transition to offshore sandstones and siltstones (FA6), and offshore calcareous mudstones (FA7).

- Based on surface interpretations, focusing on major erosional features and major landward or basinward shifts in facies, the Canal have been divided into six Tectono-Stratigraphic Units. The earlier interpreted “Corinth Marls” deposits are separated into Tectono-Stratigraphic Units 1 to 5 with deposition in lacustrine and marine environment.

- Tectono-Stratigraphic Units 1 to 3 are comprised within a fluvial-lacustrine basin, showing an overall progradation of the lacustrine deposits.

- Tectono-Stratigraphic Unit 4 is deposited during a highstand in sea level, with deposits of shoreface sandstones to offshore marine marlstones and siltstones, following a major

sea level rise that have changed the deposits in the Canal from lacustrine to offshore marine.

- Tectono-Stratigraphic Unit 5 is deposited during a highstand in sea level with deposits ranging from foreshore conglomerates to offshore marine marls. It is separated from Tectono-Stratigraphic Unit 4 by a relative fall in sea level. The Unit have after deposition been subjected to subaerial exposure on the horst, with karst and calcrete along its upper boundary. The Unit is eroded and missing from the outcrops NW of the horst.

- Tectono-Stratigraphic Unit 6 consist of three transgressive sets of foreshore conglomerates to shoreface sandstones deposited in a marine environment. It is separated from Tectono-Stratigraphic Unit 5 by a fall in sea level. Each transgressive set is capped by a fall in relative sea level which have allowed the creations of wave-eroded cliffs on each of the sets upper boundary.

- Correlation of known ages of stratigraphic units with the Glacio-Eustatic Sea Level Curve indicate deposition during five MIS highstands for Tectono-Stratigraphic Units 4 to 6, with deposition of the lacustrine deposits of Tectono-Stratigraphic Unit 1 to 3 during a Glacio-Eustatic lowstand. This infers deposition controlled mainly by Glacio-Eustatic Sea Level changes, with local faults within the Canal affecting thicknesses and local variations in relative sea level.

- The correlated ages from the Glacio-Eustatic Sea Level Curve have made it possible to correlate several of the key stratal surface found in the Canal, with major unconformities and flooding surfaces in the close by Lechaion Gulf, Alkyonides Gulf and the Gulf of Corinth.

- The Tectono-Stratigraphic Evolution is interpreted as lacustrine lowstand deposits depositing between 620 000 and 690 000 years ago, overlain by five low-frequency (100 000 year) cycles of marine highstand deposition during the past 620 000 years.

8. Bibliography

Armijo, R., Meyer, B., Hubert, A. and Barka, A., 1999. Westward propagation of the North Anatolian fault into the northern Aegean: Timing and kinematics. Geology, 27(3): 267-270.

Armijo, R., Meyer, B., King, G., Rigo, A. and Papanastassiou, D., 1996. Quaternary evolution of the Corinth Rift and its implications for the Late Cenozoic evolution of the Aegean. Geophysical Journal International, 126(1): 11-53.

Aurell, M., Bádenas, B., Bosence, D. and Waltham, D., 1998. Carbonate production and offshore transport on a Late Jurassic carbonate ramp (Kimmeridgian, Iberian basin, NE Spain): evidence from outcrops and computer modelling. Geological Society, London, Special Publications, 149(1): 137-161.

Bell, R., McNeill, L., Bull, J., Henstock, T., Collier, R. and Leeder, M., 2009. Fault architecture, basin structure and evolution of the Gulf of Corinth Rift, central Greece. Basin Research, 21(6): 824-855.

Bell, R.E., 2008. Tectonic Evolution of the Corinth Rift. PhD Thesis, University of Southampton.

Bohacs, K.M., Carroll, A.R., Neal, J.E. and Mankiewicz, P.J., 2000. Lake-basin type, source potential, and hydrocarbon character: an integrated sequence-stratigraphic-geochemical framework. Lake basins through space and time: AAPG Studies in Geology, 46: 3-34.

Briole, P., Rigo, A., Lyon-Caen, H., Ruegg, J., Papazissi, K., Mitsakaki, C., Balodimou, A., Veis, G., Hatzfeld, D. and Deschamps, A., 2000. Active deformation of the Corinth rift, Greece: results from repeated Global Positioning System surveys between 1990 and 1995. Journal of Geophysical Research: Solid Earth (1978–2012), 105(B11): 25605-25625.

Brooks, M. and Ferentinos, G., 1984. Tectonics and sedimentation in the Gulf of Corinth and the Zakynthos and Kefallinia channels, western Greece. Tectonophysics, 101(1): 25-54.

Burch, J.B., 1989. North American freshwater snails. Malacological Publications.

Campbell, C.V., 1971. Depositional model--Upper Cretaceous Gallup beach shoreline, Ship Rock area, northwestern New Mexico. Journal of Sedimentary Research, 41(2).

Carroll, A.R. and Bohacs, K.M., 1999. Stratigraphic classification of ancient lakes: Balancing tectonic and climatic controls. Geology, 27(2): 99-102.

Cartwright, J., Bouroullec, R., James, D. and Johnson, H., 1998. Polycyclic motion history of some Gulf Coast growth faults from high-resolution displacement analysis. Geology, 26(9): 819-822.

Catuneanu, O., 2002. Sequence stratigraphy of clastic systems: concepts, merits, and pitfalls. Journal of African Earth Sciences, 35(1): 1-43.

Cavinato, P., Gliozzi, E. and Mazzini, I., 2000. AAPG Studies in Geology# 46, Chapter 49: Two Lacustrine Episodes During the Late Pliocene-Holocene Evolution of the Rieti Basin (Central Apennines, Italy).

Changsong, L., Eriksson, K., Sitian, L., Yongxian, W., Jianye, R. and Yanmei, Z., 2001. Sequence architecture, depositional systems, and controls on development of lacustrine basin fills in part of the Erlian Basin, northeast China. AAPG bulletin, 85(11): 2017-2043.

Charalampakis, M., Lykousis, V., Sakellariou, D., Papatheodorou, G. and Ferentinos, G., 2014. The tectono-sedimentary evolution of the Lechaion Gulf, the south eastern branch of the Corinth graben, Greece. Marine Geology, 351: 58-75.

Clifton, H., 2006. A reexamination of facies models for clastic shorelines. SPECIAL PUBLICATION-SEPM, 84: 293.

Clifton, H.E., Hunter, R.E. and Phillips, R.L., 1971. Depositional structures and processes in the non-barred high-energy nearshore. Journal of Sedimentary Research, 41(3).

Collier, R.E.L., 1988. Sedimentary facies evolution in continental fault-bounded basins formed by crustal extension: the Corinth basin, Greece, University of Leeds.

Collier, R.E.L., 1990. Eustatic and tectonic controls upon Quaternary coastal sedimentation in the Corinth Basin, Greece. Journal of the Geological Society, 147: 301-314.

Collier, R.E.L. and Dart, C.J., 1991. Neogene to Quaternary rifting, sedimentation and uplift in the Corinth Basin, Greece. Journal of the Geological Society, 148: 1049-1065.

Collier, R.E.L., Leeder, M.R., Rowe, P.J. and Atkinson, T.C., 1992. Rates of tectonic uplift in the Corinth and Megara Basins, Central Greece. Tectonics, 11(6): 1159-1167.

Collier, R.E.L. and Thompson, J., 1991. Transverse and linear dunes in an Upper Pleistocene marine sequence, Corinth Basin, Greece. Sedimentology, 38: 1021-1040.

Collinson, J., Mountney, N. and Thompson, D., 2006. Sedimentary Structures. Terra Publishing.

Cutler, K., Edwards, R., Taylor, F., Cheng, H., Adkins, J., Gallup, C., Cutler, P., Burr, G. and Bloom, A., 2003. Rapid sea-level fall and deep-ocean temperature change since the last interglacial period. Earth and Planetary Science Letters, 206(3): 253-271.

DeMets, C., Gordon, R.G., Argus, D. and Stein, S., 1990. Current plate motions. Geophysical journal international, 101(2): 425-478.

Dewey, J.F. and Sengor, A.M.C., 1979. Aegean and surrounding regions: complex multiplate and continuum tectonics in a convergent zone. Geological Society of America Bulletin, 90(1): 84-92.

Dia, A., Cohen, A., O'nions, R. and Jackson, J., 1997. Rates of uplift investigated through 230 Th dating in the Gulf of Corinth (Greece). Chemical Geology, 138(3): 171-184.

Doutsos, T., Kontopoulos, N. and Poulimenos, G., 1988. The Corinth-Patras rift as the initial stage of continental fragmentation behind an active island arc (Greece). Basin Research, 1(3): 177-190.

Doutsos, T. and Piper, D.J., 1990. Listric faulting, sedimentation, and morphological evolution of the Quaternary eastern Corinth rift, Greece: first stages of continental rifting. Geological Society of America Bulletin, 102(6): 812-829.

Flotté, N., Sorel, D., Müller, C. and Tensi, J., 2005. Along strike changes in the structural evolution over a brittle detachment fault: Example of the Pleistocene Corinth–Patras rift (Greece). Tectonophysics, 403(1-4): 77-94.

Ford, M., Rohais, S., Williams, E.A., Bourlange, S., Jousselin, D., Backert, N. and Malartre, F., 2013. Tectono-sedimentary evolution of the western Corinth rift (Central Greece). Basin Research, 25(1): 3-25.

García-García, F., Soria, J.M., Viseras, C. and Fernández, J., 2009. High-Frequency Rhythmicity in a Mixed Siliciclastic–Carbonate Shelf (Late Miocene, Guadix Basin, Spain): A Model of Interplay Between Climatic Oscillations, Subsidence, and Sediment Dispersal. Journal of Sedimentary Research, 79(5): 302-315.

Gawthorpe, R. and Leeder, M., 2000. Tectono-sedimentary evolution of active extensional basins. Basin Research, 12(3-4): 195-218.

Helland-Hansen, W. and Martinsen, O.J., 1996. Shoreline trajectories and sequences: description of variable depositional-dip scenarios. Journal of Sedimentary Research, 66(4).

Hiroki, Y. and Masuda, F., 2000. Gravelly spit deposits in a transgressive systems tract: the Pleistocene Higashikanbe Gravel, central Japan. Sedimentology, 47(1): 135-149.

Hodgetts, D., 2009. 11 LiDAR in the Environmental Sciences: Geological Applications. Laser Scanning for the Environmental Sciences: 165.

Hongxing, G. and Anderson, J.K., 2007. Fault throw profile and kinematics of Normal fault: conceptual models and geologic examples. Geol. J. China Univ, 13(75): e88.

Hunt, D. and Tucker, M.E., 1992. Stranded Parasquences and the Forced Regressive Wedge Systems Tract - Deposition during base-level fall. Sedimentary Geology, 81(1-2): 1-9.

Jackson, J., King, G. and Vita-Finzi, C., 1982. The neotectonics of the Aegean: an alternative view. Earth and Planetary Science Letters, 61(2): 303-318.

Jolivet, L., 2001. A comparison of geodetic and finite strain pattern in the Aegean, geodynamic implications. Earth and Planetary Science Letters, 187(1): 95-104.

Komar, P.D. and Inman, D.L., 1970. Longshore sand transport on beaches. Journal of geophysical research, 75(30): 5914-5927.

Labeyrie, L., Duplessy, J.C. and Blanc, P., 1987. Variations in mode of formation and temperature of oceanic deep waters over the past 125,000 years. Nature, 327(6122): 477-482.

Le Pichon, X. and Angelier, J., 1979. The Hellenic arc and trench system: a key to the neotectonic evolution of the eastern Mediterranean area. Tectonophysics, 60(1): 1-42.

Le Pichon, X., Angelier, J., Osmaston, M. and Stegena, L., 1981. The Aegean Sea [and Discussion]. Philosophical Transactions of the Royal Society of London A: Mathematical, Physical and Engineering Sciences, 300(1454): 357-372.

Le Pourhiet, L., Burov, E. and Moretti, I., 2003. Initial crustal thickness geometry controls on the extension in a back arc domain: Case of the Gulf of Corinth. Tectonics, 22(4).

Lea, D.W., Martin, P.A., Pak, D.K. and Spero, H.J., 2002. Reconstructing a 350ky history of sea level using planktonic Mg/Ca and oxygen isotope records from a Cocos Ridge core. Quaternary Science Reviews, 21(1): 283-293.

Leeder, M., Portman, C., Andrews, J., Collier, R.L., Finch, E., Gawthorpe, R., McNeill, L., Perez-Arlucea, M. and Rowe, P., 2005. Normal faulting and crustal deformation, Alkyonides Gulf and Perachora peninsula, eastern Gulf of Corinth rift, Greece. Journal of the Geological Society, 162(3): 549-561.

Lubeseder, S., Redfern, J. and Boutib, L., 2009. Mixed siliciclastic-carbonate shelf sedimentation—Lower Devonian sequences of the SW Anti-Atlas, Morocco. Sedimentary Geology, 215(1): 13-32.

Mandic, O., Kurečić, T., A Neubauer, T. and Harzhauser, M., 2015. Stratigraphic and paleogeographic significance of lacustrine mollusks from the Pliocene Viviparus beds in central Croatia. Geologia Croatica, 68(3): 179-207.

McClusky, S., Balassanian, S., Barka, A., Demir, C., Ergintav, S., Georgiev, I., Gurkan, O., Hamburger, M., Hurst, K. and Kahle, H., 2000. Global Positioning System constraints on plate kinematics and dynamics in the eastern Mediterranean and Caucasus. Journal of Geophysical Research: Solid Earth (1978–2012), 105(B3): 5695-5719.

McKenzie, D., 1970. Plate tectonics of the Mediterranean region. Nature, 226(5242): 239-243.

McKenzie, D., 1972. Active tectonics of the Mediterranean region. Geophysical Journal International, 30(2): 109-185.

McKenzie, D., 1978. Active tectonics of the Alpine—Himalayan belt: the Aegean Sea and surrounding regions. Geophysical Journal International, 55(1): 217-254.

Murakoshi, N. and Masuda, F., 1992. Estuarine, barrier-island to strand-plain sequence and related ravinement surface developed during the last interglacial in the Paleo-Tokyo Bay, Japan. Sedimentary geology, 80(3): 167-184.

Murray-Wallace, C., Farland, M., Roy, P. and Sollar, A., 1996. Unravelling patterns of reworking in lowstand shelf deposits using amino acid racemisation and radiocarbon dating. Quaternary Science Reviews, 15(7): 685-697.

Nemec, W. and Steel, R.J., 1984. Alluvial and coastal conglomerates: their significant features and some comments on gravelly mass-flow deposits.

Nicholls, R. and Webber, N., 1987. The past, present and future evolution of Hurst Castle Spit, Hampshire. Progress in Oceanography, 18(1): 119-137.

Nixon, C.W., McNeill, L.C., Bull, J.M., Bell, R.E., Gawthorpe, R.L., Henstock, T.J., Christodoulou, D., Ford, M., Taylor, B. and Sakellariou, D., 2016. Rapid spatiotemporal variations in rift structure during development of the Corinth Rift, central Greece. Tectonics.

Nury, D., 2000. AAPG Studies in Geology# 46, Chapter 34: Lacustrine Oligocene Basins in Southern Provence, France.

Odin, G.S. and Matter, A., 1981. Origin of Glauconites. Sedimentology, 28(5): 611-641.

Olsen, P.E., 1990. Tectonic, climatic, and biotic modulation of lacustrine ecosystems—examples from Newark Supergroup of eastern North America. Lacustrine basin exploration: Case studies and modern analogs: AAPG Memoir, 50: 209-224.

Papanikolaou, I.D., Triantaphyllou, M., Pallikarakis, A. and Migiros, G., 2015. Active faulting at the Corinth Canal based on surface observations, borehole data and paleoenvironmental interpretations. Passive rupture during the 1981 earthquake sequence? Geomorphology, 237: 65-78.

Rarity, F., Van Lanen, X., Hodgetts, D., Gawthorpe, R., Wilson, P., Fabuel-Perez, I. and Redfern, J., 2014. LiDAR-based digital outcrops for sedimentological analysis: workflows and techniques. Geological Society, London, Special Publications, 387(1): 153-183.

Reading, H.G., 2009. Sedimentary environments: processes, facies and stratigraphy. John Wiley & Sons.

Roberts, S. and Jackson, J., 1991. Active normal faulting in central Greece: an overview. Geological Society, London, Special Publications, 56(1): 125-142.

Rohais, S., Joannin, S., Colin, J.-P., Suc, J.-P., Guillocheau, G. and Eschard, R., 2007. Age and environmental evolution of the syn-rift fill of the southern coast of the gulf of Corinth (Akrata-Derveni region, Greece). Bull. Soc. géol., 178: 231-243.

Sanders, D. and Pons, J.M., 1999. Rudist formations in mixed siliciclastic-carbonate depositional environments, Upper Cretaceous, Austria: stratigraphy, sedimentology, and models of development. Palaeogeography, Palaeoclimatology, Palaeoecology, 148(4): 249-284.

Shackleton, N.J., 2000. The 100,000-year ice-age cycle identified and found to lag temperature, carbon dioxide, and orbital eccentricity. Science, 289(5486): 1897-1902.

Siddall, M., Chappell, J. and Potter, E.-K., 2007. 7. Eustatic sea level during past interglacials. Developments in Quaternary Sciences, 7: 75-92.

Siddall, M., Rohling, E.J., Almogi-Labin, A., Hemleben, C., Meischner, D., Schmelzer, I. and Smeed, D., 2003. Sea-level fluctuations during the last glacial cycle. Nature, 423(6942): 853-858.

Taylor, B., Weiss, J.R., Goodliffe, A.M., Sachpazi, M., Laigle, M. and Hirn, A., 2011. The structures, stratigraphy and evolution of the Gulf of Corinth rift, Greece. Geophysical Journal International, 185(3): 1189-1219.

Vita-Finzi, C. and King, G., 1985. The Seismicity, Geomorphology and Structural Evolution of the Corinth Area of Greece. Philosophical Transactions of the Royal Society of London. Series A, Mathematical and Physical Sciences: 379-407.

von Freyberg, B., 1973. Geologie des Isthmus von Korinth. Junge, Universitäts-Buchdruckerei.

Waelbroeck, C., Labeyrie, L., Michel, E., Duplessy, J.C., McManus, J., Lambeck, K., Balbon, E. and Labracherie, M., 2002. Sea-level and deep water temperature changes derived from benthic foraminifera isotopic records. Quaternary Science Reviews, 21(1): 295-305.

White, R.S., Spence, G.D., Fowler, S.R., McKenzie, D.P. and Westbrook, G.K., 1987. Magmatism at rifted continental margins. Nature, 330: 439-444.

Willsey, S.P., Umhoefer, P.J. and Hilley, G.E., 2002. Early evolution of an extensional monocline by a propagating normal fault: 3D analysis from combined field study and numerical modeling. Journal of Structural Geology, 24(4): 651-669.

Internet references

Benson, A.J. 2016. *Viviparus subpurpureus*. USGS Nonindigenous Aquatic Species Database, Gainesville, FL. http://nas.er.usgs.gov/queries/FactSheet.aspx?SpeciesID=2769 Revision Date: 6/3/2013. Accessed 4th of July 2016.

NOAA, 2015. *What is LIDAR?* National Oceanic and Atmospheric Administration – U.S. Government. http://oceanservice.noaa.gov/facts/lidar.html Revision Date: May 29, 2015. Accessed 15th of February 2016

Lauritzen, Stein-Erik. (2011). *Karst*. Store Norske leksikon. https://snl.no/karst. Accessed 12th of July 2016

Appendix

Legend

Lithology

Konglomerat

Sand

Siltsone

Marl

Mudstone

Body fossils

Bivalve

Coral

Gastropod

Fragmented, unidentified shells

Burrows

Structures

Trough cross-bed

Planar cross-bed

Planar conglomerate cross-bed

Planar bedded

Inclined bedded

Massive

Cemented carbonate band

Erosional surface

Abbreviations

cl - clay
si - silt
vf - very fine sand
f - fine sand
m - medium sand
c - coarse sand
vc - very coarse sand
g - granules
p - pebbles
c - cobbles

FNX-FNX: Located between Fault North X and Fault North X

Logs in 1:20 scale. Vertical scale in centimetres

Tectono-Stratigraphic Unit 1 - Stratal Unit 2
Log 2 - FN1-FS1

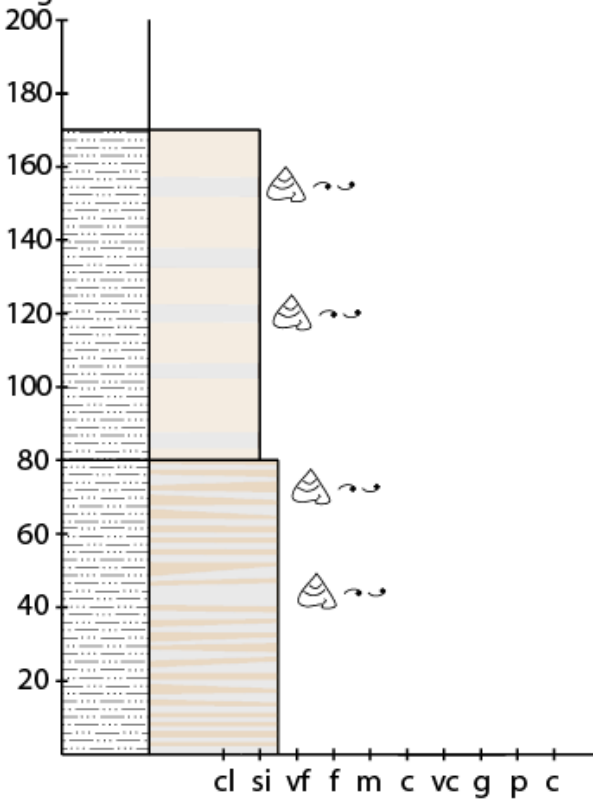

Tectono-Stratigraphic Unit 1 - Stratal Unit 2
Log 4 - FN1-FS2

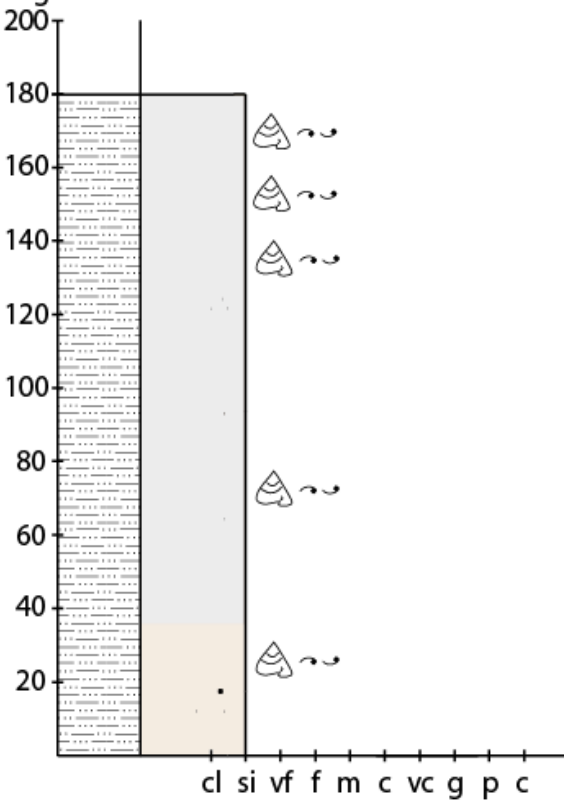

Tectono-Stratigraphic Unit 1 - Stratal Unit 2
Log 1 - FN1-FS1

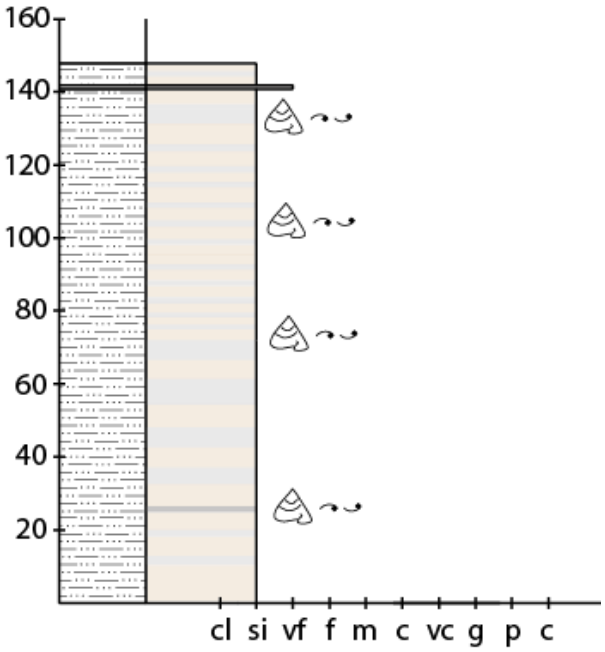

Tectono-Stratigraphic Unit 1 - Stratal Unit 2
Log 3 - FN1-FS1

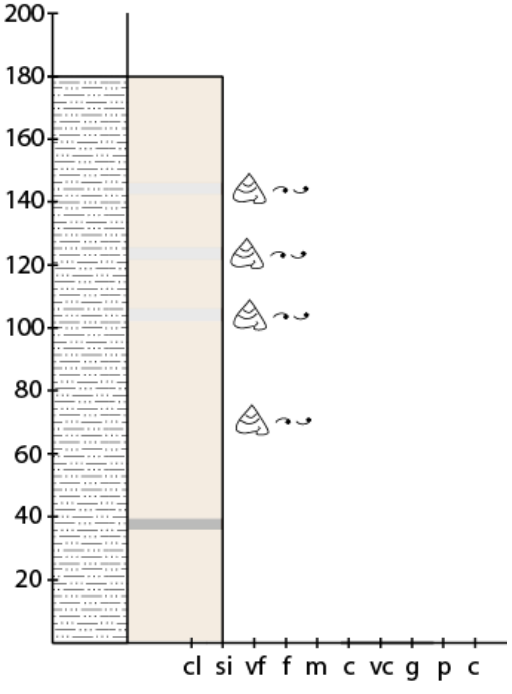

Tectono-Stratigraphic Unit 1 - Stratal Unit 2
Log 6 - FN1-FS1

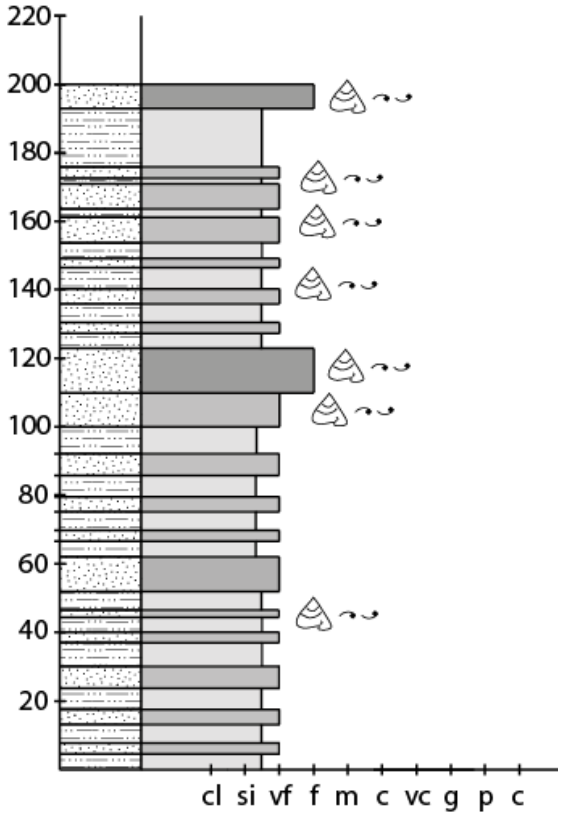

Tectono-Stratigraphic Unit 1 - Stratal Unit 2
Log 8 - FN1-FS1

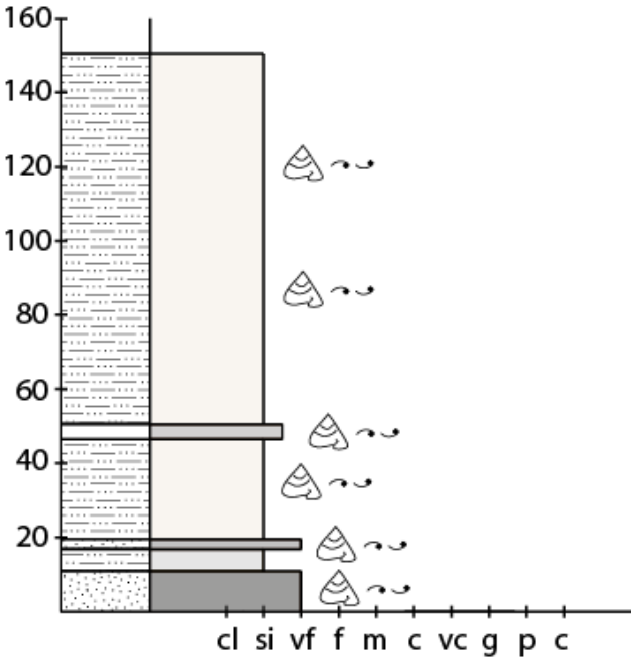

Tectono-Stratigraphic Unit 1 - Stratal Unit 2
Log 5 - FN1-FS1

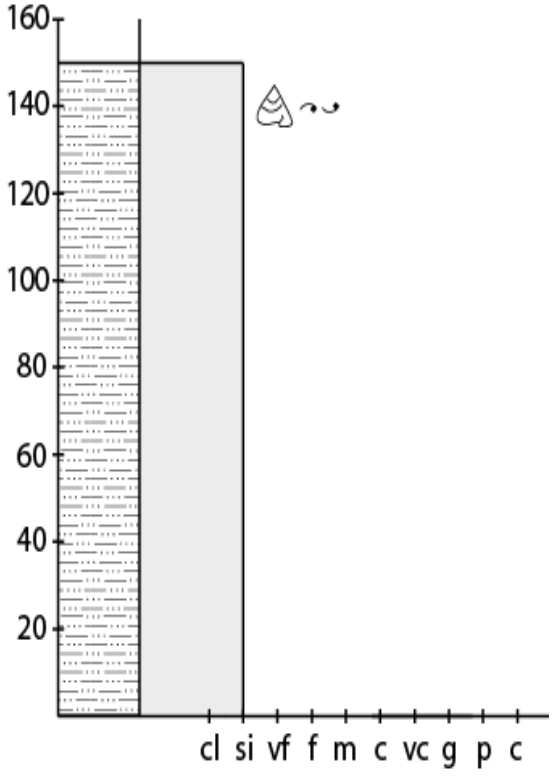

Tectono-Stratigraphic Unit 1 - Stratal Unit 2:
Log 7 - FN1-FS1

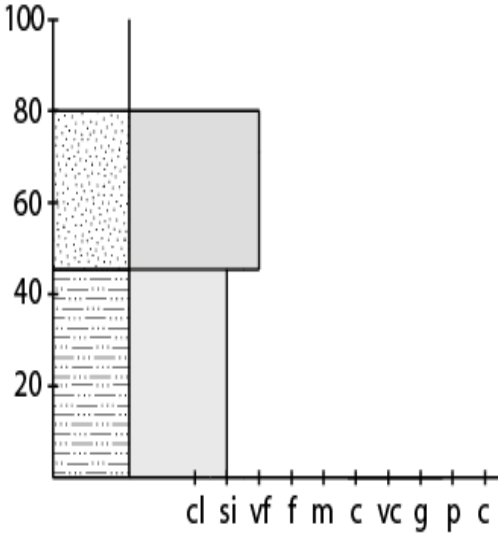

Tectono-Stratigraphic Unit 2 - Stratal Unit 3 - Log 1 - FN1-FS1
Tectono-Stratigraphic Unit 1 - Stratal Unit 2 - Log 9 - FN1-FS1

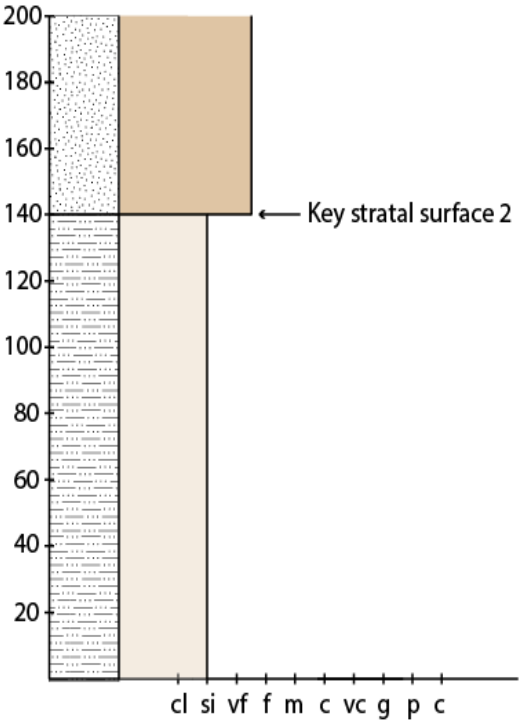

Tectono-Stratigraphic Unit 2
Log 2 - FN1-FN1.1

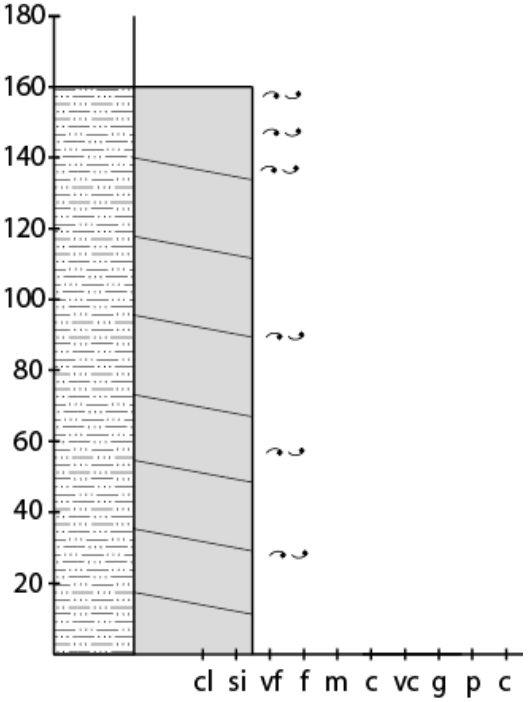

Tectono-Stratigraphic Unit 1 - Stratal Unit 2
Log 9 - FN1-FS1

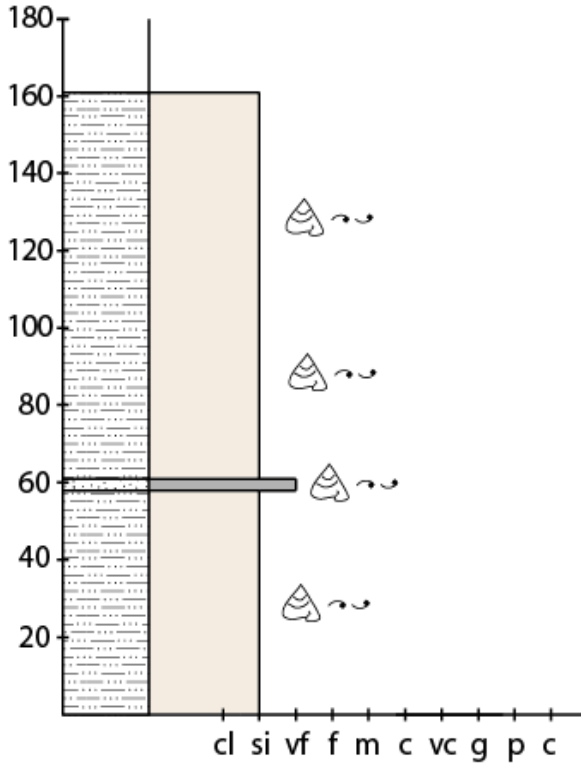

Tectono-Stratigraphic Unit 2
Log 1 - FN1-FN1.1

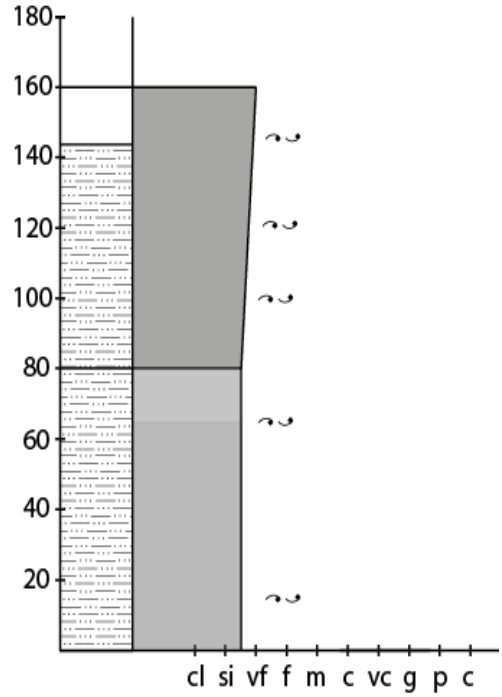

Tectono-Stratigraphic Unit 2
Log 4 - FN1-FN1.1

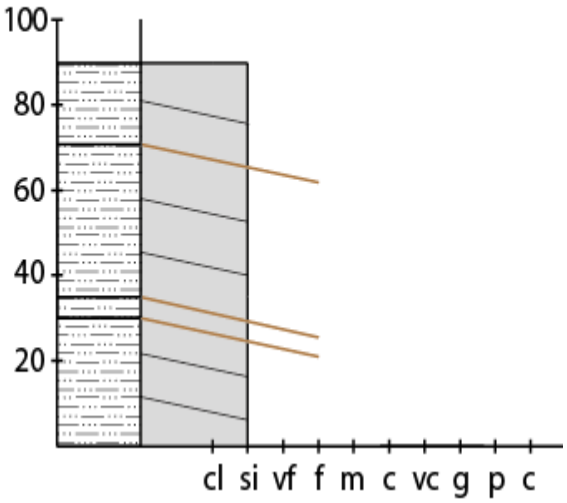

Tectono-Stratigraphic Unit 2
Log 6 - FN1-FN1.1

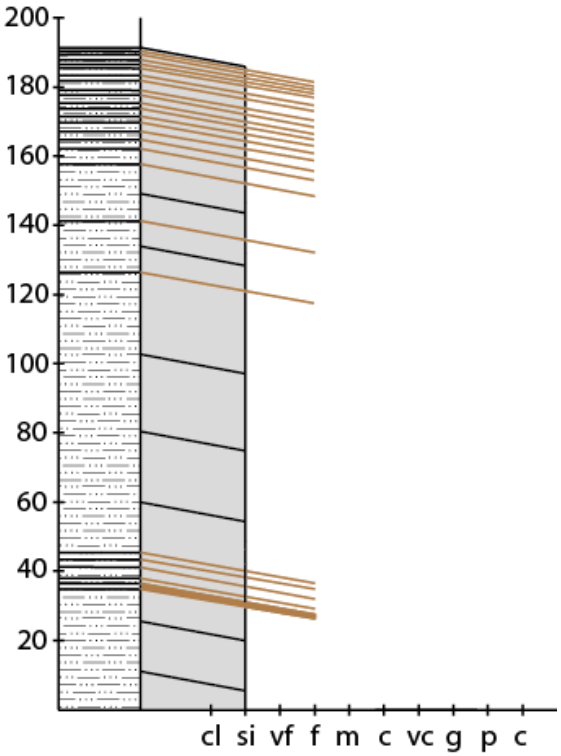

Tectono-Stratigraphic Unit 2
Log 3 - FN1-FN1.1

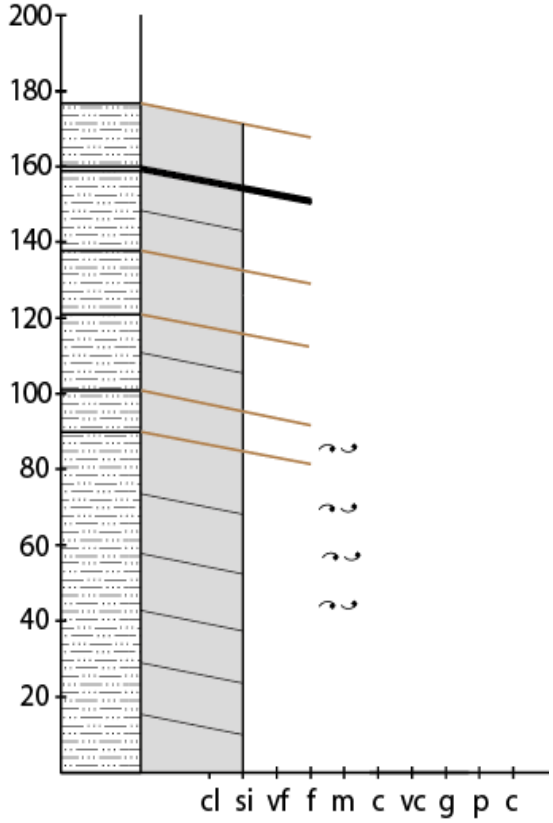

Tectono-Stratigraphic Unit 2
Log 5 - FN1-FN1.1

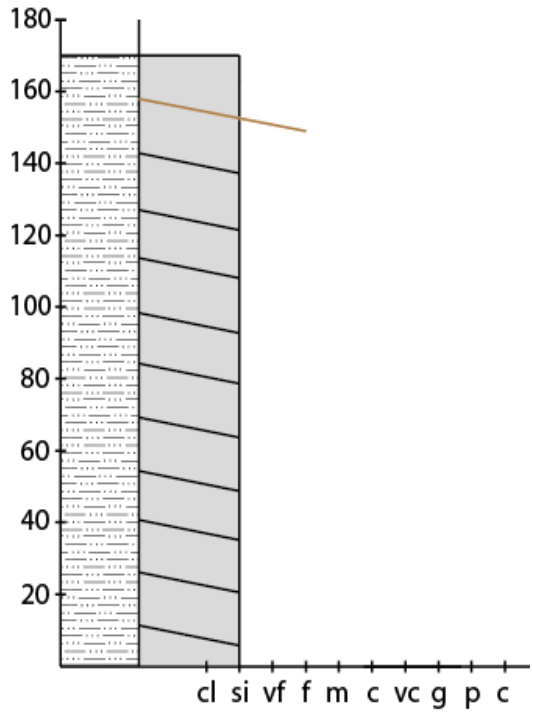

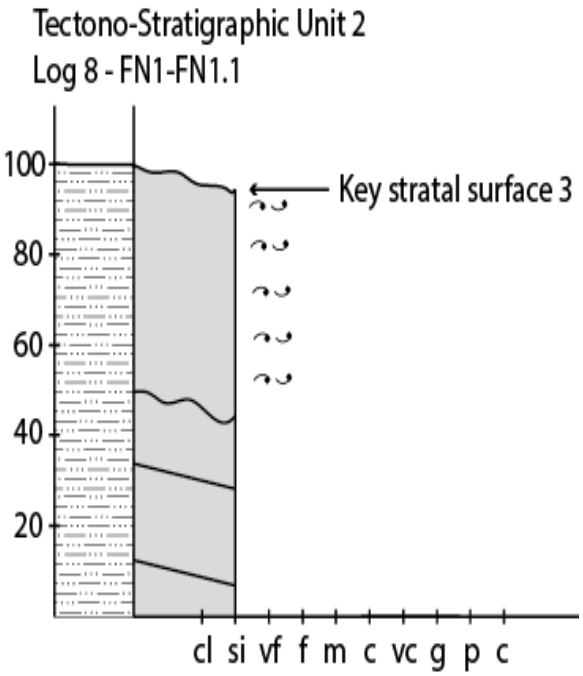
Tectono-Stratigraphic Unit 2
Log 8 - FN1-FN1.1
100
80
60
40
20
Key stratal surface 3
cl si vf f m c vc g p c

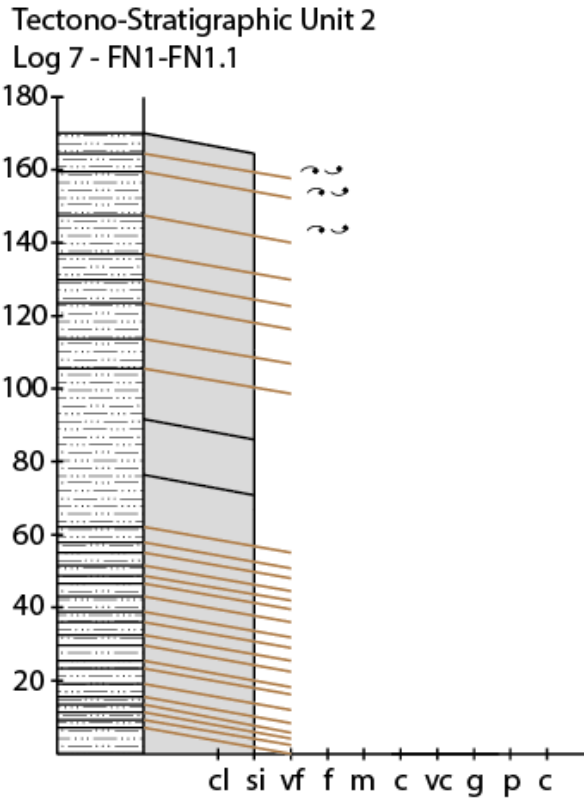
Tectono-Stratigraphic Unit 2
Log 7 - FN1-FN1.1
180
160
140
120
100
80
60
40
20
cl si vf f m c vc g p c

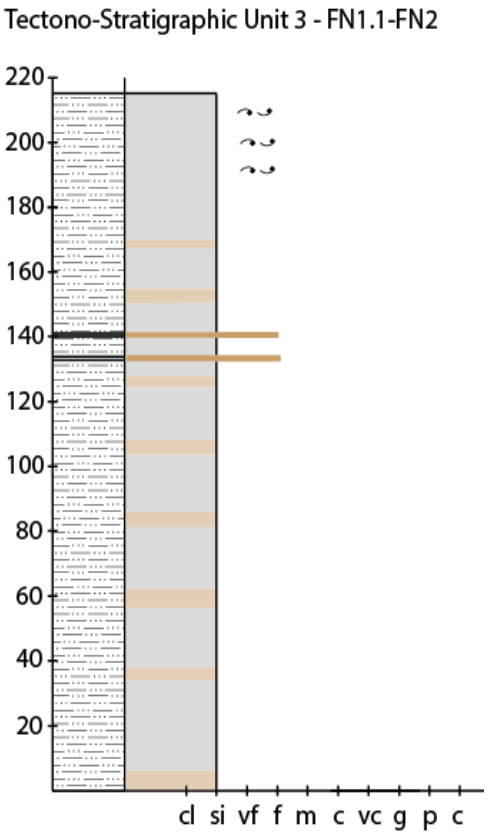
Tectono-Stratigraphic Unit 3 - FN1.1-FN2
220
200
180
160
140
120
100
80
60
40
20
cl si vf f m c vc g p c

Tectono-Stratigraphic Unit 3 - FN2-FN3

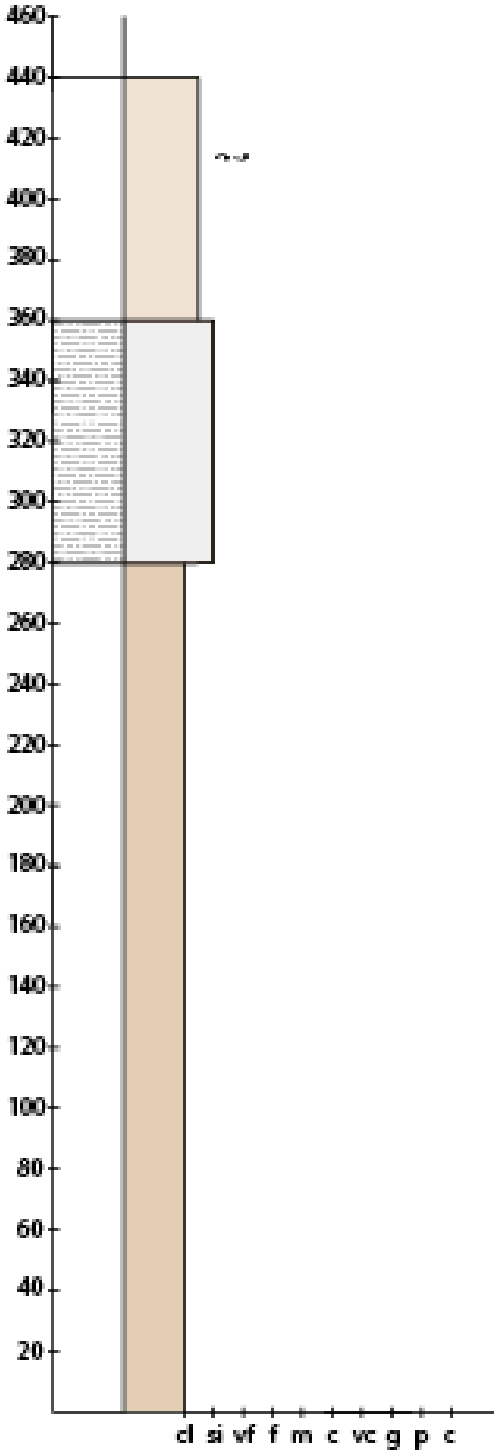

Tectono-Stratigraphic Unit 3 - Log 2 - FN3-FN4

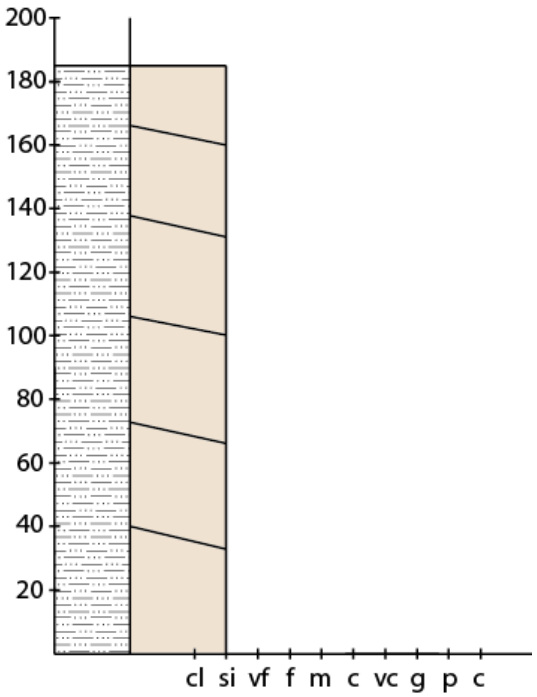

Tectono-Stratigraphic Unit 3- Log 1 - FN3-FN4

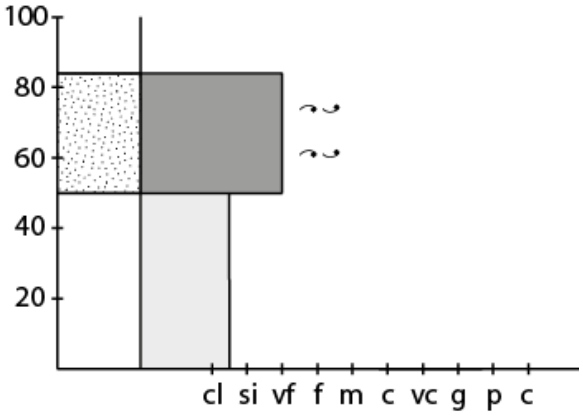

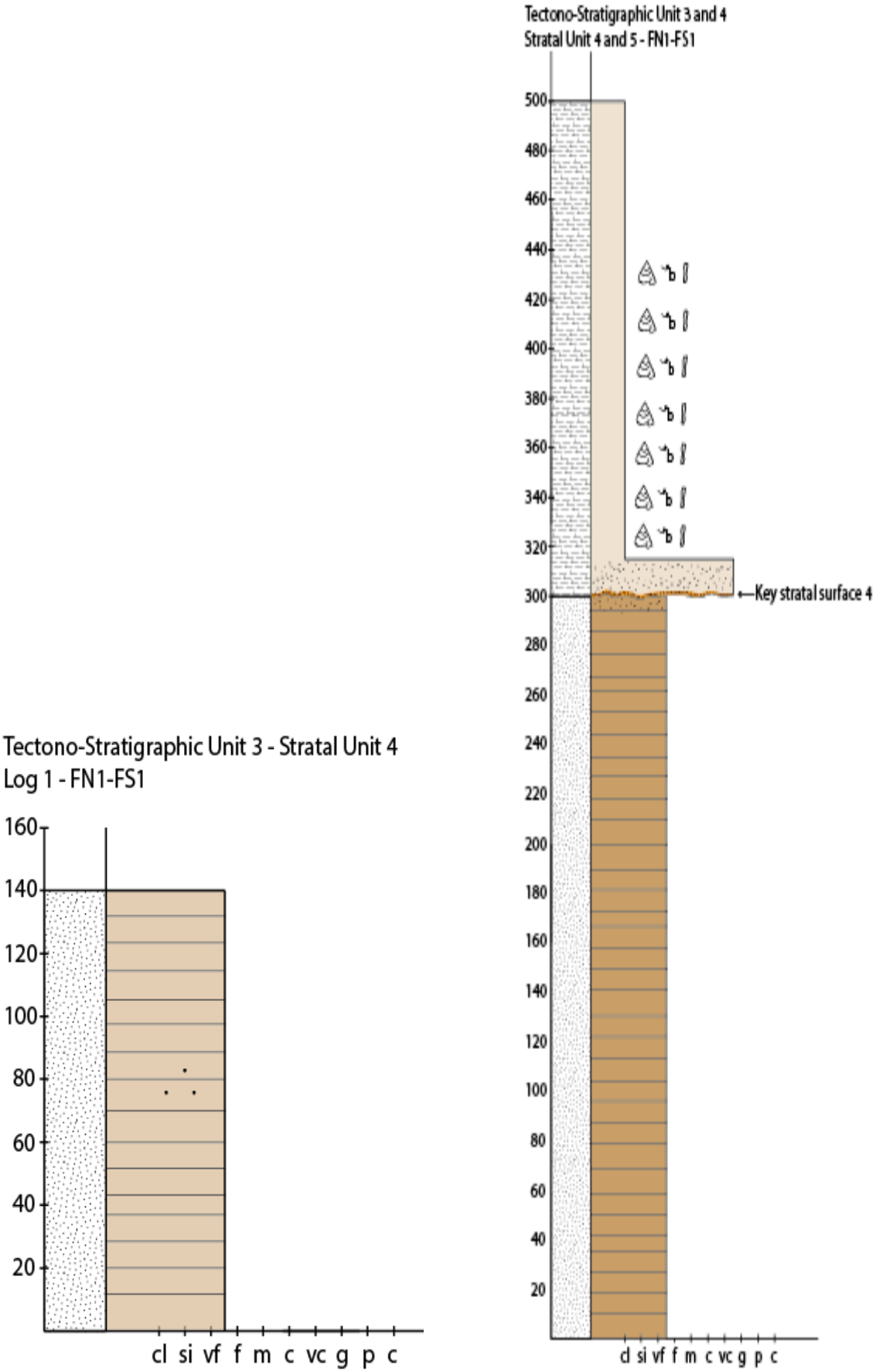
Tectono-Stratigraphic Unit 3 and 4
Stratal Unit 4 and 5 - FN1-FS1
500
480
460
440
420
400
380
360
340
320
300
280
260
240
220
200
180
160
140
120
100
80
60
40
20
Key stratal surface 4
cl si vf f m c vc g p c

Tectono-Stratigraphic Unit 3 - Stratal Unit 4
Log 1 - FN1-FS1
160
140
120
100
80
60
40
20
cl si vf f m c vc g p c

Tectono-Stratigraphic Unit 4 - FN1-FS1

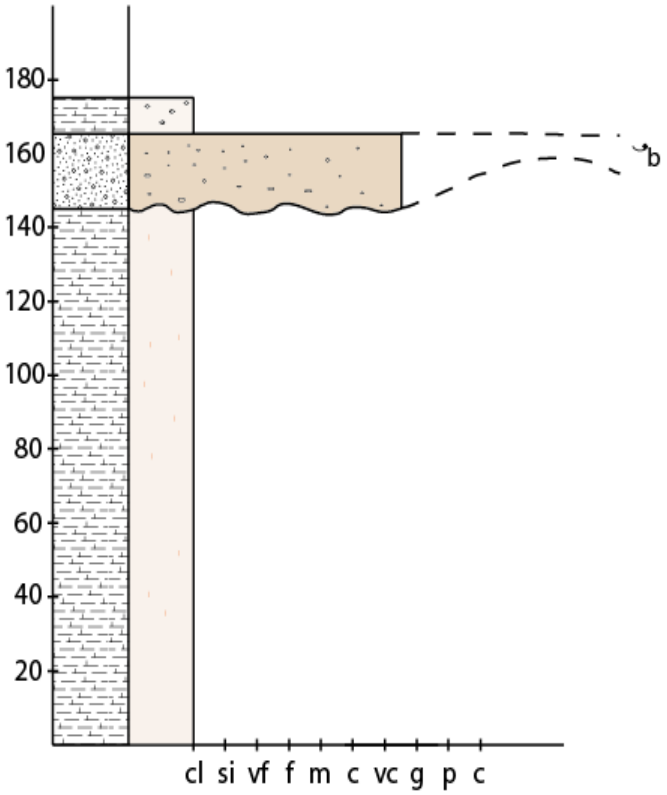

Tectono-Stratigraphic Unit 4 - FN1-FS1

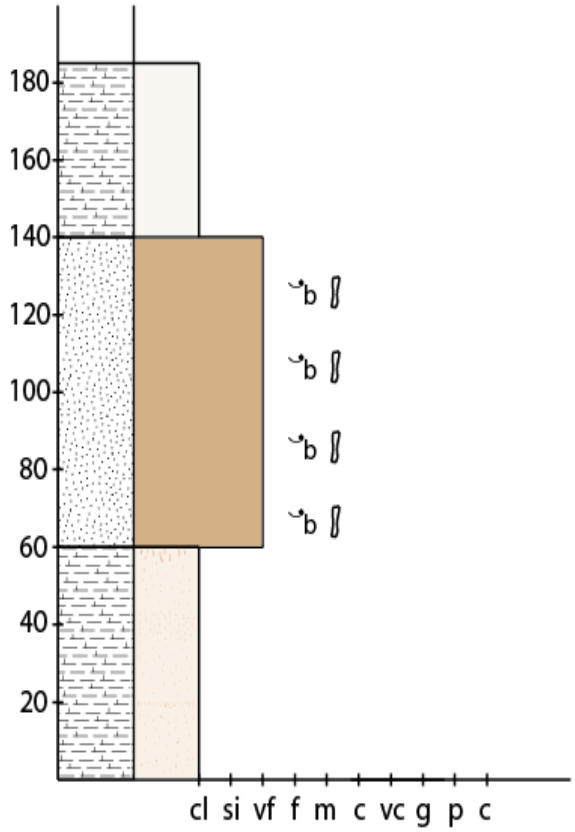

Tectono-Stratigraphic Unit 4 - FN1-FN1.1

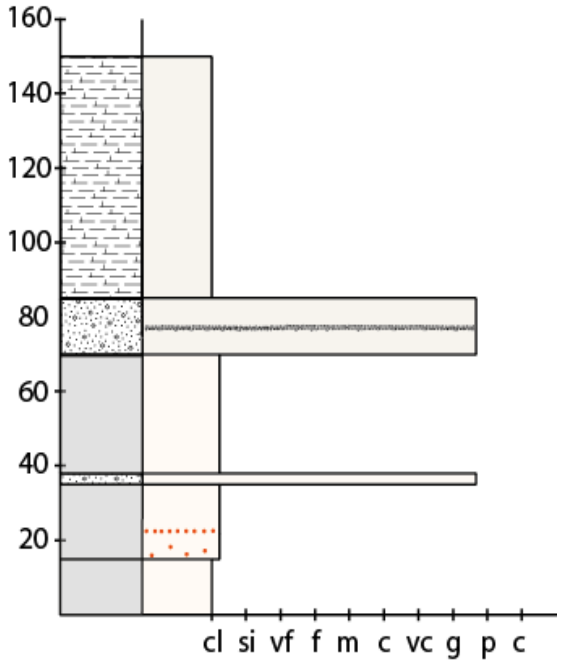

Tectono-Stratigraphic Unit 4 - FN4-FN5

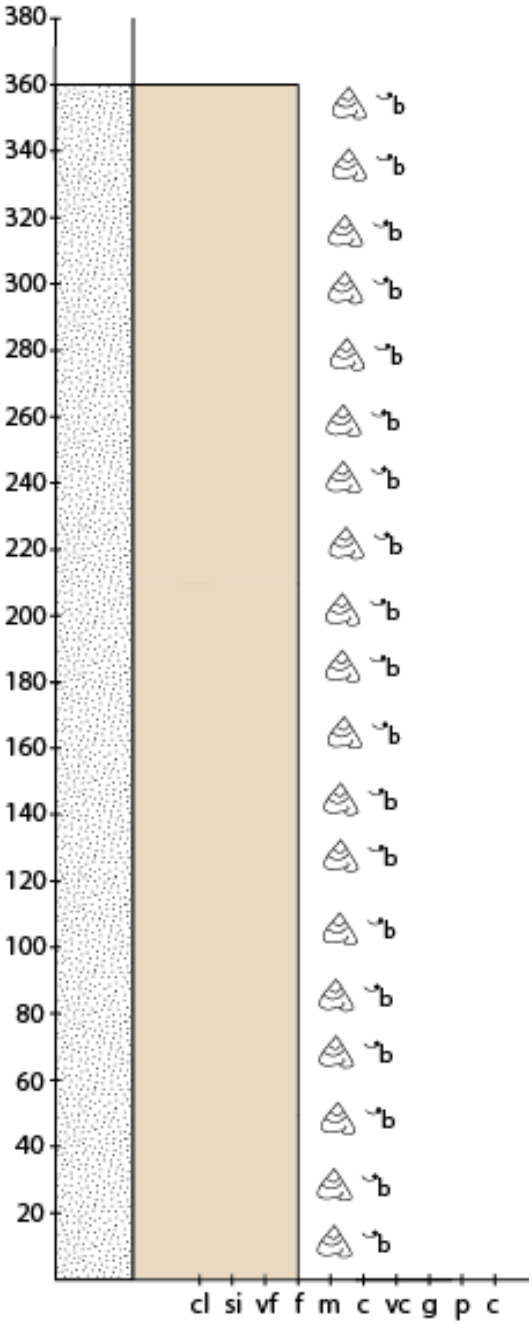

Tectono-Stratigraphic Unit 4 - Log 2 - NW of FN6

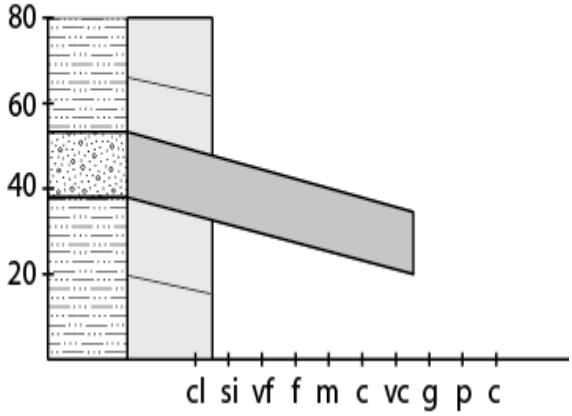

Tectono-Stratigraphic Unit 4 - FN5-FN6

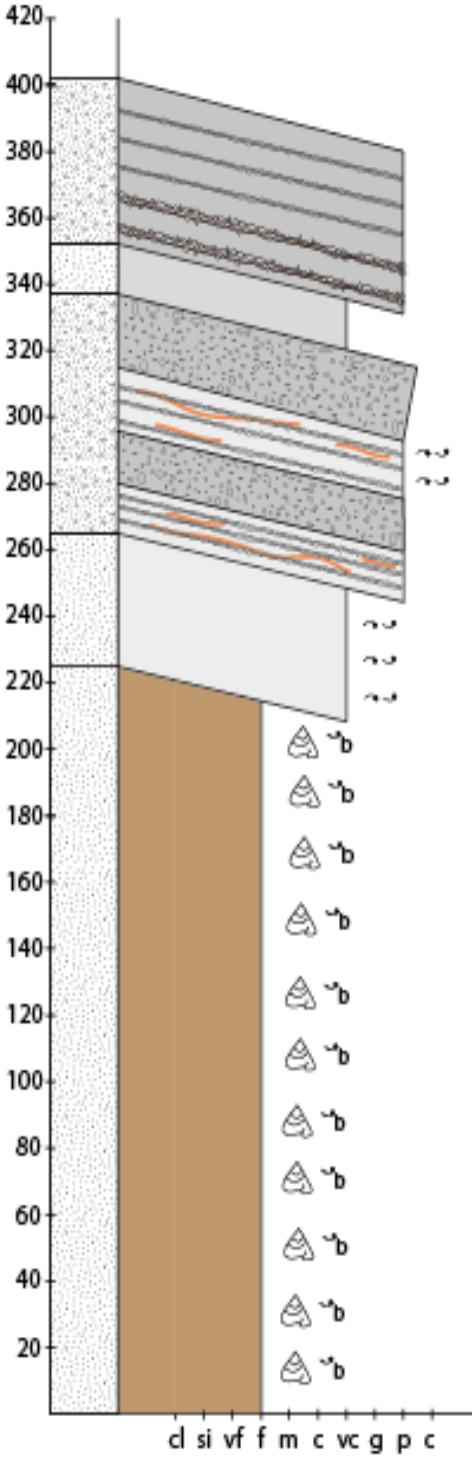

Tectono-Stratigraphic Unit 4 - Log 1 - NW of FN6

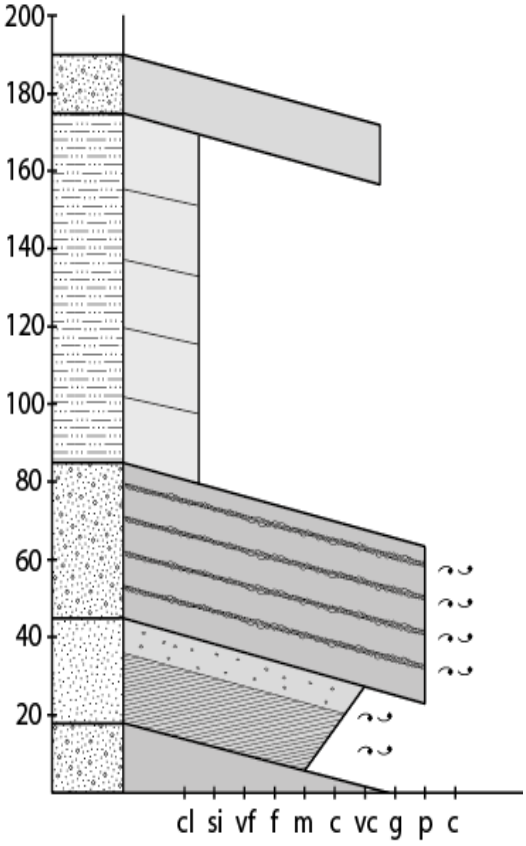

Tectono-Stratigraphic Unit 4 - Log 4 - NW of FN6

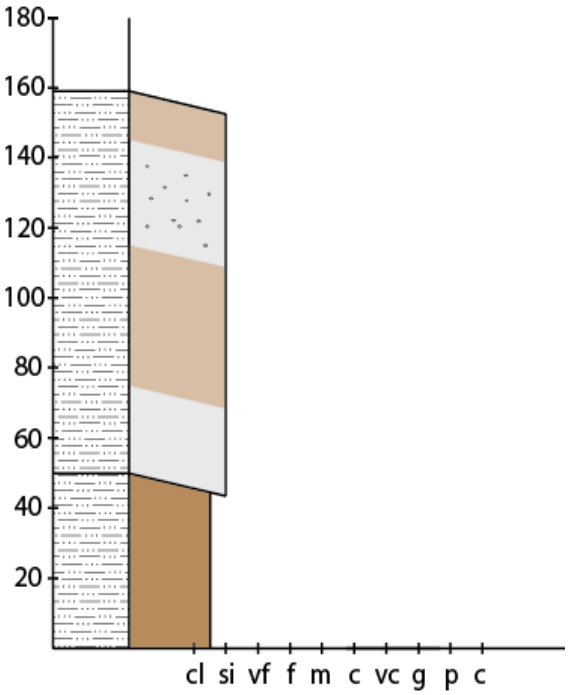

Tectono-Stratigraphic Unit 4 - Log 6 - NW of FN6

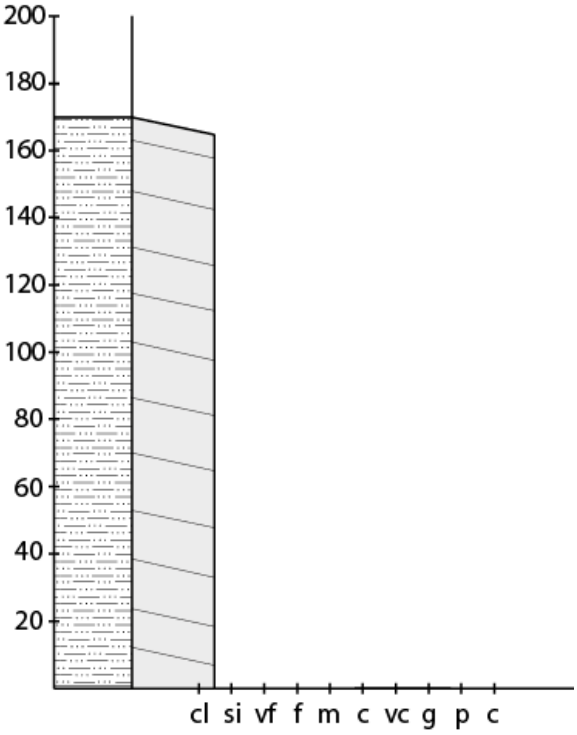

Tectono-Stratigraphic Unit 4 - Log 3 - NW of FN6

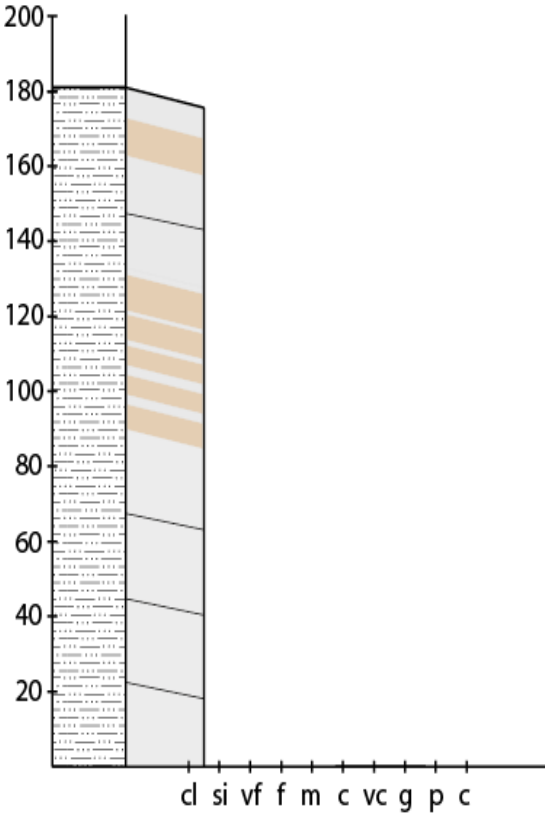

Tectono-Stratigraphic Unit 4 - Log 5 - NW of FN6

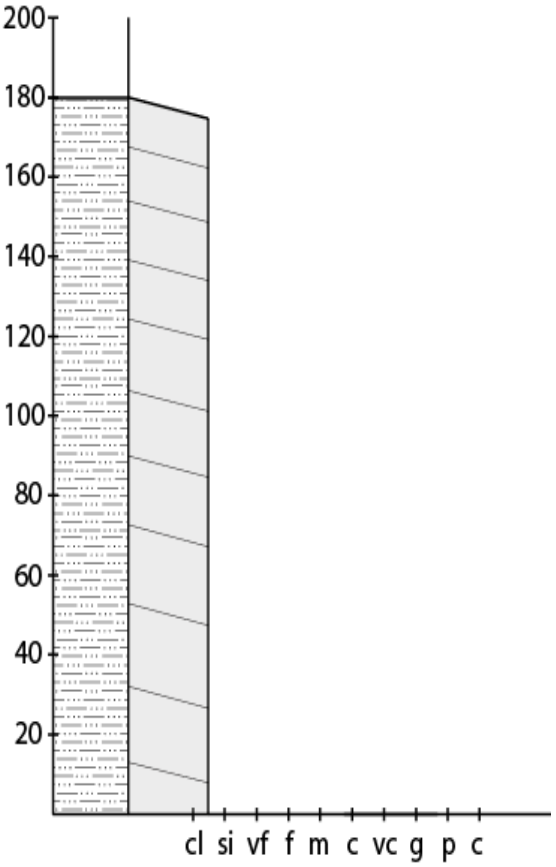

Tectono-Stratigraphic Unit 6 - Stratal Unit 9
FN1-FN2

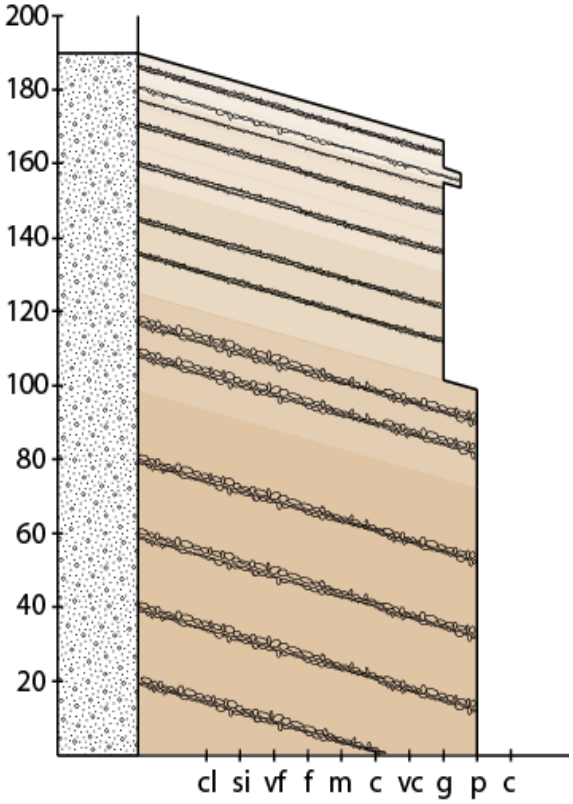

Tectono-Stratigraphic Unit 6 - Stratal Unit 10
FN2-FN3

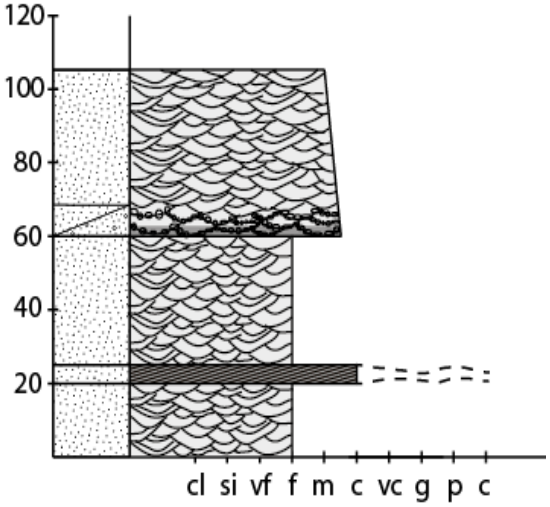

Tectono-Stratigraphic Unit 6 - Stratal Unit 9 - 20 cm
Tectono-Stratigraphic Unit 4 - Log 7 - NW of FN6

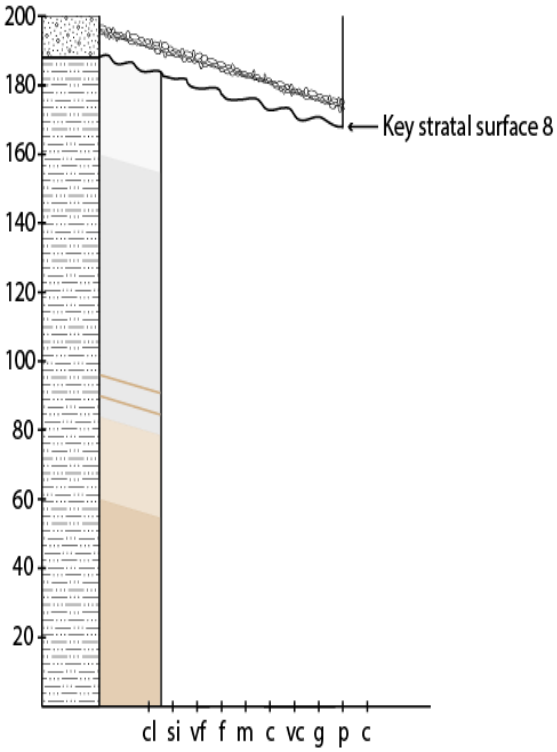

Tectono-Stratigraphic Unit 6 - Stratal Unit 9 - NW of FN6

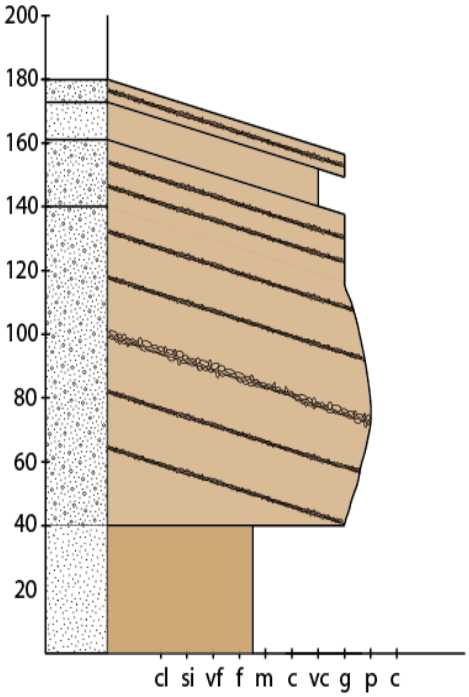

Tectono-Stratigraphic Unit 6 - Stratal Unit 10
Log 1 - FN3-FN4

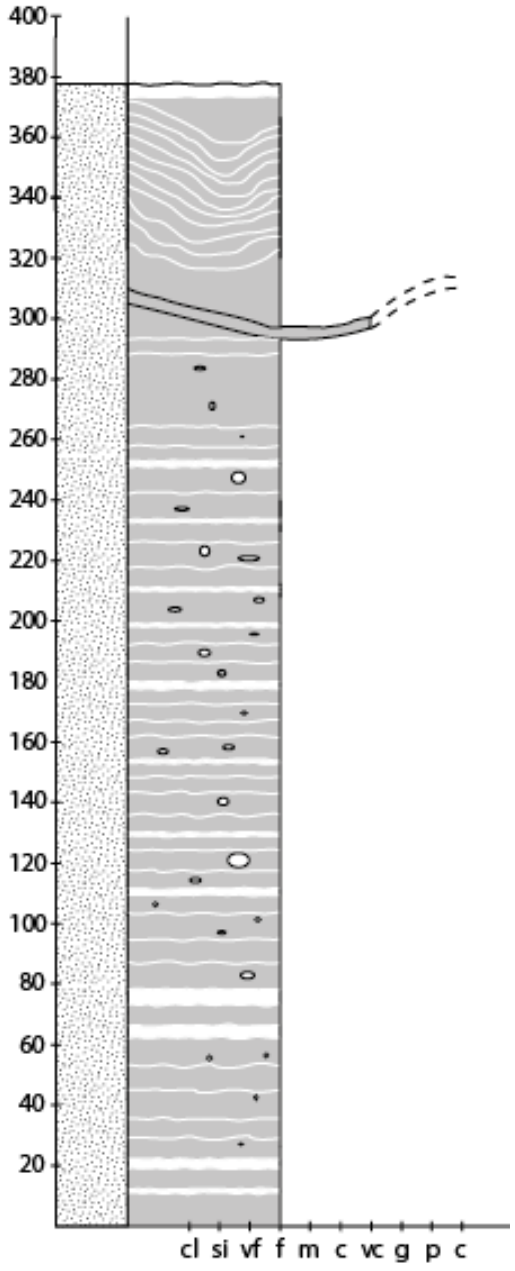

Tectono-Stratigraphic Unit 6 - Stratal Unit 10
Log 2 - FN3-FN4

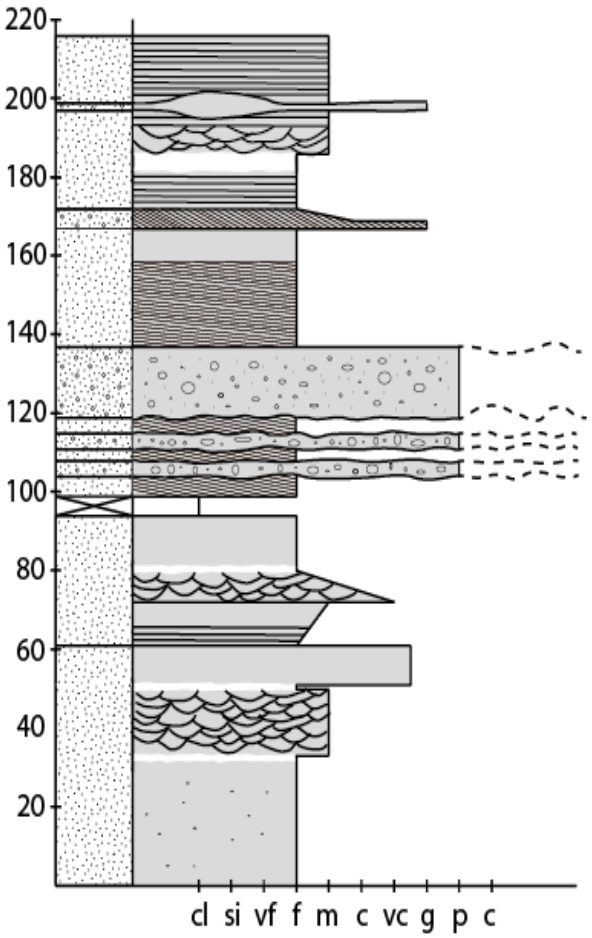

Tectono-Stratigraphic Unit 6 - Stratal Unit 10
Log 2 - FN4-FN5

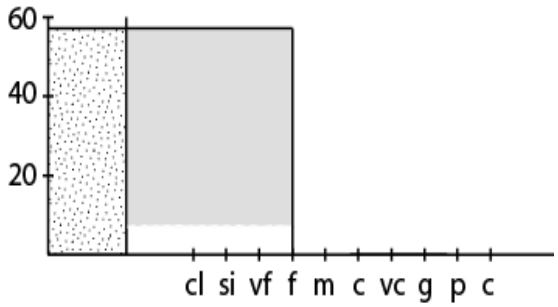

Tectono-Stratigraphic Unit 6 - Stratal Unit 10
Log 4 - FN4-FN5

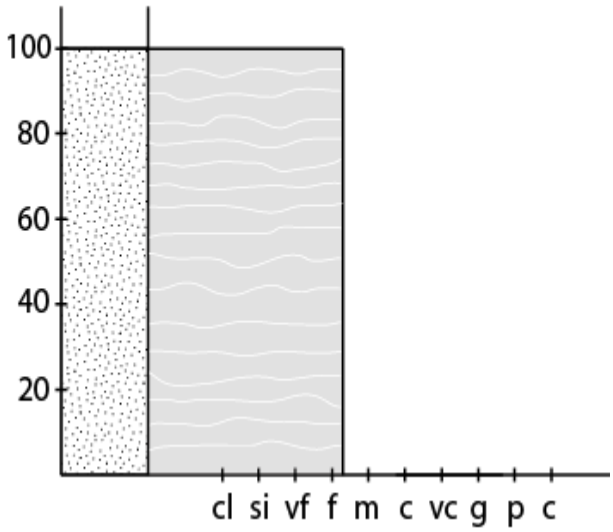

Tectono-Stratigraphic Unit 6 - Stratal Unit 10
Log 1 - FN4-FN5

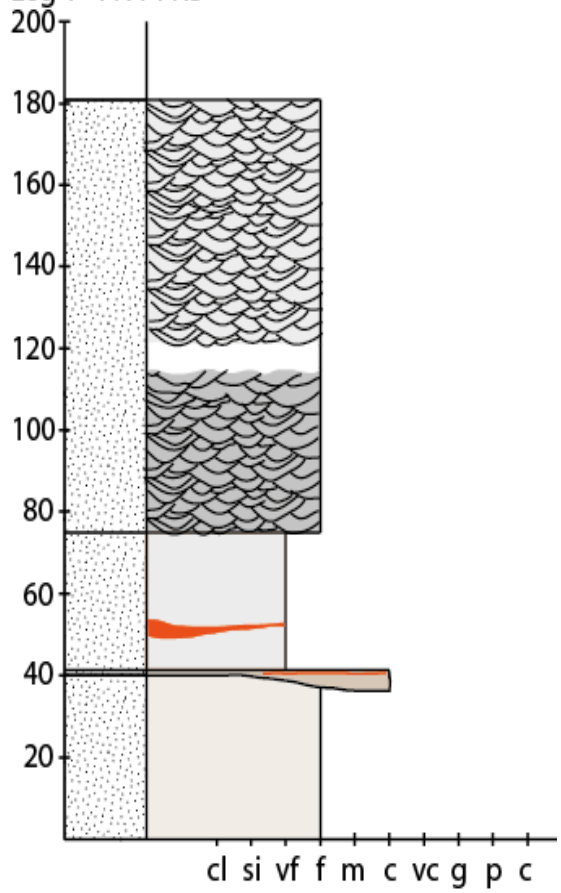

Tectono-Stratigraphic Unit 6 - Stratal Unit 10
Log 3 - FN4-FN5

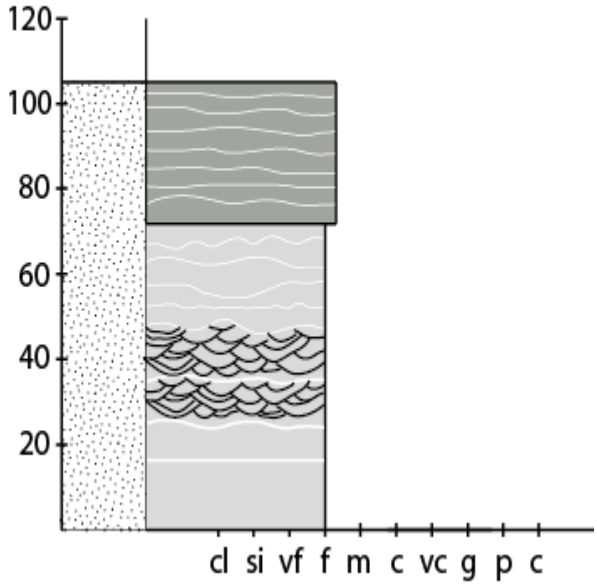

Tectono-Stratigraphic Unit 6 - Stratal Unit 10
Log 6 - FN4-FN5

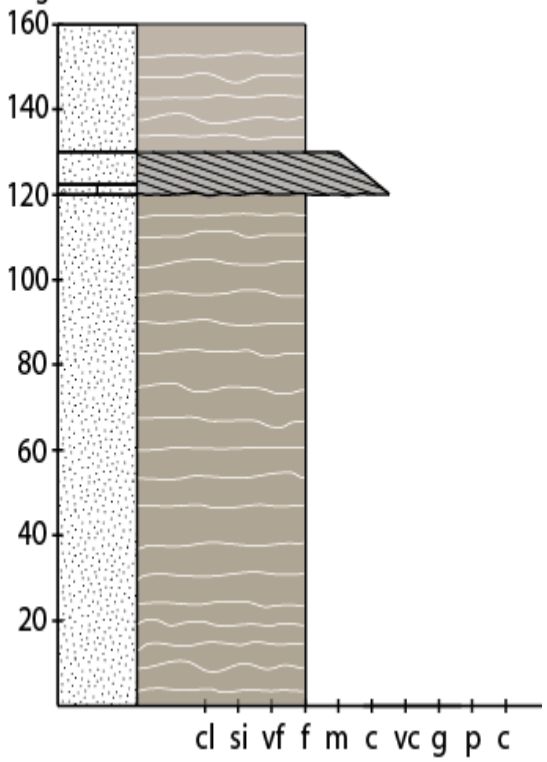

Tectono-Stratigraphic Unit 6 - Stratal Unit 10
NW of FN6

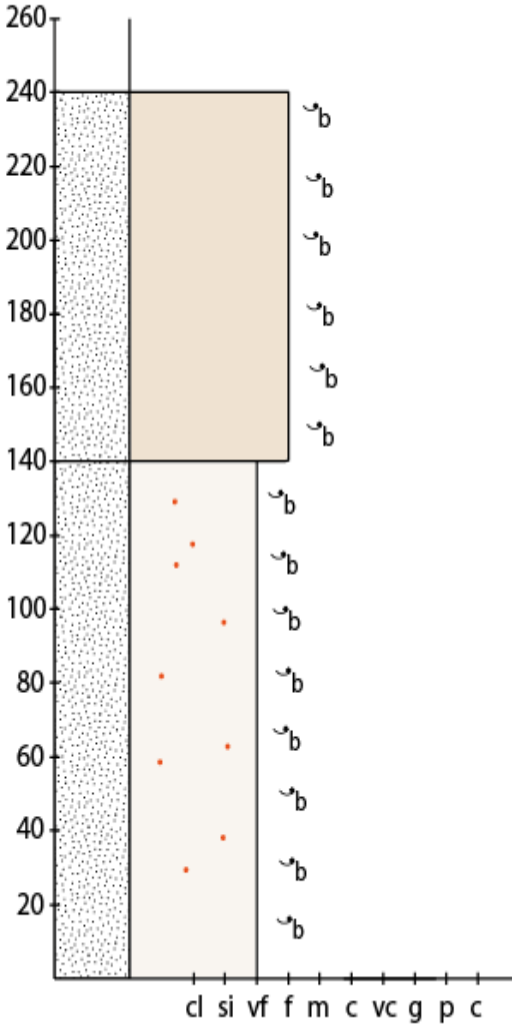

Tectono-Stratigraphic Unit 6 - Stratal Unit 10
Log 5 - FN4-FN5

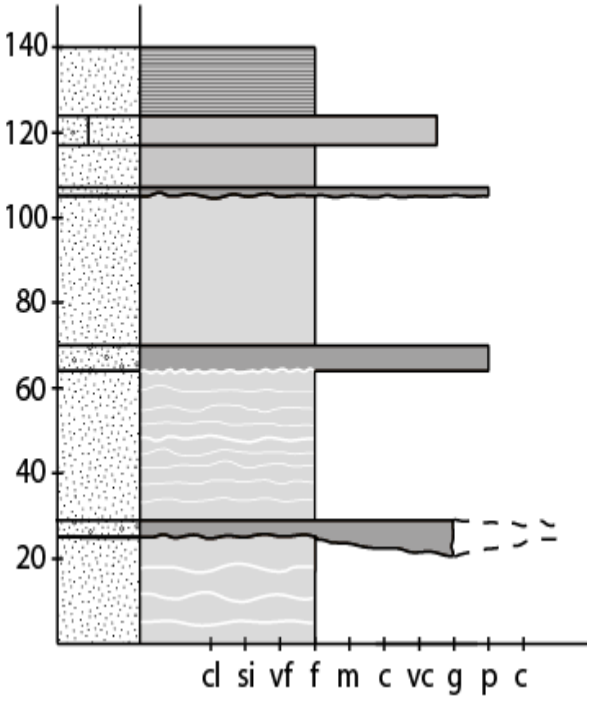

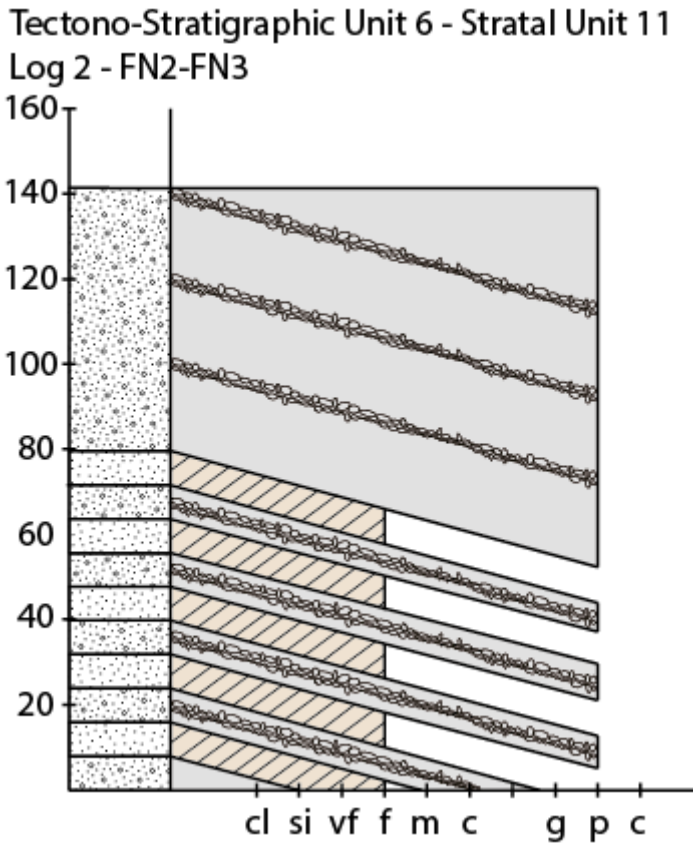
Tectono-Stratigraphic Unit 6 - Stratal Unit 11
Log 2 - FN2-FN3
160
140
120
100
80
60
40
20
cl si vf f m c g p c

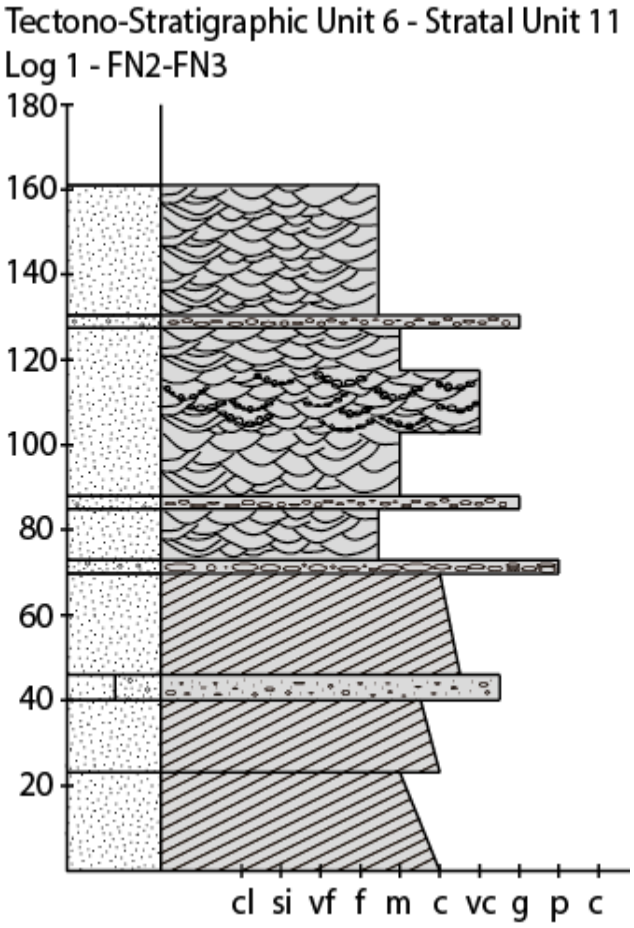
Tectono-Stratigraphic Unit 6 - Stratal Unit 11
Log 1 - FN2-FN3
180
160
140
120
100
80
60
40
20
cl si vf f m c vc g p c

Tectono-Stratigraphic Unit 6 - Stratal Unit 12
Log 2 - NW of FN 6

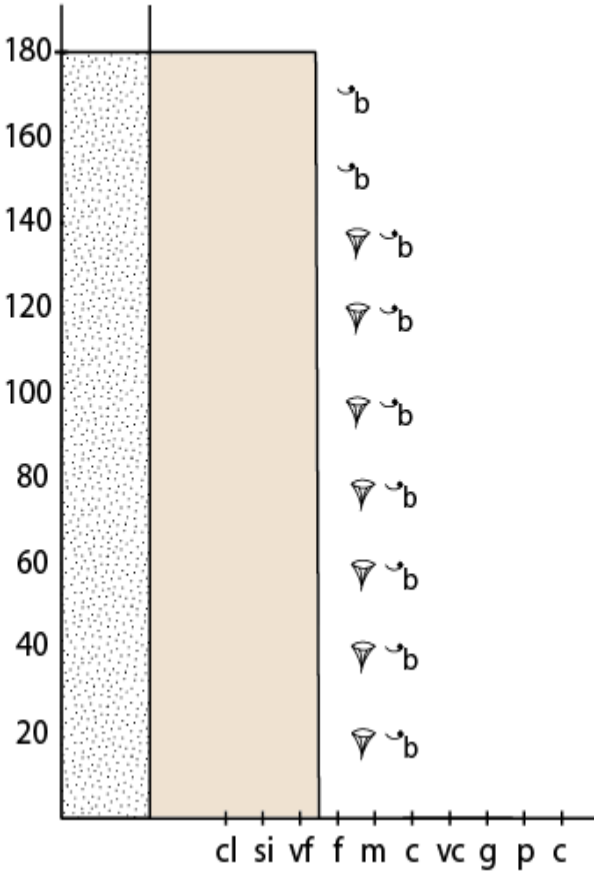

Tectono-Stratigraphic Unit 6 - Stratal Unit 14
Log 2 - NW of FN6

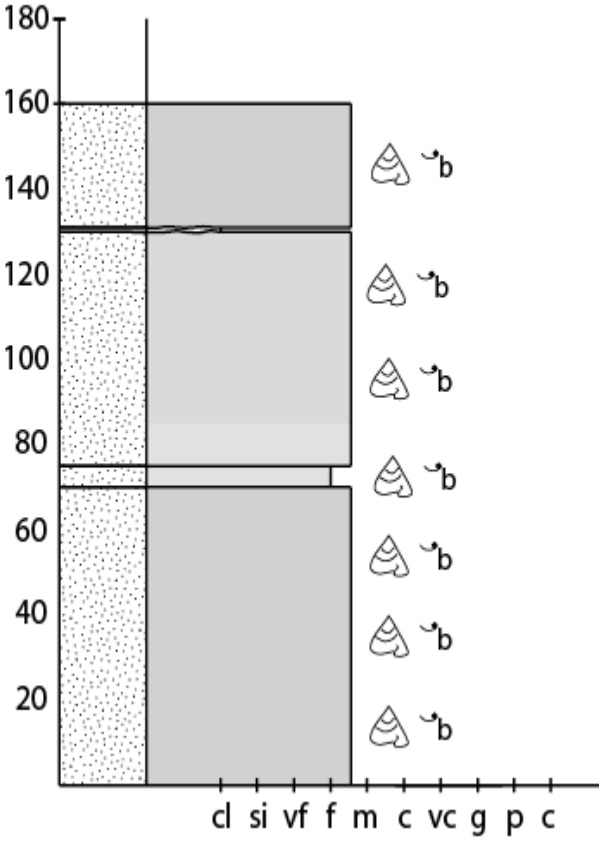

Tectono-Stratigraphic Unit 6 - Stratal Unit 12
Log 1- NW of FN6

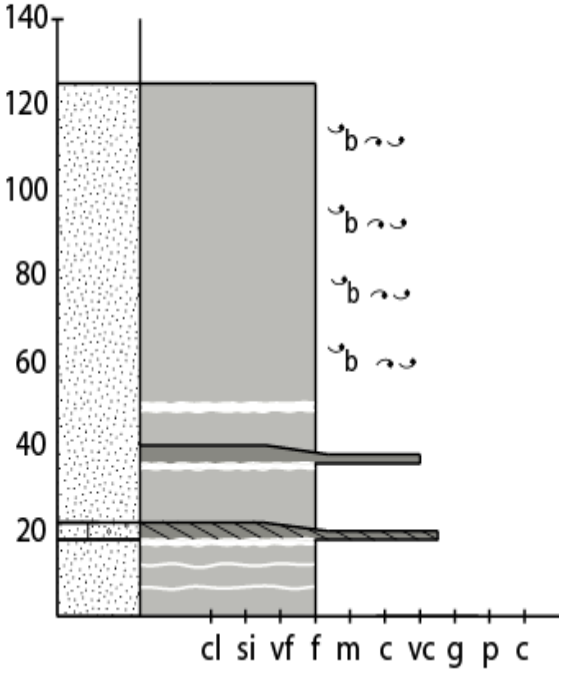

Tectono-Stratigraphic Unit 6 - Stratal Unit 14
Log 1 - NW of FN6

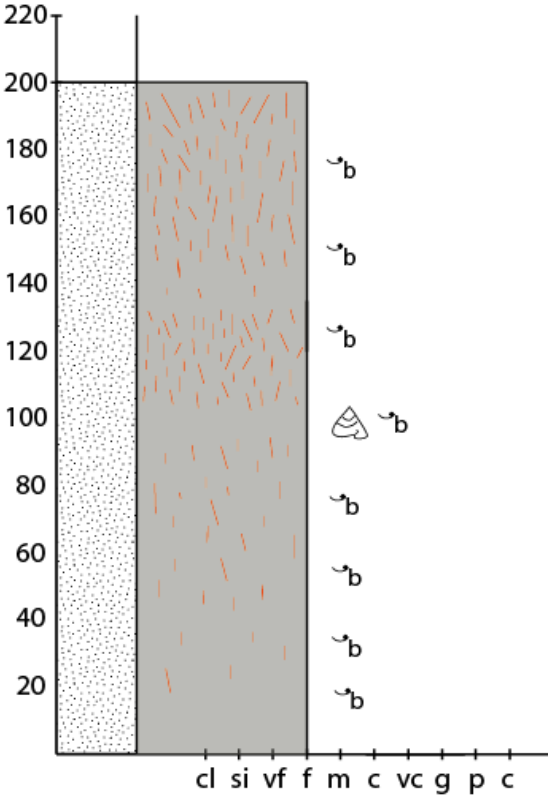

Table 1: The table features dip and strike measurements of individual surfaces throughout the canal. Not every identified surface is present in the table, due to interpretation on only one canal margin. Interpretation on just one margin does not allow measurements of dip and strike in ArcGIS. This is the reason for no data presented from the 1st fault block towards SE. X = Unidentified mistake with data recordings

Fault Blocks	Surfaces	Average dip	Avg. Strike	Avg. dip Direction	C. dip-direction (From ArcMap)
NW of FN6	13	1.7	195	285	NW-W
	11	3 (4.6 last 100 NW)	207	297	NW-W
	10.3	4.3	218	308	SE & NW-N
	10	5.7 (with cliff)	192	282	W
	9	3	198	288	W
	8	2.4	191	281	W
FN5 – FN6	10	5.3	231	321	NW
	9	2.3	215	305	NW
	8	4	201	291	W-NW
	4.3	7	227	317	NW
	4.3	6.5	213	303	W-NW
FN4 – FN5	9	3	236	326	NW
	8	3.1	218	308	NW
FN3 – FN4	9	1.9	238	328	NW
	8	2	241	331	N-NW
	4	1.2	244	344	N
	3.2	3.1	234	324	NW
	3.1	2.9	239	329	NW
FN2 – FN3	9	2.6	22	317	NW
	8	4	232	323	NW
	4	2.1	219	309	NW
	3.2	2.9	228	318	NW
	3.1	3.4	230	320	NW
	3	2.3	115	205	SW
FN1 – FN2	10	1.6	241	331	NW-N
	9	1.7	240	330	NW
	8	2.6	228	318	NW
	3	4.5	214	304	W-NW
Central Horst	8	2.3	245	335	N-NW (Cliff W)
	6	3.7 (N-dip)	254	344	N/E/SE
	5	0.9	349	79	NE-E
	4.1	4.6 & 1.2	252	342 & 88	N & E
	4	2.4 & 1.5	250	340 & 98	N & E
	3	3 (NW to 240 m, NE-flat)	328	318	NW, N & NE
	1.2	1.9 (NW to 220, NE-flat)	225	315	NW, N & NE
	1.1	2.5	254	344	N & NE
	1	7.4	272	02	N
FS2 – FS3	7	1.1	260	350	N
	6.1	1.2	250	340	N

	6	0.7	270	0	N
	5	0.9 (After faults)	228	318	N-NW
	4	1.8 (After faults)	258	348	N
FS3 – FS4	8	3.1	265	355	N
	7	3	266	356	N
	6	2.8	271	01	N
	5	2.23	257	347	N
	3	3.3	263	353	N
FS4 – FS5	8.1	3.1	221	311	NW
	8	3.4	240	330	NW
	7	4.7	238	328	NW
	6	3.6	240	330	NW
	5.1	4.2	236	326	NW
	5	4.7	224	314	NW
	4	4.3 (before fault)	225	315	NW (before fault)
	3	4.5 (before fault)	232	323	NW (before fault)
FS5 – FS6	8.2	4.6	248	338	N-NW
	8	3.3	259	349	N-NW
	6	3.5	251	341	N
	5.2	4.1	238	328	NW
	5.1	4	232	322	N-NW
	5	5.6	242	332	N-NW
FS6 – FS7	7	4.5	211	301	NW
	6.2	5.3	255	345	N
	6	5.1	259	349	N
	5.2	4.9 (last 35) & 3.4 (whole)	235	325	NW & SW/W
	5.1	X	234	324	NW & E
	5	5.1	230	320	NW
FS7 – FS8	8.1	4.1	215	305	NW-W
	8	6.2	230	320	NW
	7	7.5	241	331	NW
	6.2	8.4	242	332	NW
	6	7.9	239	329	NW
	5.3	7.3	241	331	NW
	5.2	8.3	231	321	NW
	5.1	7.9	229	319	NW
	5	5.5 (Last 55 m)	221	311	NW